Facilitating the Technical Network Integration of Distributed PV Generation

Author:
Heslop, Simon

Publication Date:
2016

DOI:
https://doi.org/10.26190/unsworks/19640

Facilitating the Technical Network Integration of Distributed PV Generation

Simon Heslop

A thesis submitted for the degree of

Doctor of Philosophy

School of Electrical Engineering and Telecommunications
The University of New South Wales
Sydney, Australia

August 2016

THE UNIVERSITY OF NEW SOUTH WALES
Thesis/Dissertation Sheet

Surname or Family name: **HESLOP** Other name/s: **Francis**

First name: **Simon**

Abbreviation for degree as given in the University calendar: **PhD**

School: **Electrical Engineering and Telecommunications** Faculty: **Engineering**

Title: **Facilitating the Technical Network Integration of Distributed PV Generation**

Abstract 350 words maximum

Whilst the existing electricity grid can accommodate distributed PV generation, higher penetration levels may have a number of adverse impacts requiring management. The thesis focuses on two of these issues; voltage variability and voltage rise, with contributions to the successful technical integration of distributed PV generation made in three areas. Firstly, the thesis examines the characterisation of PV generation variability. Comprehensive characterisation of PV generation variability is necessary for network service providers to plan appropriately for high penetration distributed PV. The thesis contributes to this area by demonstrating a comprehensive characterisation which describes the behaviour of PV generation variability over the course of the day and over the course of the year. The second is the development of a method for estimating the amount of PV generation a low voltage feeder can accommodate without exceeding upper voltage limits. A novel method is developed through the examination of the relationship between voltage rise, PV generation levels and distribution feeder characteristics. The method is implemented in a simple software tool through which network operators can quickly and easily determine approximate values of maximum PV generation for their distribution feeders. The third thesis contribution is an investigation into methods for integrating PV systems, controllable loads and other devices such as electrical storage, to manage distribution voltage levels. A review of the literature in this area found a focus on methods for minimising excessive voltage rise due to PV generation. The work presented in this thesis contributes to this area by presenting an argument for a more balanced approach to distributed voltage management, one which investigates minimising voltage excursion as a whole, not just voltage rise caused by PV generation. Also presented is an original distributed voltage control method using residential PV systems and controllable loads to ensure voltage levels, upper and lower, are maintained within regulation limits. The method requires no new communication infrastructure and is shown to be more efficient and equitable than similar methods currently proposed in the literature.

Simon Francis Heslop	James Hazelton	31 August 2016
Signature	**Witness Signature**	**Date**

FOR OFFICE USE ONLY **Date of completion of requirements for Award:**

Originality Statement

I hereby declare that this submission is my own research and to the best of my knowledge it contains no materials previously published or written by another person, or substantial proportions of material which have been accepted for the award of any other degree or diploma at UNSW or any other educational institution, except where due acknowledgement is made in the thesis. Any contribution made to the research by others, with whom I have worked at UNSW or elsewhere, is explicitly acknowledged in the thesis. I also declare that the intellectual content of this thesis is the product of my own research, except to the extent that assistance from others in the project's design and conception or in style, presentation and linguistic expression is acknowledged.

Simon Francis Heslop
31 August 2016

Copyright Statement

Simon Francis Heslop
31 August 2016

Authenticity Statement

I certify that the Library deposit digital copy is a direct equivalent of the final officially approved version of my thesis. No emendation of content has occurred and if there are any minor variations in formatting, they are the result of the conversion to digital format.

Simon Francis Heslop
31 August 2016

Abstract

Whilst the existing electricity grid can accommodate distributed PV generation, higher penetration levels may have a number of adverse impacts requiring management. The thesis focuses on two of these issues; voltage variability and voltage rise, with contributions to the successful technical integration of distributed PV generation made in three areas. Firstly, the thesis examines the characterisation of PV generation variability. Comprehensive characterisation of PV generation variability is necessary for network service providers to plan appropriately for high penetration distributed PV. The thesis contributes to this area by demonstrating a comprehensive characterisation of PV generation variability which describes the behaviour of PV generation variability over the course of the day and over the course of the year. The second is the development of a method for estimating the amount of PV generation a low voltage feeder can accommodate without exceeding upper voltage limits. A novel method is developed through the examination of the relationship between voltage rise, PV generation levels and distribution feeder characteristics. The method is implemented in a simple software tool through which network operators can quickly and easily determine approximate values of maximum PV generation for their distribution feeders. The third thesis contribution is an investigation into methods for integrating PV systems, controllable loads and other devices such as electrical storage, to manage distribution voltage levels. A review of the literature in this area found a focus on methods for minimising excessive voltage rise due to PV generation. The work presented in this thesis contributes to this area by presenting an argument for a more balanced approach to distributed voltage management, one which investigates minimising voltage excursion as a whole, not just voltage rise caused by PV generation. Also presented is an original distributed voltage control method using residential PV systems and controllable loads to ensure voltage levels, upper and lower, are maintained within regulation limits. The method requires no new communication infrastructure and is shown to be more efficient and equitable than similar methods currently proposed in the literature.

Acknowledgements

I would like to express my gratitude to the following people who have contributed towards the completion of this thesis

Firstly I would like to thank my supervisors Ass. Prof. Iain MacGill, Prof. John Fletcher and Dr. Anna Bruce for their guidance and advice.

I would especially like to thank my family for all their support throughout my PhD candidature.

I would like to thank Tim Moore (Bacchus), Greg Platt and Daniel Rowe of the CSIRO Energy Centre, Newcastle for their assistance and for providing PV generation data.

I would also like to thank Simon Lewis of Endeavour Energy for providing network data, helping me with DIgSILENT, providing DIgSILENT files and advice on electrical network operation.

Finally I would like to thanks my fellow PhD students whose company I have enjoyed over the last few years, and made this PhD a memorable experience. You are all equally wonderful so I'm going to list you in alphabetical order; Ali, Graham, Hamed, James, Johanna, John, Long Seng, Peerapat, Pei Yao and Sebastian.

Publications Arising from the Thesis

- Heslop, S. and MacGill, I., *Operational characteristics of a cluster of distributed photovoltaic systems*. In *Innovative Smart Grid Technologies Asia (ISGT), 2011 IEEE PES*. 2011. [1]
- Heslop, S. and MacGill, I., *A simple method for predicting the output of dual-axis tracking systems from fixed-tilt system outputs*. In *Australian Universities Power Engineering Conference (AUPEC), 2012 22nd Australasian*. 2012. IEEE. [2]
- Heslop, S. and MacGill, I., *Comparative analysis of the variability of fixed and tracking photovoltaic systems.* Solar Energy, 2014. **107**: p. 351-364. [3]
- Heslop, S., MacGill, I., Fletcher, J. and Lewis, S., *Method for Determining a PV Generation Limit on Low Voltage Feeders for Evenly Distributed PV and Load.* Energy Procedia, 2014. **57**: p. 207-216. [4]
- Heslop, S., MacGill, I. and Fletcher, J., *Voltage Probability Analysis – PV and Load in Low Voltage Networks.* In *Asia Pacific Solar Research Conference 2015.* 2015. http://apvi.org.au/solar-research-conference/proceedings-from-past-conferences/ [5]
- Heslop, S., MacGill, I. and Fletcher, J., *Maximum PV generation estimation tool for residential low voltage feeders: First-stage*. in *2015 IEEE Power & Energy Society General Meeting*. 2015. IEEE. [6]
- Heslop, S., MacGill, I. and Fletcher, J., *Maximum PV generation estimation method for residential low voltage feeders.* Sustainable Energy, Grids and Networks, 2016. **7**: p. 58-69. [7]

Acronyms

ADMD	After Diversity Maximum Demand
AVR	Automatic Voltage Regulator
BOM	Australian Bureau of Meteorology
CAISO	California Independent System Operator
CHP	Combined Heat and Power
CSIRO	Commonwealth Science and Industrial Research Organisation
CT	Current Transformer
DG	Distributed Generation
DKASC	Desert Knowledge Australia Solar Centre
DNI	Direct Normal Insolation
DNO	Distribution Network Operator
DPVG	Distributed PV Generation
DSE	Distributed State Estimation
DSL	DIgSILENT Scripting Language
DSM	Demand Side Management
DTx	Distribution Transformer
ERCOT	Electric Reliability Council of Texas
ESS	Energy Storage System
EWH	Electric Water Heater
IBR	Inclining Block Rate
IOP	Increment of Power
LDC	Line Drop Compensator
LV	Low Voltage
LVP	Low Voltage Point
LVR	Line Voltage Regulator
MADG	Maximum Allowable Distributed Generation
MPPT	Maximum Power Point Tracking
MPVG	Maximum PV Generation
MPVGEM	Maximum PV Generation Estimation Method
MV	Medium Voltage
NREL	National Renewable Energy Laboratory
OLTC	On-load Tap Changing (transformer)
PCC	Point of Common Coupling
PSPC	Power Set Point Control
PV	Photovoltaic
PWM	Pulse Width Modulation
RES	Renewable Energy Sources
SRRL	Solar Radiation Research Laboratory
STx	Substation Transformer
THD	Total Harmonic Distortion
VSPC	Voltage Set Point Control

Table of Contents

List of Figures

List of Tables

1 Introduction

1.1 Growth of Distributed Photovoltaic Generation

Growth in global installed Photovoltaic (PV) capacity has been remarkable over the past decade. Globally, the total installed capacity was 5.1 GW in 2005, this had increased exponentially to 227 GW by 2015 [8]. This is also the case for Australia. As of June 2016, total installed PV capacity was 5.3 GW, approaching 10% of total installed generation capacity. This is an increase from insignificant levels in 2009 [9]. For 2016, 5.3 GW represents approximately 20% of average evening peak demand and 24% of average midday demand [10]. The majority of this increase in deployment is grid-connected PV; small scale (<5 kW), distributed, single-phase residential systems connected to the Low Voltage (LV) distribution network. The growth in Distributed PV Generation (DPVG) adds a potentially new and disruptive component to the electricity network. At high penetration levels, the expected impacts of DPVG include an increase in the incidence of voltage rise, reverse power flow, an increase in voltage variability and harmonics and lastly, protection and safety concerns during islanding events [11, 12]. The key benefit of an increase in DPVG is a reduction in CO_2 emissions. PV generation is a clean source of power and if its increase in turn reduces fossil fuel generation then CO_2 emissions, as well as other pollutants associated with fossil fuel combustion, will also reduce. It is also renewable, and doesn't rely upon a finite feed stock such as coal, gas or uranium. There are also possible technical and financial benefits to an increase in DPVG. DPVG has the potential to reduce peak commercial loads and the Loss of Life (LoL) of Substation Transformers (STx) [13]. This is also shown to be the case for Distribution Transformers (DTx) [14, 15]. DPVG may also improve reliability and stability for remote sections of network [16]. When combined with storage, DPVG can potentially reduce network operating costs and be a financially superior alternative to conventional network augmentation for constrained sections of network [17].

The potential benefits of DPVG justify an investigation into facilitating its integration into the electricity grid such that its net benefits to the electricity sector are maximised. This thesis focusses on the management of the technical network challenges associated with an increase in DPVG. Two potential impacts are examined, the increase in both voltage variability and voltage rise. For DPVG to be successfully integrated into the electricity grid, these impacts need to be managed.

1.2 Key Technical Network Challenges with DPVG

Technical Challenge 1: An increase in DPVG will result in an increase in voltage variability due to fluctuations in DPVG output and load variations. This will potentially lead to breaches of voltage fluctuation regulation limits and an over-operation of voltage management equipment, increasing maintenance requirements and decreasing equipment life. A comprehensive characterisation of PV generation variability is required to accurately quantify voltage fluctuation induced by PV generation variability. This is necessary to determine the impact on voltage management equipment and to assist network operators design appropriate voltage management for sections of network with high levels of DPVG.

Technical Challenge 2: DPVG can cause voltage rise along a line when generation exceeds demand. To avoid PV deployment that is likely to cause excessive voltage rise, it is necessary to quantify the relationship between voltage rise, PV penetration levels, load and PV distribution and feeder impedance.

Technical Challenge 3: The development of voltage and demand management solutions by Distribution Network Operators (DNOs) in response to increasing levels of DPVG, and also in anticipation of future increased deployment of DPVG, is currently a time-consuming and resource-intensive exercise. The development of tools designed to assist in this task are therefore potentially valuable, and would make network operators more likely to appropriately consider DPVG in their planning.

Technical Challenge 3: There is concern that existing voltage regulation equipment and methods may not be able to manage the increase in voltage variability and voltage rise introduced by high penetration DPVG. Investigation into new voltage management equipment and techniques is required to mitigate the introduced voltage variability and voltage rise.

1.3 Focus of the Thesis and Research Aim

The overall aim of this thesis is to contribute towards the successful integration of DPVG into Australia's electricity network, and is considered a further step in the transition of Australia's generation portfolio from non-renewable to clean and renewable generation. Integration would be considered successful when DPVG is a useful contributor to the overall electricity network operational objective of reliable and efficient supply of electrical energy to consumers. Whilst the thesis is orientated around Australia's electricity distribution network, the contributions of the thesis are relevant, albeit possibly to a lesser extent, to non-Australian distribution networks which are similar operationally, and with similar operational guidelines.

The thesis presents original research that aims to address the technical challenges raised in Section 1.2 hence contributing towards successful integration of DPVG. This undertaken work is as follows:

- In response to technical challenge 1), a comprehensive characterisation of PV generation variability is presented. The characterisation is split according to season, week and hour. High resolution PV generation data is also used in one study so that its characterisation accurately represents changes in PV generation due to cloud transients. The study also categorises the analysis according to day type.
- In response to technical challenge 2), an examination of the relationship between Maximum PV Generation (MPVG), feeder characteristics and load conditions is conducted.
- In response to technical challenge 3), an innovative method for calculating the MPVG for LV feeders is presented. The method is derived analytically and has the capacity to be applied to all distribution network feeders.
- In response to technical challenge 4) a probabilistic voltage and household impact analysis case study is conducted for a number of voltage management options. The aim of this study is to demonstrate a balanced approach to distributed voltage management.
- In response to technical challenge 4) an original distributed voltage control method is proposed. The method controls PV inverters to ensure an upper

voltage limit is not exceeded and controllable loads to ensure a lower voltage limit is not exceeded. The method ensures both a minimisation of intervention and a fair distribution of intervention actions among PV inverters and controllable loads. Local measurements only are required to implement the control method.

1.4 Organisation of the Thesis

The thesis consists of three parts. The first part (Chapter 2) is an investigation into the potential impacts of high-penetration PV on the electricity grid and following this, a review of existing research which investigates preventative measures for the two key impacts identified in Chapter 2, voltage rise and voltage variability. The second part (Chapter 3) presents the research objectives, resulting from a knowledge gap analysis of the literature. The third part (Chapters 4 - 6) presents the novel contributions of the thesis, research which addresses the knowledge gaps identified in Chapter 3.

- **Chapter 2** presents a literature review consisting of two parts. The first (Section 2.1) is an investigation into the potential impacts of high-penetration PV on the electricity grid. The second (Sections 2.2-2.5) is a further review of the literature, based on the two key impacts associated with high-penetration PV that were identified from this initial work, voltage rise and voltage variability. The second part consists of three sections: characterising PV generation variability, the relationship between voltage rise, PV generation and feeder characteristics, methods for determining the MPVG for a section of LV network or feeder and novel distributed voltage management methods.
- **Chapter 3** presents a knowledge gap analysis of the literature reviewed in the second part of Chapter 2, Sections 2.2-2.5. Developing methods to address these knowledge gaps form the research objectives of the thesis. The knowledge gap analysis consists of three sections. Section 3.1 identifies knowledge gaps in the literature presenting research characterising PV generation variability. Section 3.2 identifies knowledge gaps in the literature presenting methods for determining the MPVG for a section of LV network or feeder, and it also identifies the limitations in current DNO PV installation assessment processes. Section 3.3 identifies

knowledge gaps in the literature presenting new distribution voltage management techniques.

- **Chapter 4** presents novel research on the characterisation of PV generation variability. The first part (Section 4.1) addresses a number of characterisation knowledge gaps identified in Section 3.1. A characterisation of PV generation variability is conducted for a number of different PV technologies and tracking types including fixed-tilt, single-axis and dual-axis tracking PV systems. The data used for the characterisation is taken from a number of PV systems located at the Desert Knowledge Australia Solar Centre [18]. The data is actual measured PV generation data with a sample resolution of 5 min for the year 2010. The characterisation is split according to season, week and hour. The second part (Section 4.2) also addresses a number of characterisation knowledge gaps identified in Section 3.1. High resolution PV generation data is used to characterise the PV generation variability for a cluster of small-scale PV systems. This data is sourced from the Commonwealth Science and Industrial Research Organisation (CSIRO) Energy Centre in Newcastle, Australia. The study utilises actual PV generation data and so accurately represents distributed PV generation behaviour. The characterisation concentrates on variability hour to hour, and also categorises the analysis according to day type. Day type is defined according to cloud cover: sunny, partly cloudy and majority cloud. It also investigates aggregate generation variability.
- **Chapter 5** consists of two parts. The first part (Section 5.1) presents an examination of the relationship between MPVG, feeder characteristics and load conditions. General relationships are identified through analysis of the results and under simplifying conditions, an innovative method developed for deriving the MPVG. This research addresses the MPVG knowledge gaps and limitations in current DNO PV installation assessment processes identified in Section 3.2. The second part (Section 5.2) presents a novel method for calculating the MPVG that is more sophisticated than that proposed in Section 5.1. It surpasses the method presented in Section 5.1 in terms of potential application under realistic network conditions. It more comprehensively addresses the MPVG knowledge gaps and limitations in current DNO PV installation assessment processes identified in Section 3.2.

- **Chapter 6** also consists of two parts. The first part (Section 6.1) presents a high-penetration PV case study, where a probabilistic voltage and household impact analysis is conducted for a number of voltage management options. The results of the analysis are examined to select the most appropriate voltage management solution, which most effectively minimises voltage excursion as a whole. The study demonstrates a balanced approach to distributed voltage management. This research addresses a number of voltage management knowledge gaps identified in Section 3.3. The second part (Section 6.2) presents an original distributed voltage control method. The method controls PV inverters to ensure an upper voltage limit is not exceeded and controllable loads to ensure a lower voltage limit is not exceeded. The method uses both a voltage and a power set point for control; this ensures both a minimisation of intervention and a fair distribution of intervention among PV inverters and controllable loads. Local measurements only are required to implement the control method. This research addresses a number of voltage management knowledge gaps identified in Section 3.3.
- **Chapter 7** concludes the thesis, identifying the novel aspects and the main contributions. It also discusses opportunities and possible directions for future work building on the findings of the research efforts presented in the thesis.

2 High-penetration PV – Impacts and Integration

This chapter consists of two parts. The first (Section 2.1) is an investigation into the potential impacts of high penetrations of PV on the electricity grid The second (Sections 2.2-2.5) is a further review of the literature, based on the two key impacts associated with high-penetration PV identified in the first part, voltage rise and voltage variability. The second part is a review of research associated with managing the integration of high-penetration PV into the electricity network.

The aim of Section 2.1 is to identify the potential impacts of high-penetration PV as raised in the literature. The original work contributed in the thesis (Chapters 4 - 6) is not considered a direct extension or improvement on the work presented here. In Sections 2.2-2.5, the general aim of this section is to summarise the findings. Whilst some comment on how the work could be improved may be given, the specific manner in which the author claims to make improvements on the existing literature, and how it is linked to Chapters 4 - 6, is described in Chapter 3.

2.1 The Potential Network Impacts of High-penetration PV

A high level review of the impacts of high-penetration PV is conducted in [11], raising a number of concerns. It suggests that, at sufficiently high PV penetration levels, fluctuation in voltage levels due to fluctuations in PV generation could result in excessive operation of On-load Tap Changing (OLTC) transformers. The impact of reverse power flow on DTx operation and longevity, un-intentional islanding and voltage rise are also discussed. Un-intentional islanding occurs when PV systems continue to inject power into the local network despite being isolated from the main grid due to breaker operations or an equipment fault. Distribution system protection schemes are normally designed under the assumption that power flows from the substations to the end users. If a fault takes place and a breaker opens, all circuits downstream would be de-energised. However, this is not the case when distributed PV systems are present. Thus, it is possible that an island with power generation and consumption is created and this raises concerns with respect to equipment and personnel safety. Therefore, all PV inverters are required to include an effective islanding detection method [19]. In [12], the potential impacts of high-penetration PV are also summarised. As in [11], reverse power flow, voltage rise and voltage fluctuations are again mentioned. It is also noted that reverse power flow may affect overcurrent protection co-ordination and the operation of Line Voltage Regulators (LVR) and/or Line Drop Compensators (LDC). Regarding voltage rise, it also raises the issue of constant impedance loads consuming more power when operating at a higher voltage. Phase imbalance due to PV generation, occurring when PV systems are not installed equally across the phases, is also a possibility [20, 21]. There is also concern that existing voltage regulation equipment may not be able to manage the increase in voltage variability and voltage rise caused by high-penetration PV [22, 23]. Not all the potential impacts of high-penetration PV raised by papers such as [11] have received equal attention in the literature. The majority of interest lies in the areas of voltage rise, the impacts resulting from the increase in voltage and power variability, harmonics, and at the system level, system flexibility. A general definition of system flexibility is the system's ability to balance load and generation. In [24], a measure of system flexibility is given as the fraction of peak load below which conventional generators can operate. The literature review conducted in this section (Section 2.1) focusses on these areas.

2.1.1 Increased Voltage Variability

2.1.1.1 Over-operation of Voltage Regulation Equipment

PV generation is expected to increase voltage variability in the distribution network, and there are concerns that this will lead to increased operation of voltage regulation equipment. Equipment such as voltage-controlled capacitor banks, OLTCs, and line LVRs [12]. Increased operation increases maintenance requirements and reduces equipment life.

In [25], the impact of introduced PV generation variability on the number of daily tap changes for a distribution STx is examined. The STx is 20 MVA, 69 kV / 12.47 kV, $\Delta -$ Y connected, servicing two residential feeders, tap range is ±10% with 32 steps. The PV penetration level is 20% of STx capacity, or 4 MW. The study is conducted over three summer days, load data is actual measured data taken from the network whilst PV generation data is derived from local insolation measurements. A sample resolution of 1 min is assumed. It is also assumed that all PV systems experience the same insolation. The study finds that the number of tap changes at 20% PV penetration over the period simulated was 160, 4 times greater than at 0% PV penetration.

A study [26] investigates how voltage levels, in the presence of high-penetration PV, can be better maintained using an advanced form of OLTC and Automatic Voltage Regulator (AVR) control. Instead of maintaining the substation secondary voltage in a pre-set tolerance band, which is done by a conventional OLTC control, an advanced OLTC control method based on the accurate Distribution State Estimation (DSE) result is developed, to keep the voltage in the whole network within the desirable range. The HiPerDNO project [27] is used to develop the DSE. The DSE control method is then tested on an actual rural Medium Voltage (MV) network. Actual solar irradiation values are used along with synthesized load profiles. The behaviour of 40 MV/LV STx units are examined, each substation is equipped with a load model and a scalable PV system. Results show that voltage levels are better managed, but at the expense of increased numbers of tap-changer operations. For a 10% PV penetration level (0.4 MW), over a 1-week period, the number of tap operations increased from less than 10 to over 30.

A new method for controlling MV/LV OLTC, in the presence of high-penetration PV, is also proposed in [28], where a voltage range is programmed into the OLTC as opposed to a fixed voltage target. When voltage range is used the OLTC only operates when either the upper or lower voltage limit of the voltage range is exceeded. PV generation data is actual 15 min data, for one year, taken from a PV plant located at Leibniz University in Hannover. The results of the study show that voltage is maintained within limits for both fixed and ranged voltage input control but the number of tap operations under fixed voltage is much greater. For the period simulated, more than 10000 tap operations were recorded for each PV penetration scenario under fixed voltage. Under ranged voltage control the number of tap operations is around 95% less for all PV penetration scenarios.

The above studies show that variable generation from PV increases voltage variability and leads to an increase in the number of OLTC transformer tap operations. The concern that existing voltage regulation equipment may not be able to manage the increase in voltage variability raises the question of how the growing range of distributed devices might offer new voltage management techniques for mitigating the increase in voltage variability (and voltage rise) caused by high-penetration PV. Section

2.1.6 describes the direction of further review conducted in this area.

2.1.1.2 Breach of Voltage Fluctuation Limits

There is also concern that the variability of high-penetration PV generation will result in breaches of voltage fluctuation limits. Papers [29] and [30] both present case studies examining voltage fluctuation levels in the presence of high-penetration PV.

In [29] the test system is a 10-bus test system, consisting of three conventional generators, 1154 MW, 4004 MW and 1736 MW. A large scale concentrated PV plant is added to the network (on its own bus), sized between 333 MW and 1065 MW. Insolation data, sampled at 1 s, input into a standard PV generation model [31], is used to produce PV generation data. The insolation data is for a typical cloudy day and is used to examine the potential change in voltage levels due to changes in PV generation. For 864 MW of PV generation (13% penetration), it is shown that voltages at the PV system bus can drop 5% within 5 s. The relevant Australian standard [32] specifies that a maximum 3% change in voltage is permissible, for the test system in [29], a PV penetration level above 5% will breach this limit. PV penetration is defined as the ratio of PV generation to total generation.

In [30], a 1 MW PV system is connected to a sports stadium in Taiwan. An hourly PV generation profile is derived from a combination of solar irradiation and panel temperature measurements. Referring to Figure 2.1, voltage is measured at one end of the test system (bus MU67); with the PV system located at the other (bus MF65). Bus MF65 is considered the end of the distribution feeder when the tie switch between bus 4 and 5 is closed. Historical measured hourly demand at bus MU67 is used for the study. The study finds that at 1 MW, the hourly change in voltage is 0.75%. This is well within operating constraints of 2.5%, and the Australian limit of 3%. A system size of 3.5 MW is required to reach 2.5%. Unfortunately, the paper doesn’t specify what 3.5 MW is as a percentage of load, peak or otherwise.

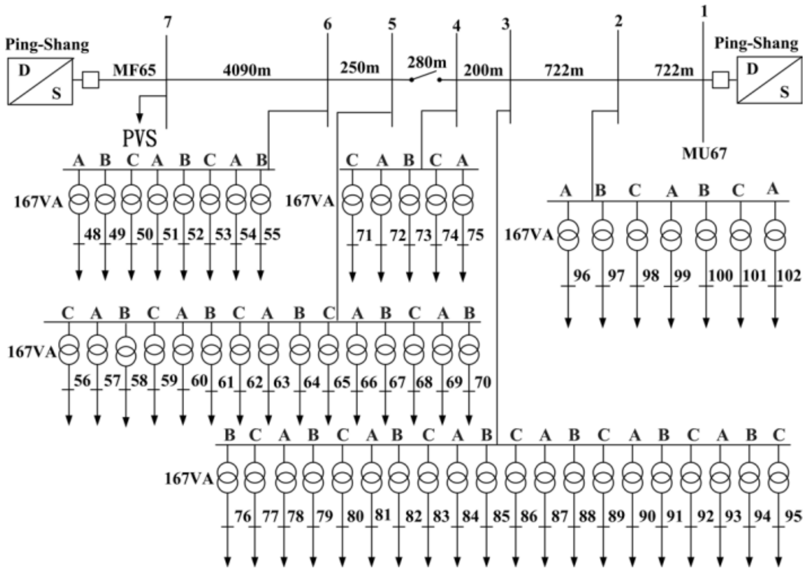

Figure 2.1 One-line diagram of test system [30]

The above studies show that breaches of voltage fluctuation limits may occur if the PV penetration level is high enough. A potential problem identified from review of these studies is whether the PV generation data sets used are adequate to accurately evaluate voltage fluctuation levels. A more comprehensive characterisation of PV generation variability may be required. Section 2.1.6 describes the direction of further review conducted in this area.

2.1.2 Voltage Rise

It is intuitive that increasing levels of PV penetration will result in increases in voltage rise and violations of steady state voltage limits [33], and this is most likely to occur during periods of light load and high PV generation. From [34], Figure 2.2 illustrates the basic relationship between PV, load and voltage rise. Looking at the top two figures, during times of heavy (or nominal) load, PV will offset the voltage drop to some degree but not enough for voltage rise to occur. Looking at the lower two figures, during times of light load, when PV generation may exceed load demand, voltage rise can occur.

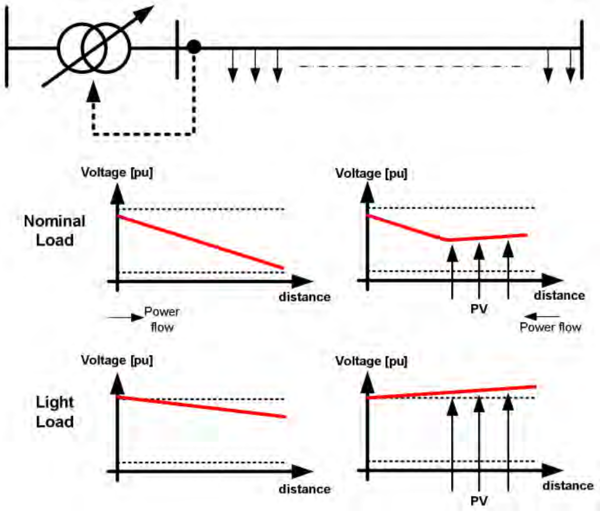

Figure 2.2 PV, load and voltage rise [34]

Studies showing that high PV penetration leads to voltage rise include [34] and [35]. A test network in [34] is used to determine the voltage rise due PV generation. The network and power flow analysis is conducted using PSCAD, the voltage profile along the length of the feeder, with and without PV generation, is then determined, see Figure 2.3. The voltage rise along the length of the feeder due to the PV generation is clearly illustrated.

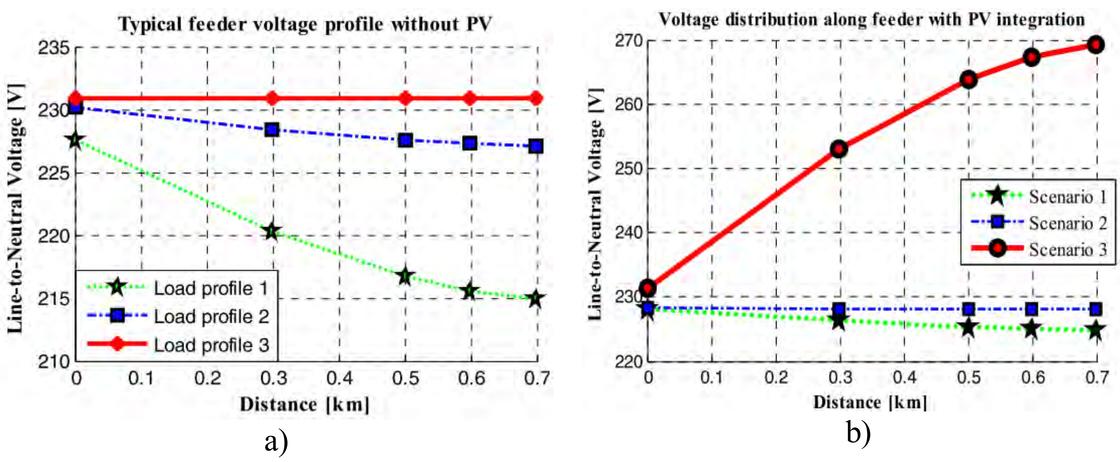

Figure 2.3 Voltage profile along test feeder a) Without PV and b) With PV [34]

In [35], the test network used for analysis is residential, and includes 629 residential PV systems. The PV generation was derived from insolation measurements, taking into account cell operating temperature. A 3-phase unbalanced power flow calculation was conducted on the test network and the time series voltage, with a 1 min sample resolution, was recorded for two houses, before and after the PV system is installed. The results are shown in Figure 2.4. The increase in voltage during the day at the two houses, when the PV systems are generating, is evident.

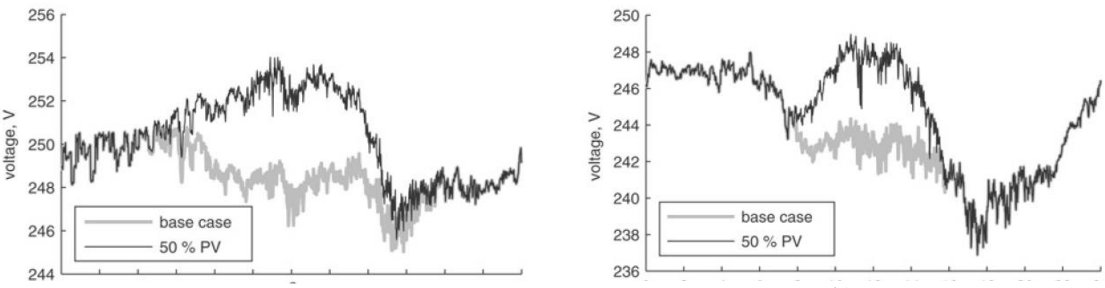

a) b)

Figure 2.4 Modelled voltage before and after PV systems are installed at one of the houses for a) a summer day and b) a winter day [35]

The above studies show that PV generation will cause voltage rise. They do not however, accurately quantify the relationship between voltage rise, PV penetration levels, load and PV distribution and feeder impedance. Section 2.1.6 describes the direction of further review conducted in this area.

2.1.3 Voltage Imbalance

Voltage imbalance across phases, due to an imbalance in PV generation across phases is also a concern. It is intuitive that imbalance will occur when PV systems are installed in an unbalanced manner, but an imbalance in PV generation can also occur when PV systems are, generally, installed in a balanced manner across phases. This occurs due to PV systems experiencing cloud transients at different times. One study, [36], demonstrates this. In [36] the potential impacts on voltage imbalance are investigated using a 13-bus IEEE test feeder, where clouds are simulated to move across the network, influencing the generation levels of PV systems dispersed across the network. Results show that some feeders experience a phase voltage imbalance of up 0.3pu, although the significance of this is not discussed. A voltage variation sensitivity method is proposed as a means to identify feeders at risk of voltage imbalance, and suggests reconfiguring the network to minimise the risk of voltage imbalance.

Existing power flow analysis software often does not have the capability to conduct power flow analysis for imbalanced 3-phase, 4-wire lines, which needs to take into account the mutual coupling between phases. This is required for analysis of voltage imbalance due to PV generation. A new line model which does take into account mutual coupling is proposed in both [37] and [38]. The development of work in this area highlights its importance, and allows for other researchers to perform impact studies with imbalanced loads and PV generation.

Strategies to mitigate voltage imbalance are proposed in both [39] and [40], from the same author of [38]. In both [39] and [40], battery storage is utilised to ensure that power on all phases is maintained in balance. In [39] a centralised battery storage system (CES) is used, with all PV system inverters connected to the CES via dedicated DC link. In [40] battery storage located at the household is controlled to manage power balance across phases. For both studies a comprehensive communication network is assumed between all devices. The mitigation strategy is dynamic, unlike the network reconfiguration solution proposed in [36].

Whilst voltage imbalance is obviously a concern, the solutions suggested above appear to be either ambitious or impractical, requiring extensive communication infrastructure as is the case of [39] and [40], or resource and labour intensive, as is the case of feeder reconfiguration proposed in [36]. In the opinion of the author this indicates that the likelihood of such strategies being implemented, at least in the near future, is not great. It may be that another alternative is required, one may not necessarily be as effective, but has less barriers to implementation. The thesis doesn't contribute any original work in the specific area of voltage imbalance across phases but does so in the related area of voltage rise, an area where a variety of ambitious strategies have also been proposed. For this thesis, the approach is taken that the solution needs to simple rather than complicated. This is demonstrated in work on estimating PV generation capacity for LV feeders in Section 5.2 and in a new method for managing voltage rise using distributed devices (PV inverters and air-conditioners) in Section 6.2.

2.1.4 Harmonics

Harmonics produced by PV systems is another cause of concern. PV cells generate DC; this current is then converted to AC through an inverter. The conversion process, normally using Pulse Width Modulation (PWM), produces harmonics [41]. Also, PV inverters can trigger parallel resonance due to interaction between line inductance, capacitance of load at residences and injected harmonic currents [42].

The research presented in this section investigates the impact of introduced Total Harmonic Distortion (THD) into the electrical network due to PV inverters. A study is referred to in [11], where a 56 kW PV system (equating to 37% PV penetration) contributed just 0.2% to harmonic voltage distortion levels, far less than a conventional household load. It was concluded that harmonics would not be a problem as long as the PV inverters were well designed.

In [42], an investigation into PV generation related power quality problems is undertaken. The analysis covers generated current harmonics, the effect of background voltage distortion in the network, and the possible resonances between PV inverters and the network. The test network is a Dutch residential network. The majority of households (197) have a large-scale PV systems installed. The planned maximum PV generation capacity is expected to be 36 MW; the capacity of the existing 197 PV systems is not stated. All are roof mounted PV systems connected on three 400 V network sections, each supplied from a separate 10-kV/400-V transformer. Simulation results found that under normal supply voltage conditions (THD = 3% is the Dutch average) the inverters operate well, but at slightly increased levels of distortion currents.

In [43], generation measurements were taken over several days during October 2007 of a 20 kWp PV plant in Northern Greece. The measurements capture the harmonic impact of the PV plant in different weather conditions. The harmonic profile of the PV system contains the amplitude and the angle shift of current harmonics as a function of the fundamental current and voltage waveforms, and the solar insolation. The aim of this study is to identify the harmonic behaviour as a function of solar insolation. Results of the study find the voltage THD remained low at all times. Dominant current harmonics observed through the measurement campaign are of the 3^{rd}, 5^{th}, 7^{th}, 9^{th} and 11^{th} order. During the day all harmonics maintained a certain proportion to the fundamental, but during the morning and evening harmonics increased substantially, the 3^{rd} order especially. Under normal operating conditions the PV plant never causes any violation of harmonic limits. The THD at the DTx remains below 5% under all test scenarios. The presence of the PV plant only adds 0.11% to THD compared to when the PV plant is not generating.

The introduced harmonics of another 20 kWp PV system is examined in [44]. The paper finds that the distortion is mainly the 3rd harmonic, but this only contributes 0.2 V to the voltage, 0.1% of the rated voltage. This is well within limits and in terms of limits to PV penetration when THD is assessed, the size of the PV system could be increased by ten times or more. The upper voltage limit (10% of rated) would be exceeded well before the THD limit.

The studies presented in this section concluded that PV inverter generated current harmonics were not likely to reach unacceptable limits. With this finding, the research presented in this thesis focusses elsewhere. Further discussion on this is described in Section 2.1.6.

2.1.5 Loss in System Flexibility

A general definition of "System Flexibility" is the system's ability to balance load and generation. In [24], a measure of ''System Flexibility'', defined as "flexibility factor", is given as the fraction of peak load below which conventional generators can operate. A system with 0% flexibility factor would be unable to operate below annual peak load at all, while a system with 100% flexibility factor could operate down to zero load demand without significant penalties. The penalties referred to are economic. If load does drop below a systems flexibility factor, then one or more base load plants would likely be required to completely shut down for a short period of time, which would incur significant economic penalties. It is suggested in the literature that the introduction of variable generation (wind and PV) reduces system flexibility. The fast ramp rates, occurring during the morning and the evening, that are introduced by high-penetration PV makes load following more difficult. Also, the increase in net power fluctuations makes frequency control more challenging [11]. Its introduction also displaces conventional generation which would otherwise be used for load following, frequency control and auxiliary services. If conventional generation is forced offline then system flexibility is reduced.

Studies looking into the impacts of PV generation on system flexibility include [45] where historical data was obtained for wind, load and solar for the California Independent System Operator (CAISO). This data was projected forward for modelling 20% renewable penetration by 2010 (2010T) and 33% renewables by 2010 (2010X) and

2020 (2020). A study was then carried out examining the impact of intermittent generation on grid operation. This included an analysis on the variability of system load as well as wind and solar generation over time frames: hourly, 5 min, and 1 min. Net load duration curves are given for the 3 years under the 2010X scenario. Curves show that for approximately the last 100 hours, net loads drop to levels likely to present operational challenges to CAISO. It also claims a required increase in system flexibility of 40% for the 2020 scenario (33% renewables) for normal load conditions and 50% for light load (greater impact of renewables). Due to increased variability the number of start/stops increases and sustained load ramps (up and down) steepens. Also, load following capability will need to increase due to renewables by approximately 8% above what is required for variation in load alone.

In [46], the impact of high-penetration PV in the Western Interconnection is examined. The WestConnect group consists of utilities operating in Arizona, Colorado, Nevada, New Mexico and Nevada. The paper examines the impact of 25% solar penetration. The model includes details of load, all generation, and major transmission limitations for the year 2017. PV penetration is defined as PV energy generated as a percentage of total energy generated. The paper looks into the displacement of conventional generation and found that for a week in July (summer) the solar generation displaces about 10% of the combined cycle plants and all of the peaking gas turbine generation. For a week in April (spring) the impacts are even greater; again all of the peak gas turbine is displaced and almost all of the combined cycle plants. There is also at times a significant reduction in coal fired generation, halving reduced by 25% most days and 50% for two days. During these periods where load is reduced to such an extent that base load (coal fired) generation is displaced; base load generation will likely need to continue running at a loss as their start/stop cycling time is too long. A similar study is conducted in [24], for the Electric Reliability Council of Texas (ERCOT).

The above studies show that large amounts of PV generation can lead to a reduction in system flexibility. However in Australia, a significant reduction in system flexibility due to PV are unlikely, this is due to the nature of its deployment. As such further research focuses on distribution level impacts as opposed to system level. Further discussion on this is described in Section 2.1.6.

2.1.6 Summary and Further Review

The key impacts of high-penetration PV identified in the literature include increased voltage variability, voltage rise, harmonics and loss in system flexibility.

Increase in Voltage Variability: Variable generation from PV increases voltage variability and this is shown to lead to an increase in the number of OLTC transformer tap operations. Breaches of voltage fluctuation limits may also occur if the PV penetration level is high enough. It is questionable, however, whether the PV generation data sets used in these studies are adequate to properly evaluate the impacts of high-penetration PV, and hence determine the impact on voltage management equipment[1]. A more comprehensive characterisation of PV generation variability may be required. Such a characterisation of PV generation variability would also assist network operators design appropriate voltage management equipment for sections of network with high levels of distributed PV deployment. A review of the literature on the characterisation of PV generation variability is presented in Section 2.2.

Voltage Rise: PV generation will cause voltage rise; the extent of voltage rise is dependent upon PV penetration in conjunction with load and PV distribution and feeder impedances. To assist in the avoidance of PV deployment likely to cause excessive voltage rise, it is necessary to quantify the relationship between voltage rise, PV penetration levels, load and PV distribution and feeder impedance. The literature review presented in Section 2.3 discusses studies to date investigating this relationship.

PV Generation Limits: An examination into the relationship between voltage rise, PV penetration, load and PV distribution and feeder impedance leads to the question of how much PV generation can a section of network or feeder accommodate without exceeding voltage regulation limits? Section 2.4 examines research to date developing methods for estimating a PV generation limit.

[1] Although the three studies on equipment over-operation in Section 2.1.1.1 examine the impact on OLTC transformers; the findings have implications for all types of voltage management equipment, and distribution voltage management generally.

Adequacy of Existing Voltage Management Techniques: There is concern that existing voltage regulation equipment may not be able to manage the increase in voltage variability and voltage rise caused by high-penetration PV; this raises the question of how the growing range of distributed devices[2], might offer new voltage management techniques for mitigating the increase in voltage variability and voltage rise caused by high-penetration DPVG? Section 2.5 examines research to date on new distributed voltage management techniques, using distributed devices, designed to assist in the integration of DPVG. Innovative Demand Side Management (DSM) techniques are also covered in this section.

Harmonics: All studies presented discussing harmonics as a potential impact concluded that, for their particular case study, PV inverter generated current harmonics were not likely to reach unacceptable limits. With increasing levels of PV penetration, harmonics will increase, but as stated in [44], breaches of other power quality limitations, and probably network capacity, will likely occur long before limits on harmonics are reached. With this finding, the research presented in this thesis focusses elsewhere.

Loss in System Flexibility: Whilst the potential impact of high-penetration PV on system flexibility is certainly important, it is a system level impact. The deployment of PV in Australia to date is primarily small-scale generators at the distribution level. The extent of the deployment, whilst large in terms of number of systems, is not yet at a capacity to cause system level impacts. By virtue of this, thesis research beyond this point focusses on distribution level impacts as opposed to system level.

2.2 Characterisation of PV Generation Variability

As noted in Section 2.1.6, it is questioned whether the PV generation data sets used in these studies are sufficiently adequate to properly evaluate the impacts of high-penetration PV, and to properly determine the impact on voltage management equipment, a comprehensive characterisation of PV generation variability may be required. This section presents a review of the literature on the characterisation of PV generation variability.

[2] Distributed devices used for distributed voltage management include distributed generation, battery storage and controllable loads for example, to maintain distribution network voltage levels within regulation limits.

The studies examined in this section provide a characterisation of PV generation variability. Their contribution can be grouped into two categories: studies of PV generation variability for a single PV system and studies of aggregated PV generation variability for multiple PV systems or within a large scale PV plant.

2.2.1 Single PV System

High resolution (1 second) insolation[3] sampling [47] shows that within 1 second, due to cloud transients, changes in insolation levels of up to 68% are possible. But this is for a singular insolation measurement device, with a very small footprint. PV generation is directly proportional to insolation levels, but for a PV system to exhibit a similar change in generation in 1 second, in terms of percentage of rated power, it would have to be small, with an equivalent footprint to the insolation measurement device. The shadow cast by a singular cloud in an otherwise cloudless sky would cover a small PV system almost instantly, therefore also reducing its PV generation capacity as a percentage of its rated power by 100% almost instantly. But for a solar farm, the shadow cast by a singular cloud only covers a fraction of the farms total area, and thus reducing the farms PV generation capacity as a percentage of its rated power by only a small percentage. Footprint increases with PV generation capacity, thus larger PV systems will exhibit lower variability, as a percentage of rated power.

In [48], using 1 min solar insolation and weather data from the National Renewable Energy Laboratory (NREL) Solar Radiation Research Laboratory (SRRL), and a modified version of the PVWatts model [49], the generation for a fixed-tilt PV system with latitude tilt was calculated. The frequency (number of hours per year) of ramp rates (percentage of PV capacity) over 1 min and 15 min intervals is calculated. Results show the cumulative number of hours of ramp rates over 10% is approximately 200 hours. Assuming an average of 8 PV generation hours a day, this is approximately 6% of the time. Similar levels of variability are recorded for a 3 kW system in [50]. In [50], the probability density of ramp rates for time intervals ranging from 1 second to 1 hour are calculated, results show that variability increases with increasing time interval. In [48],

[3] Note that the majority of studies use solar insolation, or insolation, measurements to conduct their characterisation. As PV generation is directly proportional to insolation levels, the findings of studies using insolation measurements are therefore directly applicable to PV generation

these ramp rates are taken from insolation measurements and therefore translate to generation variability for a small-scale PV system, this is confirmed by the 3 kW system in [50] which exhibits similar levels of variability. PV systems of this size will not introduce voltage variation into the local network significant enough to breach the 3% voltage change limit in the Australian standard [32]. Although, where the generation from individual small-scale PV systems will not introduce significant voltage fluctuation into the local network, a cluster of small-scale PV systems, with their generation considered in aggregate, may. This is investigated further in section 2.2.2.

Comparing results from [50] and [48], in [50] the 1 min variability is far greater than the 15 min variability, yet the opposite is the case in [48]. This may have something to do with the sample period; in [50] the sample period is over a year while in [48] the sample period is over one summer month (June). The difference in variability gives weight to the argument that PV generation variability, for singular PV systems at least, varies across the year. A comprehensive PV generation variability characterisation should therefore cover an entire year.

Also in [50], the average hourly change in PV generation, split according to month, is calculated. Results confirm that PV generation variability varies from month to month, where a difference of over 5% average PV generation variability between some months is evident. It is also the case on an hour-to-hour basis, with more positive ramps in the mornings and more negative ramps in the afternoons. The data used for this analysis is derived from the clearness index. The clearness index is "a measure of how the actual irradiance for a period of given time deviates from the irradiance for a perfectly clear day" [50]. The resolution is hourly, and therefore unable to capture the variation in PV generation due to cloud transients. This could explain why PV generation variability is close to zero around midday. Either that or the negative and positive ramps around this time balance to give a zero average. So, whilst [50] confirms that PV generation variability varies from month to month, higher resolution sampling is required to capture the changes in generation due to cloud transients

From the above studies it can be ascertained that due to cloud transients, for singular PV systems, large changes in generation in short times frames are possible. It is also the case that it is necessary to use high resolution data to capture effect of cloud transients.

Small-scale PV systems do exhibit high levels of generation variability but this will not necessarily translate into high voltage variability at the local network due to their small capacity. Finally, it is shown that the variability of PV generation will differ according to the time frame analysed.

2.2.2 Aggregation of PV Systems

Where the generation from individual small-scale PV systems will not introduce significant voltage fluctuation into the local network, a cluster of small-scale PV systems, with their generation considered in aggregate, may. According to [51], at the penetration level where PV generation becomes significant, the PV systems can no longer be thought of as individual generators; their combined effects must be considered. But, whilst a large cluster of PV systems may have a large combined capacity, if they are spread out over a large area, either geographically or electrically, then their equivalent penetration level will be small. PV systems may be close geographically but are located on different feeders and therefore distributed electrically.

It is claimed in [47] that a 68% change in PV generation is possible, but this is only for a singular small-scale PV system. The combined generation of a cluster of PV system considered in aggregate doesn't exhibit such large changes in generation, due to the fact that not all PV systems are going to experience the same cloud transients at the same time. The combined generation is therefore not as variable; this is known in the literature as the "smoothing effect". To explain further, if all systems were (somehow) located at the one location, then a transient cloud over the location would give one large generation dip. However, if these systems are spread out geographically the time at which the same transient cloud passes over each PV system will differ, giving a number of smaller generation dips, a smoothing out of the one large generation dip. Figure 2.5 from [52] illustrates the smoothing effect, showing how the aggregated generation from a cluster of distributed PV systems is less variable than a singular system.

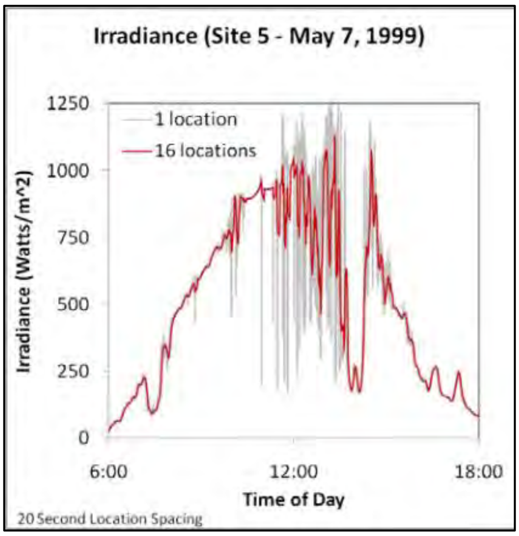

Figure 2.5 Reduction in variability when generation is aggregated from a cluster of PV systems – illustration of the smoothing effect [52]

Research [53] has modelled the smoothing effect, introducing a measure of aggregate variability, relative output variability. The relative output variability is the ratio of the aggregate variability for a cluster of PV systems and the variability of an individual PV system within the collection. The cluster of PV systems are assumed to be spread across a sufficiently large area so as not to experience the same insolation. The relative output variability is calculated for all PV systems within the collection (N). The mean of the relative output variability, with increasing N, is defined by the relationship (2.1).

$$Relative\ output\ variability = \frac{1}{\sqrt{N}} \tag{2.1}$$

Figure 2.6 shows how the relative output variability decreases with N for a cluster of PV systems.

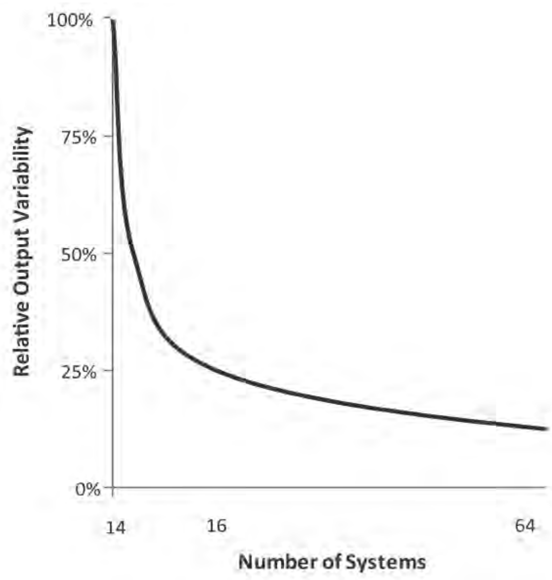

Figure 2.6 Relative output variability versus number of systems N [53]

The smoothing effect does not just occur for a cluster of PV systems, but also within larger capacity PV plant. The smoothing effect increases with footprint. Analysis in [52] shows how a 30 kW PV system, for all time intervals (1 s to 10min), exhibits less variability than an insolation sensor, variability decreasing further for a 13.2 MW PV plant. Figure 2.7 confirms the diversity in PV generation within a PV plant [52]. Figure 2.7 gives the correlation in power between all inverters relative to one inverter; within the 13.2 MW plant.

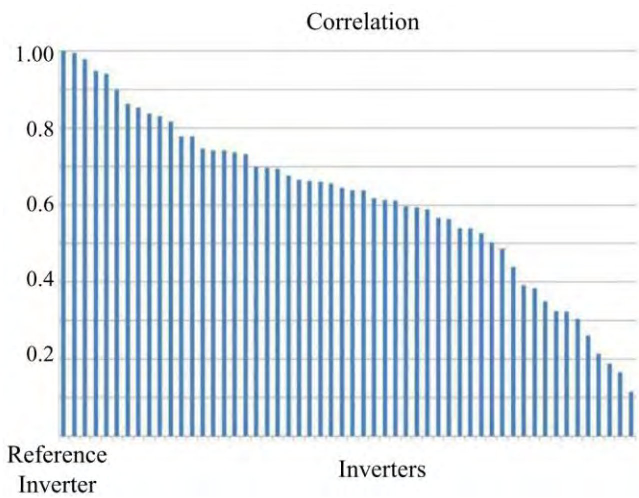

Figure 2.7 1 min correlation in power between all inverters relative to one reference inverter, within a 13.2 MW plant [52]

Finally, an examination of solar insolation correlation and distance is conducted in [54]. In [54], the changes in solar insolation for different time intervals as a function of distance between sites is plotted. Results show that correlation reduces exponentially with distance, for all time intervals, though at different rates of decay. The rate of decay is similar to (2.1), and gives weight to the argument that it is a reduction in solar insolation correlation between sites which leads to the reduced aggregate variability.

The above studies show that when the total PV generation from a cluster of systems is considered in aggregate, the combined variability is less than that of an individual system, referred to as the "smoothing effect". Also, that the aggregate variability for a cluster of systems, relative to the variability of a singular system, reduces exponentially with a linear increase in the number of systems. It is therefore important that when characterising PV generation variability for a cluster of small-scale PV systems, their generation should be considered in aggregate. This is also the case for large scale solar plants.

2.2.3 Summary

The key findings from the literature can be summarised as follows

- Due to cloud transients, for singular PV systems, large changes in generation in short times frames are possible. This is confirmed in [47], which shows that a rapid change in insolation in seconds is possible. This would also be the case for PV generation, as it is directly proportional to insolation levels other factors being held constant. This finding indicates that when analysing PV generation variability it is necessary to use high resolution data to capture effect of cloud transients.
- Small-scale PV systems do exhibit high levels of generation variability [48] but this will not necessarily translate into high voltage variability at the local network due to their small capacity.
- Variability of PV generation will differ according to the time frame analysed. This is confirmed in [48] and [50], with results showing that different variability probabilities occur for different time frames. Therefore, when investigating the variability of PV generation it is important to conduct analysis across a range of time frames.

- It is likely that PV generation variability itself varies across the course of the year. This argument is supported results from [48], which shows more variability at 1 min intervals than at 15 min, while results in [50] show the opposite; this is likely due to the data sample period. In [50] the sample period is a year while in [48] it is for one summer month. PV generation variability will also vary across the course of the day; this argument is support by results in [50].
- When the total PV generation from a cluster of systems is considered in aggregate, the combined variability is less than that of an individual system. This is called the “smoothing effect”; Figure 2.5 illustrates the “smoothing effect” of geographical diversity. The same smoothing effect is also seen in large scale centralised PV plants [52].
- Generally, the aggregate variability for a cluster of systems, relative to the variability of a singular system, reduces exponentially with a linear increase in the number of systems, defined by equation (2.1) from [53]. This relationship is linked to the level of correlation between sites, indicated by findings presented in [54].

When the above findings are examined in the context of how to characterise PV generation variability it is important to understand that high resolution data is required to capture the effects of cloud transients. Also, when investigating distributed PV generation, their behaviour also needs to be considered in aggregate. PV generation variability will itself also vary throughout the day, from hour-to-hour, and also over the course of the year. A thorough characterisation of PV generation variability would therefore cover an entire year and also examine variability in hourly segments. Finally, deriving PV generation data from insolation or satellite measurements may not be necessarily accurate. To ensure accuracy, the PV generation dataset should be obtained from actual PV system measurement.

2.3 The Relationship between PV Generation, Feeder Characteristics and Voltage Levels

As noted in Section 2.1.6, to assist in the avoidance of PV deployment likely to cause excessive voltage rise, it is necessary to quantify the relationship between voltage rise, PV penetration levels, load and PV distribution, and feeder impedance. The research presented in this section reviews studies investigating this relationship.

In [55], the relationship between PV inverter and load power factor and voltage rise is examined. Also, using a test feeder, the study investigates how total PV generation capacity is influenced by its distribution. The amount of PV generation the feeder can accommodate without breaching the upper voltage limit is the total PV generation capacity. PV systems are assumed to be evenly distributed along the length of the feeder. The conventional relationship between voltage and power between two points on a feeder is given by equations (2.2) and (2.3). Where E_L and E_G are the voltages at the two points, R and X is the line impedance between them, δ is the power angle and P_L and Q_L is the real and reactive power at point L.

$$P_L = \frac{1}{R^2 + X^2}[R(E_L E_G cos\delta - E_L^2) + X(E_L E_G sin\delta)] \tag{2.2}$$

$$Q_L = \frac{1}{R^2 + X^2}[R(E_L E_G sin\delta) - X(E_L E_G cos\delta) - E_L^2] \tag{2.3}$$

For the purposes of this study [55], the solution to the above equations has been normalised, giving (2.4). A derivation of (2.4) can be found in [56].

$$2e^2 = \left|1 - 2p(r + q) \pm \sqrt{1 - 4[(r + q)p + (1 - rq)^2 p^2]}\right| \tag{2.4}$$

Where

$$p = \frac{XP_L}{E_G^2} \tag{2.5}$$

$$e = \frac{E_L}{E_G} \tag{2.6}$$

$$q = \frac{Q_L}{P_L} \tag{2.7}$$

$$r = \frac{X}{R} \tag{2.8}$$

The solution to (2.4), e, is plotted with an increasing value of p for a PV inverter operating at unity power factor and load at three different power factors. The value p is equivalent to the normalised net power, PV generation minus load, at point L. Values of r = 2 and r = 1.3 are used. The plots illustrate the required value p to achieve a change in voltage limit, the difference between E_L and E_G. The plots show how the required value p to reach the voltage change limit varies with load power factor and also with r. For both values of r, a higher value of p is required to achieve the voltage change limit when load (q) is more inductive. This is also the case for a higher line X/R ratio (r).

The maximum value of p for each PV system was plotted against the number of PV systems to achieve a change in voltage limit (E_L minus E_G) between two points L and G. The maximum value of p is the value which ensures the change in voltage between the two points gives the upper voltage limit at point G. The plots show the maximum value of p decreasing exponentially with a linear increase in the number of PV systems and also a higher X/R ratio allows for more PV generation to be installed, a higher maximum value of p. Also, results show that whilst the value of p per PV system decreases exponentially with number of PV systems, the total combined value of p increases. The rate of increase takes the form of an increasing decaying exponential.

The key findings from [55] are that when load is more inductive, more PV generation is required to reach the voltage change limit. It is also discovered that the maximum PV generation (p) decreases exponentially with a linear increase in the number of PV but that the total installed PV capacity increases. Also, a higher cable X/R ratio also increases the value of p.

In [57], the variation of the voltage profile for a rural line according to PV distribution along the line is investigated. The Increment of Power (IOP) vs the number of PV systems is plotted. The IOP is defined as (2.9).

$$IOP = \frac{PV_{PVtot(n)} - PV_{PVtot(n=1)}}{PV_{PVtot(n=1)}} \times 100 \tag{2.9}$$

Results show that distributing the total PV power generated across more systems results in fewer voltage rise issues. For the test network, the line voltage is 400/230 V with a cable impedance of R=0.899 Ω/km and X=0.106 Ω/km. It is calculated that the total PV generation capacity the network can accommodate without breaching the upper voltage limit is 63 kW when PV is distributed evenly along the length of the feeder and 36 kW when the all the PV generation is located at the end of the feeder. These findings agree with those in [55].

The study in [58] confirms the influence of line impedance magnitude and line X/R ratio on voltage rise in the presence of PV generation. The voltage at the last household is calculated for a range of PV generation levels, a range of line impedance magnitudes and a constant line X/R ratio. As expected, results show the voltage increases with increased impedance magnitude and with increased PV generation. Also in [58], the voltage at the last household is calculated for a range of PV generation levels, a range of line X/R ratios and a constant line impedance magnitude. Interestingly, results show there is little variation in voltage for the range of line X/R ratios tested. This is due to the power factor of the PV inverter, operating at unity power factor, and the load at 0.95 inductive power factor. Power factors, for both load and PV, further from unity have greater interaction with the line reactance and produce greater voltage excursions. This can be confirmed through examination of the conventional power equation (2.10), where if the strength of Q is small relative to P (in the case of near-unity power factor) then the influence of X on the change in voltage will be minimal.

$$V_x = \left[\frac{V_y^2 + R_{x,y}P_y + X_{x,y}Q_y}{V_y}\right] + j\left[\frac{X_{x,y}P_y - R_{x,y}Q_y}{V_y}\right] \tag{2.10}$$

This is proven in [55], where results show more PV generation (p) is required to give the same increase in voltage (e) as the load becomes more inductive (q). This is due to more inductive load interacting with the line reactance and causing a greater voltage drop.

In [59] an analysis of voltage rise for a residential demonstration area in Ota, Japan is conducted. The demonstration area hosts approximately 2.1 MW of PV generation capacity, composed of 553 residential PV systems. The average PV system size is 4 kW and the demonstration area is approximately 1 km^2. Voltage levels were recorded at each household for a particular day; the line impedance between the household and the pole transformer households were grouped into those which experienced over voltages due to PV generation and those that didn't. A box plot of the line impedance for each group is generated. The plot shows the higher average line impedance for households which experienced over-voltages. It is not stated in the paper whether or not this is an expected result. This research further shows the influence of line impedance on voltage rise due to PV generation.

2.3.1 Summary

The key findings from the literature can be summarised as follows

- It is net load (load demand subtracted from PV generation) that determines voltage rise; therefore load also needs to be taken into account when investigating the relationship between PV generation and voltage levels.
- The distribution of PV systems and loads along the length of a feeder influence voltage rise. If the majority of PV generation is located at the end of a feeder (furthest from the DTx) and the majority of load is located at the front (close to the DTx) then excessive voltage rise is more likely than if load and PV locations were reversed.
- The voltage drop caused by load is strongly influenced by both the load power factor and the *X/R* ratio of the cable. A more inductive load power factor combined with a higher *X/R* ratio will result in a greater voltage drop. A greater voltage drop caused by the load means more PV generation can be accommodated without breaching an upper voltage limit. This discovery is made through an analysis using conventional power flow equations (2.2) and (2.3) in [55]. Evidence of the influence of cable *X/R* ratio on voltage rise is also given in [58]. The power factor of the PV inverter also has as strong influence over the PV systems influence on voltage levels. Studies presented in this section assume unity power factor for their PV inverters so it is not analysed in great detail. PV

inverter power factor influencing voltage levels makes it an effective voltage control technique; Section 2.5 discusses this topic further.

- If the number of PV systems between two points on a feeder are increased linearly, whilst being distributed evenly, to maintain the same voltage rise between the two points the generation from each PV system needs to decrease exponentially. This discovery is also made in [55].
- Considering the voltage rise between two points on a feeder due to an even distribution of PV generation. With a linear increase in the number of PV systems between the two points, to maintain the same voltage rise, the total combined generation for all PV systems increases exponentially. The rate of increase takes the form of an increasing decaying exponential. This discovery is made in both [55] and [57].
- When PV generation is greater than load, the larger the impedance between a PV system and the DTx, the greater the voltage rise between the PV system and the DTx. This discovery is made in both [58] and [59].

2.4 MPVG Estimation Methods

The question "How much PV generation can a section of network or feeder accommodate without exceeding voltage regulation limits?" was raised in Section 2.1.6. This section examines research presenting methods for estimating a PV generation limit.

Relatively simple methods proposed for estimating the maximum allowable Distributed Generation[4] (DG) are proposed in [60] and [61]. In [60], the maximum generation for a line is set to be equal to the typical minimum load, for the entire line, during PV generation hours. The approach is to ensure that no reverse power flow occurs. It also ensures that the upper voltage limit is not exceeded, but no voltage measurements are used in the estimation. In [61], a heavily simplified equation for the maximum

[4] Studies discussed in this section may refer to DG instead of PV generation. DG is any type of generation located at the distribution network level, and consists of not just PV systems but also includes wind turbines, diesel generation and Combined Heat and Power units. Fuel cells and batteries can also be considered a form of DG. A key difference between PV generation, and also wind turbines, and the other types of DG, is controllability. PV and wind turbines are not completely controllable, as they are both dependent upon an uncontrolled resource, sun or wind. Despite this difference, it can be assumed that all studies referring to DG discussed in this section are applicable to PV systems.

allowable generation for a singular PV system installed at the end of a feeder is given (2.11). The equation is designed to ensure that both current and voltage limits are not exceeded, and is dependent upon the tap setting of the STx. All variables, P_{PV}, P_{Load} and S_{Load}, are in pu.

$$P_{PV} = 2 * P_{Load} + (1 - S_{Load}) \tag{2.11}$$

The study found that voltage was more likely to limit PV generation levels the higher the STx tapping and current limits when the STx was tapped lower. Setting the STx midway between the upper and lower voltage limit was found to be a good compromise. This allowed the use of (2.11) to determine the MPVG without breaching either current or voltage limits.

The above two studies, [60] and [61], do not present a method through which true maximum allowable DG generation capacities can be calculated, only a method which ensures voltage limits are not exceeded.

In [62], an expression for calculating the voltage change on LV lines between the front of the line and a singular DG installation point is derived. Line reactance is neglected in the derivation, giving a DC calculation. This does introduce error into the estimation but it is estimated to be less than 4%. The derived equations can be used to calculate the maximum size of the DG (I_{gen}) such that an upper voltage limit (V_{max}) isn't exceeded. The voltage drop (V_{load}), up to point z, due to the cumulative load is first calculated (2.12). Load is distributed along the length of the line. Point z is the distance from the front of the line to the DG installation. The maximum voltage rise ($V_{max} - V_{LV}$) is equated to the difference between the voltage rise caused by the DG and V_{load} (2.13), from which I_{gen} can be calculated. V_{LV} is the voltage at the front of the line and r is the resistance of the line in Ω/m.

$$V_{load} = r\sqrt{3}\int_{0}^{z}\left(\int_{z}^{L} i(z)dz\right)dz \tag{2.12}$$

$$V_{max} - V_{LV} = zI_{gen} \times r\sqrt{3} - V_{load} \tag{2.13}$$

In [63] a Jacobian bus voltage sensitivity matrix is used to determine the voltage change at each bus in a distribution network due to a singular installed DG system. For a singular installed DG unit at any bus the change in voltage (according to its sensitivity) at every bus can then be calculated, this allows for the maximum allowable DG size to be calculated without causing a breach of an upper voltage limit on any bus on the network. The proposed benefit of the method is that repetitive power flow solutions are not required. Although, it still does first require the calculation of the Jacobian bus voltage sensitivity matrix. There is also an estimation error, when compared to the maximum generation calculated using conventional iterative power flow calculation. The error is found to be 3% on average.

The methods presented in the above two studies, [62] and [63], can only be applied to a singular DG installation. An MPVG estimation method should be applicable to situations where a number of DG systems are installed, not just one.

Finally, in [64], a Monte Carlo-based technique is used to assess the impacts of different PV penetrations on LV networks in order to estimate their corresponding probabilistic hosting capabilities. In this study, two networks consisting of four and six feeders are considered where loads, PV location and system size are randomly allocated. Power flow calculations are performed and the percentage of households experiencing voltage issues is identified. Results give percentage PV penetration levels that will cause a particular percentage of households for each feeder to experience voltage problems.

An MPVG estimation method should calculate the MPVG level for each installed PV system. A method which isn't computationally intensive and doesn't require power flow software would also be both more accessible and have less technical barriers preventing its use.

2.4.1 MPVG and Voltage Regulation Limits

A search of the literature on MPVG estimation methods produced a range of studies looking at factors other than voltage regulation limits to determine the MPVG, for example, [60] uses reverse power flow levels and [61] uses both voltage and current limits. In [11], a review on papers examining MPVG are discussed. A summary of the findings is presented in TABLE 2.1 from [11] which gives an estimation of the maximum PV penetration level (%) and its predicted cause.

TABLE 2.1 Summary of factors predicted to limit PV generation levels

Maximum PV penetration level (%)	Cause of upper limit	Electricity network level
5	Power balance - ability of conventional generation to follow PV generation power fluctuations caused by cloud transients	System
15	Voltage regulation – ability to maintain voltage within regulation limits during PV generation power fluctuations caused by cloud transients	Distribution
> 37	Harmonic voltage distortion exceeding regulation limits.	Distribution
1.3 - 36	Unacceptable unscheduled tie-line flows. The variation is caused by the geographical extent of the PV (1.3% for central-station PV). Results particular to the studied utility because of the specific mix of thermal generation technologies in use.	System
10	Frequency control versus break-even costs.	System
Equal to minimum load on feeder	Voltage rise. Assumes no OLTCs in the MV/LV transformer banks	Distribution
< 40	Primarily voltage regulation, especially unacceptably low voltages during false trips, and malfunctions of SVRs.	Distribution
5	This is the level at which minimum distribution system losses occurred. This level could be nearly doubled if inverters were equipped with voltage regulation capability.	Distribution
33 or ≥ 50	Voltage rise. The lower penetration limit of 33% is imposed by a very strict reading of the voltage limits in the applicable standard, but the excursion beyond that voltage limit at 50% penetration was extremely small.	Distribution

Harmonics are mentioned, but previous analysis of harmonics (Section 2.1.3), concluded that it is unlikely to be a concern. On power balance and voltage regulation, whilst there are studies on the impacts, there is little in the literature where it is shown as a determinant for MPVG. This is also the case for distribution system losses. The other impacts mentioned manifest at the system level, which is outside the scope of this thesis. This leaves voltage rise as a key determinant of MPVG at the distribution level. In Australia, the growth in PV penetration levels and their potential impact is recognised by DNOs, and the PV installation assessment process for a couple of DNOs is based on steady state voltage rise [65, 66]. The grid-connected PV inverter standard AS4777 [67] has also been updated recently to better manage voltage rise caused by PV generation. For these reasons, novel research on MPVG estimation method (Chapter 5) is orientated towards voltage rise as the determining factor.

2.5 New Distributed Voltage Management Techniques

The question was raised in Section 2.1.6, "How might the growing range of distributed devices offer new voltage management techniques for mitigating the increase in voltage variability and voltage rise caused by high-penetration DPVG?" This section examines research on new distributed voltage management techniques using distributed devices designed to assist in the integration of DPVG.

Distributed voltage management techniques using distributed devices to assist in the integration of DPVG include PV inverter real and reactive power control and PV panel re-orientation, designed to minimise voltage rise due to PV generation. More complex systems, which incorporate PV inverter control, battery storage and DSM, are designed to not just mitigate PV impacts but also to improve the voltage and power profile.

2.5.1 Real Power Curtailment

The PV inverter is capable of controlling the real power flow from the PV system, curtailed to reduce voltage levels.

An example of active power curtailment only control to mitigate voltage rise is given in [33]. In [33] an active power curtailment strategy to reduce PV power injection during peak solar insolation periods is proposed, this is to prevent violation of upper voltage limits. A large scale PV system installed in a Taipower distribution feeder was selected for testing. The proposed method of actively controlling power generation curtailment shifts the operating point of the PV system away from the Maximum Power Point Tracking (MPPT). The method is shown to be effective at ensuring the upper voltage limit is not exceeded. The key drawback of real power curtailment is reduced revenue.

A solution to the "lost revenue" problem associated with real power curtailment is storage, battery or otherwise, and/or load shifting. Load shifting is where flexible and controllable loads are made active during periods of high PV generation. With storage, the energy stored can be injected into the network at a different time, when there is little risk of excessive voltage rise. The majority of studies looking at real power curtailment therefore also incorporate storage and/or load shifting, these are discussed in Section 2.5.4 and Section 2.5.5.

The above studies show that active power curtailment can effectively mitigate excessive voltage rise but reduces production and hence revenue for the PV system owner.

2.5.2 Reactive Power Control

The PV inverter is capable of controlling the reactive power flow from the PV system. Reactive power can either be injected to increase voltage or absorbed to reduce voltage

A PV system's contribution to voltage rise can also be mitigated through reactive power absorption, with little reduction in real power generation. It may be for this reason that the majority of the literature analyses reactive power absorption for voltage management as opposed to real power curtailment.

The study in [68] provides a good overview on the effectiveness and drawbacks of using PV inverter reactive power flow control to manage voltage. The test distribution network is about 6 miles in length, loads and PV systems are simulated to be located on the secondary side of each DTx at each bus. PV penetration is defined as percentage of load. Load power factor is set to 0.92. For the first test scenario, 50% PV penetration, with PV inverters set to control voltage levels through absorption of reactive power. Results show that voltage levels are kept close to their target voltage 1 pu but at a cost, a total of 1.8 MVAr of reactive power is required to maintain a steady voltage along the length of the primary feeder, around 16% of load.

How PV inverters absorbing reactive power reduces voltage levels can be understood by again looking at the conventional power flow equation (2.15).

$$V_x = \left[\frac{V_y^2 + R_{x,y}P_y + X_{x,y}Q_y}{V_y}\right] + j\left[\frac{X_{x,y}P_y - R_{x,y}Q_y}{V_y}\right] \tag{2.14}$$

When absorbing reactive power, Q is negative and multiplied by the reactance of the line. This results in a negative change in voltage between the two points, and reducing V_x.

The second scenario again has 50% PV penetration, but with PV inverters set to control power factor. Results show that the voltage profile does rise along the length of the primary feeder but levels remain with regulation limits, the advantage is zero reactive power, giving a significant reduction in losses and demand.

The method of control, either for voltage or power factor, isn't described in [68]. For the first scenario it looks as though PV inverter reactive power is adjusted to keep the voltage at the end of the feeder at 1 pu. For the second scenario, the PV inverter ensures that reactive power flow is zero at its PCC. In relation to the first scenario, it should be noted that it isn't necessary to maintain a voltage of 1 pu; this could easily be set to 1.05 pu, the primary feeder voltage limit. A more relaxed upper voltage limit means less reactive power is required to be absorbed. Still, the study does demonstrate both the effectiveness of PV inverter reactive power control at managing voltage levels, as well as the drawbacks.

In [69], a more sophisticated method for managing voltage levels through PV inverter reactive power control is presented. The control method is fully described, unlike in [68], it's also applied to a LV section of line, making it more relevant to Australian conditions. The control method uses $Q(V)$ droop control, Figure 2.8 a), for the PV inverters with the dead-band limit, $limit_a$, see Figure 2.8 b), set according to the equivalent impedance as seen from the PCC of the PV system. As V_{max} is the same for all PV inverters, having a variable $limit_a$ results in a variable droop slope. Therefore, this process is equivalent to setting the $Q(V)$ droop parameters. Also, using the equivalent impedance to determine $limit_a$ is equivalent to using the voltage sensitivity at the PCC, as per [63].

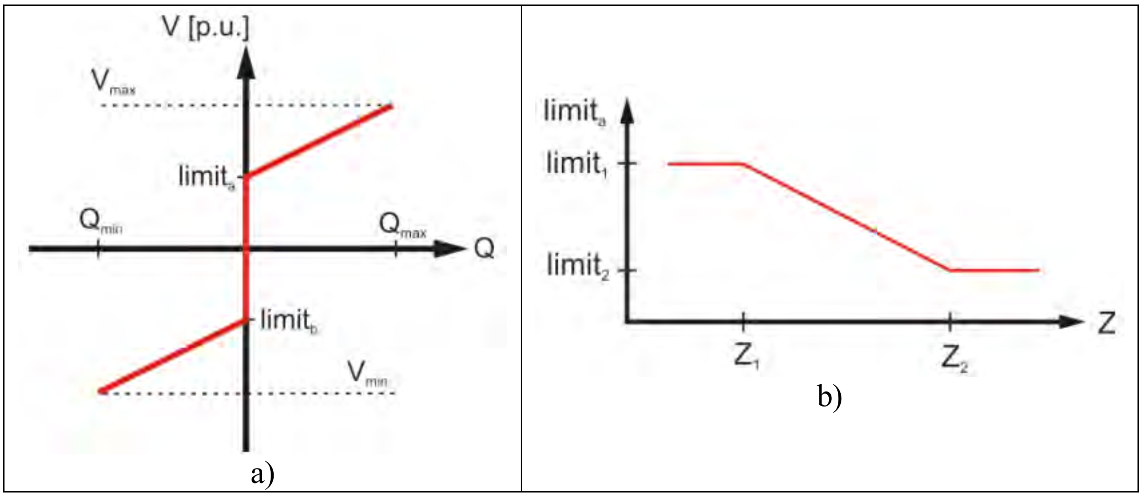

Figure 2.8 a) *Q(V)* droop control characteristics b) $limit_a$ as a function of equivalent impedance [69]

The method proposed in [69] does assume all inverters are in communication, another layer of control also ensures that the end inverter responds to high voltage first, once it has reached its *Q* limit then the next inverter begins absorbing/injecting reactive power and so on. Characteristics of the communication system, data latency for example, are not mentioned. The control method is tested on a semi-rural feeder; PV systems are evenly distributed along the length of feeder. Results show that for a total of 182 kW, a total of 40 kVAr is required to ensure voltage levels do not breach the upper voltage limit of 1.1 pu. The ratio of total reactive to total real power is 0.2. A similar voltage control scheme is proposed in [70]. In [70] all PV inverters are in communication, with each inverter communicating their equivalent line impedance to the others. The inverter with the highest impedance becomes the master and adjusts its reactive power component according to calculation, a proportion of the upper limit voltage and the nominal voltage. Again, PV systems are evenly distributed along the length of the feeder. The control scheme is tested on a LV feeder (230 V). Results show that for an average of 9.7 kW, an average of 2 kVAr is required to ensure the voltage at the end of the feeder does not breach the upper voltage limit. This is a reactive to real power ratio of 0.2, the same as that achieved in [69]. Whilst the same ratio of reactive to real power is required, in [69] this ensures a maximum voltage rise of only 3%, compared to 6% reported in [70].This indicates that the method in [69] is twice as efficient as that proposed in [70].

In [71] and [72], voltage sensitivity is again used. In [71], it is used to determine the parameters of the *Q(P)* characteristic curve for each PV inverter, namely the real power threshold and slope. In [72], the parameters of the *Q(V)* characteristic curve for each PV inverter, are calculated. The difference between [71] and [72] and the other studies mentioned is the necessary communication infrastructure. The methods proposed in [71] and [72] do not require communication between devices, only local measurements of power for [71] and voltage for [72] are required.

Another control method requiring only local measurements and no additional communication infrastructure, is proposed in [73]. In [73] DG modulates its generation to ensure a lower voltage limit is not exceeded at the end of the feeder. The voltage at the last bus is estimated from local readings of power and voltage at the distributed generator, the generator then alters its generation to sufficiently increase the voltage.

The above studies show that reactive power absorption effectively mitigates excessive voltage rise but will also increases line losses. Also, the efficiency of different reactive power absorption measures can vary, with some requiring more reactive power absorption to ensure the same percentage voltage rise isn't exceeded.

2.5.3 Panel Re-orientation

In this section the effectiveness of re-orientating the direction a PV system faces and/or adjusting the tilt to reduce output and therefore voltage rise is examined. The optimum tilt for a PV panel is approximately equal to the latitude angle at its location. The optimum direction a panel faces is south for the northern hemisphere and north for the southern hemisphere. Voltage rise reduction is achieved through two means.

1. Setting a non-optimal tilt angle and/or facing the panels in an east-west direction will reduce the peak PV generation and thus voltage rise.
2. Facing the panels in an east-west direction will also shift the time at which peak PV generation occurs. When it occurs at times of higher load then the net real power injected by the PV systems is reduced, voltage rise is also therefore reduced.

Facing PV panels in an east-west direction can also increase the coincidence of PV generation and peak load demand, thus resulting in peak load shaving and a reduction voltage drop. This coincidence varies according to PV generation and load profiles.

An example of re-orientating PV systems to an east-west direction to reduce voltage rise is given in [74]. The case study demonstrates that the 2.5% voltage rise limit is exceeded when panels are facing south, but not when facing panels are facing east-west. Re-orientation of panels to reduce output does reduce revenue for the PV system owners, and for helping to maintain voltage levels, compensation from the DNO would likely be expected (although of course being constrained down also reduces revenue. In [75], twelve months of PV production data for systems located in San Antonio, Texas, with standard south facing and west-facing orientations is examined. The study finds that west facing systems offset peak load demand. This is also the case for the study in [76], which finds that re-orientating PV systems in Hawaii to an east-west orientation better matches PV generation to peak load demand. Finally in [77], PV tilt angles for Germany are examined. The study shows that tilting PV panels at an angle greater than at latitude results in more generation during winter when load demand is greater, thus improving voltage regulation.

The above studies show that re-orientating panels can reduce voltage rise but at the expense of reduced output and therefore revenue for the system owner. Also, the extent to which voltage rise can be reduced is dependent upon the co-incidence between PV generation and peak load.

2.5.4 PV Combined with Storage and/or DSM

Methods already discussed in this section have PV voltage rise minimisation as their objective, but when PV is combined with battery storage and/or DSM, a smoothing of the voltage and power profile is also possible. For PV combined with battery storage, the battery is charged during peak PV generation times by the PV system and discharged in the evening during peak load demand times. The charging of the battery by PV reduces introduced voltage rise and fluctuation by the PV system and the discharging of the battery during peak load demand times reduces peak demand. A smoothing of the voltage and power profile is the result. For PV combined with DSM, flexible load can be shifted from peak load demand times to times of peak PV generation, again resulting in a voltage and power profile smoothing effect. The studies discussed in this section present voltage management strategies incorporating PV and either battery storage or controllable loads.

In [78], it is claimed that to minimise the introduction of fluctuating power flows into the electricity network, a solution to is to add a storage element to these nonconventional and intermittent power sources. Also, according to [79], energy storage units have long been considered as a means for improved integration of fluctuating Renewable Energy Sources (RES). It is also stated that the specific control law or operation objective makes a significant difference to the specific benefits energy storage may provide. So, PV integrated with battery storage doesn't necessarily mitigate impacts, it depends on the objective of the control strategy. In [78] for example, the PV and battery system are controlled to minimise the electricity costs of the owner.

In [80] an Energy Storage System (ESS) is combined with each PV system to ensure that the upper voltage limit is not exceeded. The method calculates a power set point for each PV+ESS. At the set point, real power from the PV system is diverted to the ESS. The power set point is determined through minimising the objective function (2.15). For a years' worth of load and PV generation data, a power flow calculation is performed, and the minimum value of $\alpha_k P_{PV,k}$ the set point for each PV system, is calculated. $\alpha_k P_{PV,k}$ is the percentage of rated power for each PV system which ensures that the upper voltage limit isn't exceeded on any bus on a test network.

$$f = \sum_{k=1}^{N} \propto_k P_{PV,k} \tag{2.15}$$

A LV residential feeder [81] is used as a case study to test the control method. The feeder is comprised of 7 buses, of which 4 out of 7 hosting PV systems, installed PV capacity is 42.6 kW. The same load and PV generation data is used for testing as was used to calculate the values of $\alpha_k P_{PV,k}$ for each PV/ESS system. Results show the effectiveness of the method at keeping voltages under the upper voltage limit (U_{max}) at bus 7. Under the same test conditions but without the voltage control method, breaches of the upper voltage limit (U_{max}) at bus 7 were recorded [82].

In [83] a charging/discharging strategy for storage devices integrated with rooftop PV is proposed. The strategy is designed to mitigate voltage fluctuation as well as minimise voltage excursion. To mitigate down ramps in voltage when PV is generating, the storage is discharged when a predetermined change in PV generation (dP_{PV}/dt) is detected. To mitigate down ramps when PV isn't generating, the storage is discharged when a predetermined change in voltage at the PCC (dV_{cc}/dt) is detected. To minimise excessive voltage rise, real power from the PV system is diverted to storage when generation exceeds a predetermined set point. To minimise excessive voltage drop, the storage is discharged when the voltage at the PCC (V_{cc}) is lower than a predetermined set point. The proposed strategy is tested on a LV residential feeder, consisting of ten households; each household has a PV and battery system installed. A typical load profile for each household is used and a particularly variable PV profile. The strategy is implemented and the voltage at the last household calculated over a 24 hour period. The voltage calculations show the effectiveness of the strategy at mitigating voltage fluctuation and minimising voltage excursion.

In [84] an energy consumption scheduling algorithm incorporates load shifting to offset voltage rise due to PV generation. At each hour, a control unit located at the household receives the pricing schedule and forecast load and PV profiles. The pricing scheme is an Inclining Block Rate (IBR) pricing scheme, this scheme encourages households to conserve energy. The IBR charges a higher rate for household energy consumption over a certain amount. The objective function, to minimise energy consumption, is solved using a Monte-Carlo technique. The technique involves generating a number of random scenarios, each scenario differs by how the loads are deferred and how the battery is charged and discharged for the coming hour. The scenario with the best solution determines the control strategy for deferrable load and battery charge/discharge over the next hour. The algorithm is tested on a LV distribution feeder consisting of ten households. Deferrable load consists of washing machines, clothes dryers, dish washers and water heaters. It is assumed that 30% of deferrable load is available at any time. Whilst the algorithm isn't designed specifically to control voltage levels, voltage rise minimisation occurs through load shifting offsetting PV generation. The algorithm is shown to be effective at mitigating voltage rise, with the voltage at one household reduced from 1.08 pu to 1.05 pu, the upper voltage limit.

The algorithm proposed in [84] requires comprehensive communication infrastructure, incorporates load and PV generation forecasting, and some complex computing. Whilst it is shown to mitigate voltage rise, voltage control is not its primary objective, and it is possible that voltage levels won't always be maintained within regulation limits. Test results for a number of different load and PV generation profiles are not given.

PV combined with battery storage is shown to effectively ensure voltages can be maintained with limits. The transferal of PV real power to either charge a battery or supply a shifted load has the same positive effect on voltage as real power curtailment but without wasting the generation.

2.5.5 DSM

DSM involves the control of flexible and controllable loads to assist in voltage management. An active load causes voltage drop along a line. A load can be controlled to switch off to minimise excessive voltage drop during periods of high load demand. A load can also be shifted, to be active whilst DG is generating, to minimise excessive voltage rise. This section discusses studies proposing DSM techniques to manage voltage levels.

In [85], a simplified test network is used to demonstrate the effectiveness of load control to manage voltage levels. The test network includes a 300 kW wind turbine with load distributed across ten busses. The wind turbine is located mid-way along the feeder. The simulation conducted is an idealised one, operating under the conditions that load can be switched without delay and there is also sufficient load available to be switched. The simulation also assumes communication infrastructure exists between all loads and the wind turbine. Results compare the voltage at the wind turbine PCC with and without load control, and show the effectiveness of DSM. This is to be expected under such ideal operating conditions.

In [86] a comprehensive voltage management strategy incorporating DSM is proposed. The proposal assumes a communication infrastructure such that the DNO has knowledge of all bus voltages, OLTC tap position and can send control signals to all participating loads. In the event of a voltage breach at a bus, loads are switched off to bring voltage levels within regulation limits. Loads to be switched off are selected according to the outcome of an optimisation problem, designed to minimise the number of loads switched off. Included in the optimisation problem is the relative voltage sensitivity between loads and the target bus and load availability constraints. When load alone is not sufficient to regulate the voltage, the OLTC is adjusted.

In [87] the possibility of sending two control signals to end users to address a large change load variation is assessed. One signal is to an interruptible load and the other is to a DG unit. The control signal would interrupt the load if currently operating in "interruptible" mode, and might also activate the DG unit if power is available. The DG considered in the paper is a micro Combined Heat and Power (CHP) unit. Signal control is based on a cost of energy minimisation function to the DNO. Using emergency load scenarios for stress testing, the study finds that interruptible load alone is not sufficient to maintain load variation within required limits and dispatchable generation is also necessary.

In [88] a scheme involving direct control of Electric Water Heaters (EWH) is proposed so that peak network imports to, and exports from, the controlled area are minimised. This objective is achieved by shifting heating periods to times with high levels of generation from the local energy sources. The scheme is tested in a LV network hosting high penetrations of PV. The hardware of the scheme is comprised of a central unit for the area being controlled and a control unit in each household. Every 5 min, the power balance for the area (generated power minus absorbed power), using historical load and PV profiles, is calculated for a selected time horizon. An optimisation problem, based on the predicted power balance, is solved such that the energy imported and exported from the area is minimised. The optimisation problem determines the EWH dispatch signals. Results presented across a four day period show the effectiveness of the scheme at reducing the voltage range. Similar DSM strategies are proposed in [89-92], where control signals are dispatched to distributed flexible loads from a central control device, often under control of the DNO.

All of the studies discussed so far in this section require some form of communication infrastructure, one load control method which doesn't, and uses local measurements only, is proposed in [93]. In [93] the locally read instantaneous voltage is compared to short term and long term moving voltage averages. The difference is input into a PI controller which controls the load demand of a controllable load, which is likely to be a water heater. The control algorithm is designed to minimize voltage fluctuation in the network, and results show its effectiveness at achieving this objective.

The above studies show that DSM is also shown to be effective at mitigating excessive voltage rise. However, in the case of limited available load for shedding, voltage levels may not always be maintained within regulation limits using DSM alone. Also, DSM control objectives are not necessarily voltage related but can still result in positive voltage outcomes.

2.5.6 Summary

The key findings from the literature can be summarised as follows

- Active power curtailment can effectively mitigate excessive voltage rise but reduces production and hence revenue for the PV system owner [33].
- Reactive power absorption is also shown to effectively mitigate excessive voltage rise but also increases line losses [68]. Also, the efficiency of different reactive power absorption measures can vary, with some requiring more reactive power absorption to ensure the same percentage voltage rise isn't exceeded [69, 70].
- Distributed voltage management techniques, including all types mentioned in this section, can be categorised according to the communication infrastructure necessary to implement the control. Communication infrastructure requirements can be categorised as follows
    1. None, where local measurements only are required.
    2. Communication between DG units.
    3. Communication between DG units as well as with a central control device.
    4. Communication between DG units, a central control device and also the DNO.
- DSM is also shown to be effective at mitigating excessive voltage rise, in the case of [85], no breaches of the upper voltage limit occur over the test period. However, in [85] it is assumed that load is always available for shedding. In the case of limited available load for shedding (or shifting), voltage levels may not always be maintained within regulation limits using DSM alone [86]. This is also shown to be the case in [87], although the DSM objective in [87] is not to maintain voltage levels but to offset fast changes in load.
- DSM control objectives are not necessarily voltage related but still result in positive voltage outcomes. In [87] the objective is to offset fast changes in load while in [88] it is to minimise the energy import/export from the control area. The beneficial side-effect of [87] is reduced voltage fluctuation and in [88]

reduced voltage excursion. This is also the case for PV combined with storage or DSM [83, 84].

- PV combined with battery storage is shown to effectively ensure voltages can be maintained with limits [80]. The transferal of PV real power to either charge a battery or supply a shifted load has the same positive effect on voltage as real power curtailment but without wasting the generation.
- Facing PV panels in an east-west direction can increase the coincidence of PV generation and peak load demand, reducing voltage drop during the peak load demand period. This coincidence will vary according to PV generation and load profiles [74]. Adjusting the tilt angle can also be beneficial, in [77] it is shown that adjusting the tilt angle results in more PV generation during winter when load demand is greatest, although of course this applies only to contexts where winter heating demand exceeds summer cooling demand.

3 Research Objectives and Thesis Methods

This chapter presents the knowledge gaps identified in the literature reviewed in Section 2.2, 2.4 and 2.5, hence specific research objectives, and then describes the method by which they are addressed in the thesis. The limitations in current DNO PV installation assessment processes are also considered in the methods development. Also argued are the limitations in current DNO PV installation assessment processes. The chapters presenting these novel thesis methods are introduced at the end of each section.

3.1 Characterisation of PV Generation Variability

3.1.1 Knowledge Gaps

Characterisation knowledge gaps identified in the literature reviewed in Section 2.2 are presented in this section.

Cloud conditions determine PV generation variability, cloud conditions are weather dependent, and weather varies throughout the year according to season.

1. A complete characterisation should cover the entire year, unlike [50], and also be broken up according to season, unlike [48].

As load demand varies throughout the day, so does PV generation variability. PV generation variability in the middle of the day will likely be greater than in the mornings or the evenings. Downward ramps would be more likely in the evenings and upward ramps more likely in the mornings.

2. It is necessary for a characterisation to be split according to hour to capture the change in PV generation variability which occurs over the course of the day. Paper [50] does characterise the PV generation according to hour for each month. However, the PV generation data set is derived from the clearness index, with a resolution of an hour, a higher resolution is required to instructively characterise hourly PV generation variability. This point is discussed further in knowledge gap 3.

The majority of the literature only investigates PV variability for time frames of 1 min or more. For the analysis in [48], the highest sample resolution is 1 min, and it is stated in [48] that higher resolution data would be needed to accurately determine the impact of high-penetration PV generation variability on grid stability. Also identified was the need to examine PV generation variability at shorter time frames as cloud transients can produce significant changes in PV generation within seconds.

3. The dataset used for the characterisation should have a sufficiently high sample resolution, no more than 10 s, to pick up changes in PV generation due to cloud transients and accurately determine the impact on grid stability.

As noted in knowledge gap 2, a complete characterisation should cover the entire year, and also drill down to the hourly level, to accurately characterise PV generation variability. This detail of characterisation also needs to be applied to a cluster of small-scale PV system, where their generation variability is considered in aggregate.

4. The same detail of characterisation described in knowledge gaps 1 and 2 should also be applied to a cluster of small-scale PV system, where their generation variability is considered in aggregate.

The majority of existing research examined performs characterisations using PV generation data derived from either insolation measurements or from satellite measurements. Ideally, when possible, the PV generation dataset should be obtained from actual PV system measurements; data of this type gives the most accurate representation of PV generation.

5. To produce the most accurate characterisation, the PV generation dataset should be obtained from actual PV system measurements.

The majority of the research focuses on fixed tilt PV systems, and those that do examine tracking PV systems do not perform a characterisation to the detail described in knowledge gaps 1 and 2.

6. This same detail of characterisation described at knowledge gaps 1 and 2 also needs to be applied to tracking PV systems

3.1.2 Methods

A comprehensive PV generation variability characterisation is one which addresses characterisation knowledge gaps 1-3 and 5. The research presented in Section 4.1 and Section 4.2, in combination, both address the above characterisation knowledge gaps identified from the literature and demonstrate a more complete and comprehensive characterisation of PV generation variability.

Single PV System: In Section 4.1 a characterisation of PV generation variability is conducted for a number of different PV technologies and tracking type including fixed-tilt, single-axis and dual-axis tracking PV system. The data used for the characterisation is taken from PV systems located at DKASC. The data is actual measured PV generation data, has a sampling resolution of 5 min and covers an entire year. The characterisation is split according to season, week and hour. This research addresses characterisation knowledge gaps 1, 2, 5 and 6.

Cluster of Distributed PV Systems: In Section 4.2, high resolution PV generation data is used to characterise the PV generation variability for a cluster of small-scale PV systems. The PV generation data is obtained from actual PV system measurements. The characterisation concentrates on variability hour to hour, and also categorises the analysis according to day type. Day type is defined according to cloud cover: sunny, partly cloudy and majority cloud. It also investigates aggregate generation variability. This research addresses characterisation knowledge gaps 2-5.

3.2 MPVG Estimation Methods

3.2.1 Knowledge Gaps

MPVG knowledge gaps identified in the literature reviewed in Section 2.4 are presented in this section.

There are a number of relevant studies [94-98] whose content has not been reviewed in Section 2.4 as they do not propose a method as such for estimating the MPVG. These studies undertake an investigation into the voltage impact of high-penetration PV. They all use test networks, case studies, with particular load and PV arrangements, to make their findings. It is possible to approximate the MPVG from the analysis, but the approximation could only be applied to the test network or ones similar, under similar PV and load arrangements. It would be difficult to apply the findings of these studies to estimate the MPVG for a range network configurations and PV and load arrangements. The study conducted in [58] is also on the voltage impact of high-penetration PV, but a comprehensive one. For varying levels of residential PV penetration, voltage level dependency on load levels, line impedance, DTx impedance and PV distribution is determined. Due to the comprehensive nature of the study, the results could be analysed and a rough MPVG estimate for other LV feeders with similar parameters, load and PV arrangements could be made. But this approach would be considered “rule of thumb” only, with uncertain levels of accuracy.

1. An approximation of the MPVG only can be derived from high-penetration PV voltage impact case studies. Also, an approximation derived from a case study has limited application under different network conditions. From comprehensive impact studies, performed under an extensive range of network conditions, only a “rule of thumb” MPVG method can be derived, with uncertain levels of accuracy.

The approaches in [60] and [61] give an estimate which safely ensures voltage limits are not exceeded, but is not calculating a true “maximum”. The approach would likely result in an estimate smaller than one which uses voltage limits.

2. A MPVG estimation method should calculate a true maximum, not just provide a method which ensures voltage limits are not exceeded.

Methods proposed in [61], [62] and [63] calculate the Maximum Allowable DG generation (MADG) for just a singular installation. For [61], this singular installation is assumed to be at the end of the feeder. For the situation most prevalent in Australian, a large number of small-scale LV distributed PV systems; these methods would be applicable for only a small number of scenarios.

3. A MPVG estimation method should be applicable to situations where a number of PV systems are installed, not just one.

The research presented in [64], a Monte Carlo-based technique, can be applied to any network with any number of PV systems installed. One drawback of the method is that it does not calculate a probabilistic MPVG for each household, only for a particular PV penetration level, which is the percentage of houses with a PV system installed. The method is also computationally intensive, requiring power flow analysis software (OpenDSS) and a comprehensive load data set.

4. An MPVG estimation method should calculate the MPVG level for each installed PV system. A method which isn’t computationally intensive and doesn’t require power flow software would also be both more accessible and have less technical barriers preventing its use.

3.2.2 Limitations in Current Industry Practise

The limitations in current DNO PV installation assessment processes are presented in this section.

Looking at current industry practise in Australia, the assessment process DNO’s undertake when a new PV installation application is received varies. Some allow PV installations only up to a set limit [99] while others set a limit based on DTx capacity [100], [101]. DNO’s experiencing greater PV penetration levels are generally more thorough, Ausgrid for example assesses each PV system to determine if “the contribution of the proposed PV installation to the steady state voltage rise on the LV distribution mains between the Point of Common Coupling (PCC) and the DTx is greater than 1% of the nominal voltage, and if the steady state voltage rise on the distributor due to all embedded generation connected is greater than 2% of the nominal voltage” [65] and if so network augmentation will be required. Ergon also undertakes a network impact assessment, but only if the PV system size is greater than 3.5 kVA [66].

5. Setting a hard limit or not assessing PV systems under a certain size has a number of shortcomings; it does not take into account the number of systems installed, their location on the LV feeder or the feeder characteristics. It can either result in excessive voltage rise or an under-utilisation of the LV feeders PV hosting capacity.

6. Setting a limit based on transformer capacity is also not ideal; DTx sizing is calculated using load demand, not DG.
7. The approach used by Ausgrid also has its limitations; a set percentage voltage rise does not take into account the DTx tap setting, a key factor when determining PV system size limits based on voltage rise. It is also iniquitous, allowing residents closer to the DTx to have larger systems compared to residents located further from the DTx, and favours early installers of PV systems.
8. The approaches currently employed by Australian DNOs when assessing new PV installation applications could therefore be more sophisticated. As stated in [102] "There is a growing need for tools to assist DNOs in managing this increase in PV penetration". A DNO could conduct a power flow calculation to determine a PV generation limit, but only for that particular network case and assumed load and PV profiles. A DNO's network typically consists of a wide range of feeder types and performing a separate power flow calculation to determine the PV generation limit for all cases where PV is being deployed would be a large and costly exercise.

3.2.3 Methods

The research presented in Chapter 5 addresses the above MPVG knowledge gaps identified in the literature and the limitations in current DNO PV installation assessment processes. The methods derived in Chapter 5 are "tools" designed to estimate the MPVG for a range of feeder configurations and PV and load arrangements. The tools proposed could relieve the need for the DNO to perform dedicated power flow calculations in every instance, and make strategy development for managing PV on their network easier.

A MPVG Estimation Method for Evenly Distributed PV Generation and Load: In Section 5.1 an examination into the relationship between MPVG, feeder characteristics and load conditions is conducted. The MPVG is determined by an upper voltage limit. For a range of feeder characteristics and load conditions, results are obtained through power flow calculations using DIgSILENT. The study assumes a number of simplifying conditions including evenly distributed PV generation and load, cable reactance of zero and load and PV system operating at unity power factor. General relationships are identified through analysis of the results, primarily though graphical means, and an innovative method developed for deriving the MPVG. The research presented in Section 5.1 is a first step attempt to address MPVG knowledge gaps 1-4 and limitations 5-8 in current DNO PV installation assessment processes.

A Comprehensive MPVG Estimation Method for Residential LV Feeders: An original method for calculating the MPVG is also presented in Section 5.2, but is more sophisticated than that proposed in Section 5.1. The method is derived analytically and can be easily implemented in spreadsheet software; no power flow software is required. The method presented in Section 5.2 can potentially be applied to a DNOs entire distribution network and more completely addresses MPVG knowledge gaps 1-4 and limitations 5-8 in current DNO PV installation assessment processes.

3.3 New Distributed Voltage Management Techniques

3.3.1 A Balanced and Practical Approach to Distributed Voltage Management

The limitations in current industry practice in relation to a balanced approach to distributed voltage management are argued in this section. A critique of the literature reviewed in Section 2.5 in relation to a balanced and practical approach to distributed voltage management is also included.

In Australia, DTx tap settings are typically set high to accommodate voltage drop associated with peak load demand. However, the high tap setting reduces the capacity for voltage rise in LV lines. If DTx tap settings were lowered then the capacity for voltage rise in LV lines would be increased and the need for PV inverter reactive power absorption and real power curtailment could potentially be reduced. Lowering DTx tap settings does increase the risk of low voltage limit breaches but it may not be significant. A recent report from an Australian DNO operating in Queensland [103] supports this argument, finding that 75% of their DTx taps were set too high. Furthermore, the risk can also be mitigated through load shedding. Heating and cooling is a large contributor to peak load demand (typically 40% of total household demand [104]) and is increasingly being provided by air-conditioning units [105], making them a good candidate for load shedding. The introduction of demand management programs for air-conditioners by one Australian DNO [106] supports this suggestion. Voltage deviations due to PV systems are under particular scrutiny, unlike similar, but negative, voltage deviations due to air-conditioning units. Air-conditioning units should therefore also contribute to the voltage management solution.

1. New voltage management approaches proposed in the literature are focussed largely on minimising the impacts of PV generation. They should instead look at voltage management requirements as a whole, with the objective of minimising voltage excursion generally, not solely voltage rise due to PV generation. Voltage management requirements can be identified through voltage impact studies, such as those conducted in [33, 35, 58].
2. A voltage impact study could also simulate a number of voltage management solutions, from which the most appropriate, possibly a combination of solutions, can be selected. This is taking a more balanced approach to distributed voltage management instead of assuming it is solely the problem of PV generation which needs to be solved. It may be that an impact study finds that adjustment of the DTx tap setting combined with air-conditioning unit load management is the most appropriate solution.
3. The majority of control schemes proposed in the literature [68-70, 85-92] also require extensive communication and control hardware, along with the scrutiny of load and PV profiles either before and/or during operation for the control algorithm to be executed. Whilst an extensive communication network is likely required as part of the transition to an electricity network dominated by distributed generation; it requires large infrastructure investment and significant operational change. This is still a time away in Australia.

Voltage management knowledge gaps 1-3 define the context in which new methods for distributed voltage management are being developed, one which does not examine voltage management needs as a whole and often requires extensive communication infrastructure.

3.3.2 The Practicality, Efficiency and Equality of Proposed Distribution Voltage Control Methods

The capability of distributed voltage control methods proposed in the literature (Section 2.5) to manage voltage levels under three guiding principles are examined in this section.

The approach is taken that distributed voltage control methods should operate under the following principles

a) Control methods should not require measurements beyond that which can be taken locally, meaning no communication infrastructure. An investigation into the effectiveness of less complex approaches, without investment in communication infrastructure, which can give immediate support to the growth of DPVG in our network, is justified.
b) Distributed voltage control should reliably ensure voltage limits are not exceeded with minimum intervention. Intervention refers to the act of controlling a generating source.
c) Intervention should be fairly distributed amongst households, according to their net load (source or sink) contribution.

Voltage management knowledge gaps in proposed distributed voltage control methods reviewed in the literature (Section 2.5) were identified by assessing their capability to manage voltage levels under the above principles

4. Studies [68-70, 85-92] all require some form of communication infrastructure; this is in breach of principle a)
5. Relevant studies which don't require communication infrastructure include [71-73] and [80]. The drawbacks of these approaches are argued in the following points.
6. According to principle b), *Q(P)* control [71], and methods using power set point only control do not minimise intervention whilst ensuring voltage levels are kept within limits. Solely using *Q(P)* or power set point only control results in unnecessary absorption of reactive power, occurring when a PV system generates power over its threshold despite voltage levels being at acceptable

levels. Unnecessary diversion of PV real power to battery also occurs when using power set point only control [80].

7. The drawback of using *Q(V)* control [72] is it doesn't necessarily distribute intervention fairly across households, principle c). A PV system generating large amounts of power relative to its neighbours will push the voltage level up for everyone, forcing intervention regardless of their net load contribution.
8. In [73], the control system is shown to be effective when employed to manage voltage drop, but would have drawbacks when employed to manage voltage rise where there is more than one distributed generator. In this case, the estimation of voltage at the end of the feeder assumes that all generation is located at the end of the feeder, when this is not case, the voltage at the end of the feeder would be over-estimated and the reduction in generation excessive, this is in breach of principle b).

3.3.3 Methods

A Balanced Approach to Distributed Voltage Management: The research presented in Section 6.1 addresses voltage management knowledge gaps 1-3. In Section 6.1, a high-penetration PV case study is presented, where a probabilistic voltage and household impact analysis is conducted for a number of voltage management options. A typical LV feeder with high penetrations of PV is used for the case study. The objective of each option is a minimisation of voltage excursions, both higher and lower. The voltage management options simulated require no additional communication infrastructure. The results of the analysis are examined to select the most appropriate voltage management solution, which most effectively minimises voltage excursion as a whole. The study demonstrates a balanced approach to distributed voltage management.

A Practical Distributed Voltage Control Method to Ensure Efficient and Equitable Intervention of Distributed Devices: The research presented in Section 6.2 addresses the voltage management knowledge gaps 4-8. In Section 6.2, an original distributed voltage control method is proposed. The method controls PV inverters to ensure an upper voltage limit is not exceeded and controllable loads to ensure a lower voltage limit is not exceeded. Air-conditioning units are considered the most appropriate controllable load. The same method can be applied to both PV inverters and controllable loads. The method uses both a voltage and a power set point for control; this ensures both a minimisation of intervention and a fair distribution of intervention among PV inverters and controllable loads. Local measurements only are required to implement the control method.

4 Comprehensive Characterisation of PV Generation Variability

Original research by the author presented in this chapter addresses the characterisation knowledge gaps defined in Section 3.1.

4.1 Single PV System

The research presented in Section 4.1 is based on the authors journal paper “Comparative Analysis of the Variability of Fixed and Tracking Photovoltaic Systems”, published in Solar Energy [3].

4.1.1 Introduction

As noted in Section 3.1.2, Section 4.1 presents a characterisation of PV generation variability is conducted for fixed-tilt, single-axis and dual-axis tracking PV system. The characterisation is performed over a year and is categorised according to season, week and hour. The data is actual measured PV generation data. As all PV systems included in the study are in close proximity, therefore experiencing the same insolation, a comparison in variability for the different PV system types is also possible. The research presented in Section 4.1 addresses characterisation knowledge gaps 1, 2, 5 and 6 defined in Section 3.1.

Research characterising the variability of PV generation has generally been associated with a high-penetration PV impact analysis. Typically the PV generation profile used for the impact analysis is presented but without an associated analysis of its dynamic behaviour, for example, [29],[42-44],[45, 46],[107-110]. Such a dynamic characterisation might include, for example, how the level of PV generation variability changes over the course of a day or season, ramp rates, temporal and spatial correlation and variability across different time scales from seconds to minutes and hours.

PV generation exhibits marked daily and seasonal cycles. It also exhibits potentially considerable variability within these cycles depending on the weather and, particularly, cloud cover. The actual operational characteristics of particular PV systems therefore depend greatly on these conditions at their particular location. However, they will also be impacted by other design and engineering choices including the technical specifications of key equipment such as the PV panels and system size, and its spatial arrangement. A particular issue is the orientation and tilt of fixed panel systems, and the potential use of tracking mechanisms or concentrator systems. Tracking systems orient the PV panels so that they follow the sun across the sky over the day. Concentrator systems orient reflecting surfaces towards the sun in a similar manner, but then concentrate this direct solar insolation onto the PV cells. The overall amount and general daily and seasonal timing of PV generation is, naturally, of key interest to PV system owners and operators as well as other electricity industry participants. This has been a key consideration in the choice between fixed and tracking systems given the greater generation during morning and evening periods of tracking systems, yet also their greater complexity and cost [111].

The research presented in Section 4.1 utilises data from a unique PV test facility located in Central Australia, The Desert Knowledge Australia Solar Centre (DKASC), to investigate and characterise the relatively short term (5 min sample resolution) variability of a range of PV systems including fixed tilt, tracking and concentrator system configurations. As the systems are all located on the one site, they experience the same solar insolation, hence supporting direct comparison of the performance of different technologies. The desert climate at the site includes both dry and wet seasons, hence well differentiated periods of generally low and high cloud cover. 5 min PV generation data is available for each system over a period of up to three years. The research characterises and compares the 5 min variability for the different system configurations by hour and season in order to better understand their possible implications for power system operation over these time scales.

A description of the DKASC site and the different PV system types is given in Section 4.1.2. Section 4.1.3 describes the different methods utilised to develop the PV variability characterisation. Section 4.1.4 presents the findings from the methods described in Section 4.1.3. Section 4.1.4 discusses the results and Section 4.1.5 gives concluding comments.

4.1.2 PV Test Systems at DKASC

DKASC is located in central Australia in the town of Alice Springs. 5 min generation

PV generation data is available for 21 PV systems of varying technologies and configurations, sized between 2-30 kW, located at one site at the edge of the town. Alice Springs has a desert climate with very little rainfall and largely clear skies during the dry season and therefore comparatively little generation variability in the PV systems due to cloud cover during that period. What rainfall there is generally occurs between November and February during the wet season with corresponding common cloud cover, and hence increased PV generation variability. The difference in cloud cover between the wet and dry season allows for an interesting variability comparison between the two seasons. Of particular value to this research project, the site allows comparison of system performance across a range of fixed, tracking and concentrating PV systems. The systems analysed consist of sixteen fixed tilt systems including amorphous, hybrid, thin film, polycrystalline and monocrystalline panels, one single-axis tracking system, three dual-axis tracking systems and one concentrating system. See TABLE 4.1 for details of these systems. The PV generation data used for the analysis consists of time synchronised, 5 min average kW samples for the years 2009-2011. It should be noted that not all systems have a full three years of data depending on the date of their installation and installed instrumentation.

TABLE 4.1 List of PV Systems at DKASC

Manufacturer	Material	Size (kW)	Tracking
BP Solar	Polycrystalline	4.95	None
First Solar	CdTe Thin Film	6.96	None
Kaneka	Amorphous	6	None
Sunpower	Monocrystalline	5.805	None
BP Solar	Polycrystalline	4.95	None
BP Solar	Monocrystalline	5.1	None
Trina	Monocrystalline	5.25	None
Kyocera	Polycrystalline	5.4	None
Sanyo	Heterojunction with Intrinsic Thin Layer (HIT)	6.3	None
Sungrid	Monocrystalline	5.04	None
Sungrid	Polycrystalline	5.04	None
Evergreen	Polycrystalline	4.92	None
Calyxo	CdTe Thin Film	5.4	None
Q-Cells	Upgraded metallurgical grade (UMG) silicon	5.85	None
Q-Cells	Polycrystalline	5.64	None
Q-Cells	Monocrystalline	5.64	None
Kyocera	Polycrystalline	5.4	Single axis
ADES	Unspecified	26.52	Dual-axis
DEGERenergie	Monocrystalline	31.5	Dual-axis
Kyocera	Polycrystalline	5.4	Dual-axis
Solfocus	High efficiency "triple junction" cells	16.8	Dual-axis concentrating

Figure 4.1 illustrates the different generation profiles of fixed orientation versus dual-axis tracking systems at DKASC over a particular day. In this case both systems use the same Kyocera polycrystalline technology and are rated at 5.4 kW. It is clear that tracking systems provide a greater overall generation than fixed tilt systems under such conditions, with the difference in generation occurring during the mornings and afternoons due to the more appropriate orientation of the panels on the tracking system as it follows the sun across the sky. Single axis tracking systems follow the sun from East to West at a fixed tilt angle to the horizon while dual axis systems also track the sun's height about above the horizon. Concentrating systems also track the sun whilst concentrating the sun's Direct Normal Insolation (DNI) on to a small yet highly efficient PV panel [112].

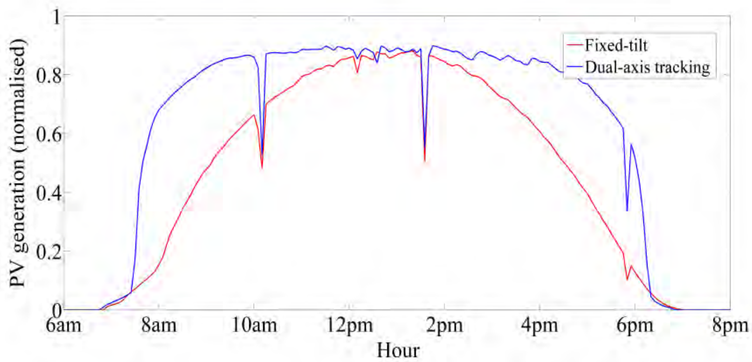

Figure 4.1 PV generation profile comparison for a dual-axis and fixed-tilt PV system at DKASC during a sunny day with only two brief periods of cloud. Both systems use polycrystalline Kyocera panels and are rated at 5.4kW

Different patterns of clouds for different positions of the sun in the sky can have very variable and somewhat surprising impacts on the total amount, and proportion of DNI versus diffuse insolation arriving on PV panels of different orientations. In this study the authors seek to characterise such differences through analysing real system generation data for a range of PV systems located at the one site and hence experiencing largely the same insolation. As an example, Figure 4.2 gives the different PV generation profiles of fixed, tracking and concentrator systems for a highly variable solar insolation day at DKASC. The generation profile of the concentrating system is clearly very different to that of the other systems, with generation often dropping to zero during periods of cloud cover while the other systems maintain at least some level of generation.

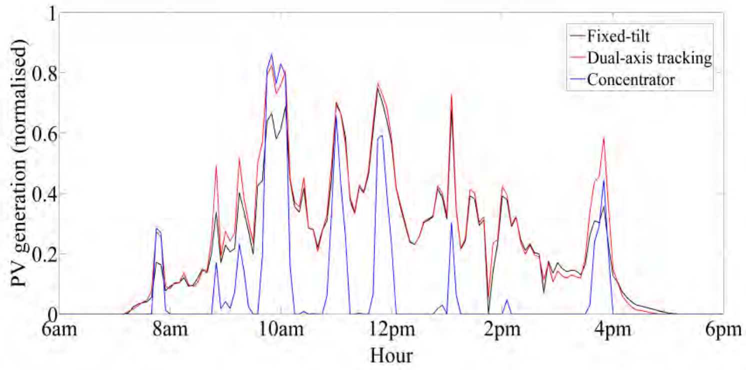

Figure 4.2 Plot of concentrating, dual-axis tracking and fixed tilt PV system generation at DKASC over a particular day highlighting the greater variability and reduced generation of the concentrating system during periods of cloud cover, and hence reduced DNI

4.1.3 Method

The time synchronised 5 min average kW data for all PV systems is publicly available and was downloaded from the DKASC website as a CSV file. The data was then cleaned (see Section 4.1.3.1) and imported into Matlab with all data analysis executed using that software. The following sections describe a number of procedures developed for this research to concisely summarise the variability of PV generation for the systems.

4.1.3.1 Data Clean-up

Data for all systems is time-synchronised, for occasions where small amounts of data was missing the values for the same times from the previous or following day were inserted. A generation of zero was assigned to larger sections of missing data – this data is later filtered out and doesn't contribute to the variability analysis.

4.1.3.2 Normalisation

As each system is of a different size, the data set for each system had to be first normalised. Normalisation was done against the rated capacity specified by the system installers, typically installed PV panel capacity, of each system.

4.1.3.3 Generation Variability

The shortest time period possible for assessing generation variability was, of course, five minutes given the five min data. Generation variability data sets were constructed from the normalised data sets by shifting each PV system data set forward by a single 5 min time sample and then subtracting the shifted data set from the non-shifted. This resulted in a new data set, consisting of 5 min percentage change in PV generation values relative to the rated capacity.

4.1.3.4 Month v Hour Generation Variability Surface Plot

Using the absolute value of the variability data sets, from this point the data is grouped into fixed, single-axis, dual-axis and concentrating data sets. The data sets were then grouped by month. Finally, the mean 5 min variability for each hour of each month was calculated. It was considered that the month versus hour surface plot gives a good indication of how climate and seasons impact on generation variability profile of PV systems. Figure 4.3 below gives a schematic of the process for fixed systems.

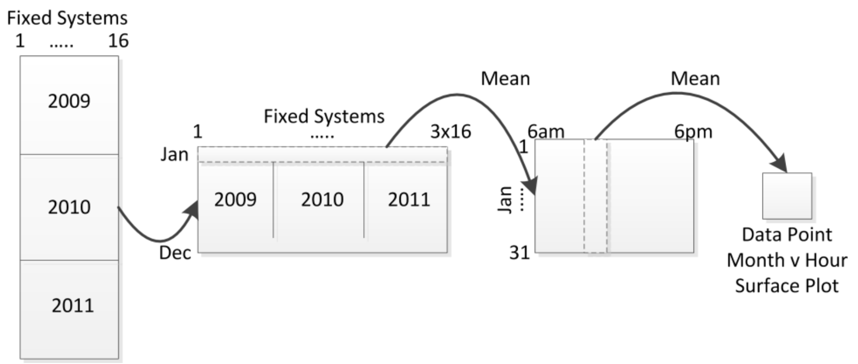

Figure 4.3 Procedure for resolving data point for month v hour generation variability surface plot

The last step in this process involves a degree of curve smoothing, where each data point is set to the value of the mean of the 3 point average in both the x-axis direction (month) and y-axis direction (hour). This method is also repeated to create a magnitude surface plot, where the normalised magnitude is used instead of the variability.

4.1.3.5 Monthly and Hourly Generation Magnitude and Variability

For each system type, the data to create the Month v Hour surface plots is used to calculate the monthly and hourly magnitude and variability. The 5 min mean of the variability and magnitude for each month and each hour is taken to achieve this. Equations (4.1) and (4.2) define this process for variability

$$V_M = \frac{(\sum_{h=1}^{H} V_{mh})}{H} \tag{4.1}$$

$$V_M = \frac{(\sum_{m=1}^{M} V_{mh})}{H} \tag{4.2}$$

Where

V_M is the mean variability for a certain month m

V_H is the mean variability for a certain hour h

H is the total number of hours

M is the total number of months

m is the month

h is the hour

4.1.3.6 Weekly Scatter Plot with Mean

For a particular technology, all the 5 min variability data points from the variability data set are collected, the 16 fixed-tilt variability data sets for example. The data for a particular hour is then extracted. The data for this particular hour is then grouped into weeks producing an array consisting of 52 columns. In the case of 16 fixed-tilt systems, there are 4032 rows; given there are 12 individual 5 min samples in one hour, 7 days in a week, 3 years and 16 systems. All zero values are then removed. Two individual five-min weekly variability means are then calculated, one for all the negative data points for each week and one for all the positive data points.

4.1.3.7 Histogram

The final analysis step is a magnitude and 5 min variability analysis for any particular month and hour. A histogram is used to achieve this. A histogram is a function that counts the number of observations that fall into each value range, known as bins. A mathematical definition is given below (4.3)

$$n = \sum_{i=1}^{k} m_i \tag{4.3}$$

Where

n is the total number of observations

k the total number of bins

i represents a value range

m_i is the number of observations that fall within the value range of i

Looking at the variability histogram, all values are between -1 and 1 and a bin size of 0.025 is used. The same is done for the magnitude except that a bin size of 0.01 is used. For a particular technology, all the 5 min variability data points and the normalised magnitude data points are collected. The data points for a particular hour during a particular month are then extracted. These data points are then assigned to a bin and the histogram developed.

4.1.4 Results

The aim of this analysis is to characterise PV generation variability across different time frames. PV systems located at the DKASC include fixed tilt, single-axis and dual-axis tracking as well as a concentrator system; a comparison in PV generation variability is therefore also possible. The first graph Figure 4.4 gives an indication of how tracking systems can be more variable than fixed system. The red plot is for tracking systems (1 single and 3 dual) while the blue plot is for a cluster of fixed tilt systems. This weather on this day is likely to have been overcast as the ramp up in the morning and ramp down in the afternoon for both types of systems is similar. If the weather was fine then the tracking systems would have far steeper ramp gradients. An overcast day can also be assumed as the spikes in generation are up instead of down, indicating a gap in the clouds as opposed to a passing cloud in a clear sky. Looking at the spikes at around 6:45am, 7.30am and around 5pm it is clear how much more a tracking system can vary during the morning and evening periods due to these changes in cloud cover. As expected, with the difference in tilt between the fixed and tracking systems reducing towards the middle of the day, the variation due to changes in cloud cover is much the same over those times.

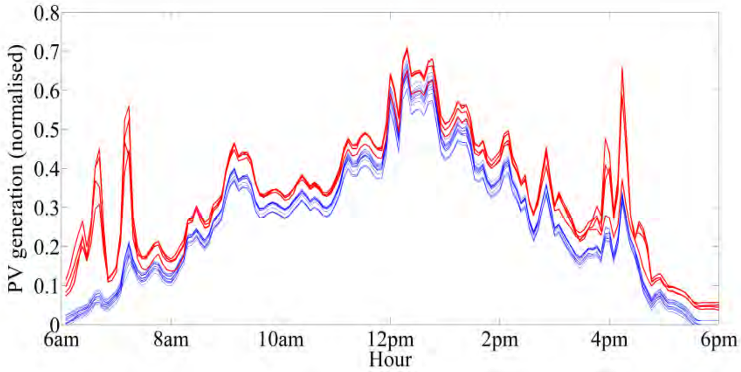

Figure 4.4 Plot showing the PV generation of a number of fixed tilt systems (blue) and 1 single-axis and 3 dual-axis tracking systems (red) over a particular day

The next two figures, Figure 4.5 and Figure 4.6 give a month v hour normalised PV generation surface plot for fixed-tilt and dual-axis tracking systems, created using method *Month v Hour generation variability surface plot* but using normalised PV generation instead of variability. Generation data from all systems was used to produce the figures. These two plots were included to communicate how PV generation varies across the course of the year. The greater generation of the dual-axis tracking systems in the morning and afternoon is made most apparent by the length of the bottom two segments, 6 – 7 am and 7 – 8 am. Looking at December for example, the fixed-tilt system is producing at 0.3 while the dual-axis tracking system is producing at 0.55. The variation in the length of these segments in Figure 4.6 reveal the degree to which the generation for dual-axis tracking systems varies across the year for this time of day, whilst staying relatively constant for fixed-tilt.

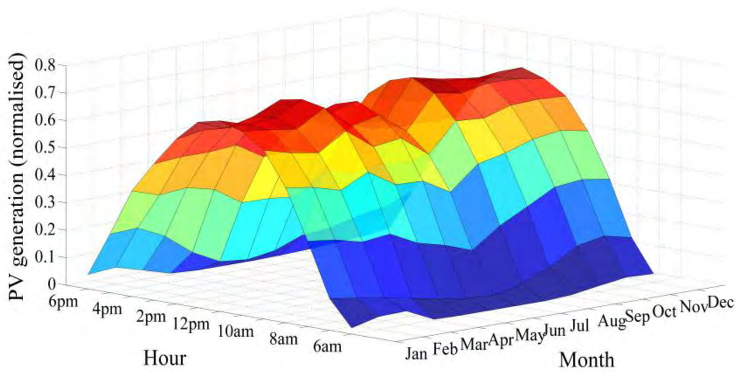

Figure 4.5 Month v hour normalised average generation surface plot for fixed-tilt systems

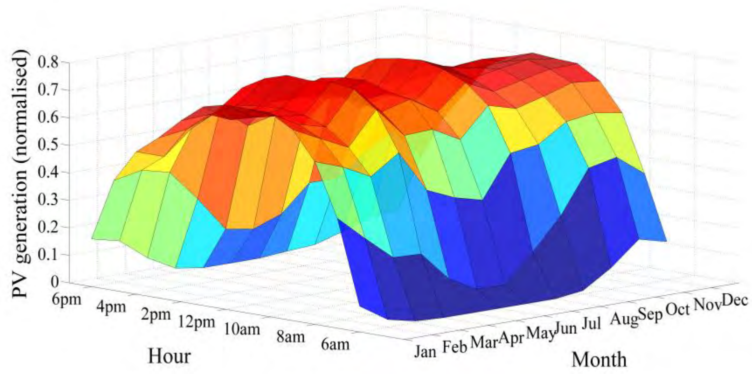

Figure 4.6 Month v hour normalised average generation surface plot for the dual-axis tracking systems

4.1.4.1 Variability Surface plots – Month v Hour

The first set of results presents the month v hour 5 min variability surface plots, these results are obtained through method *Month v Hour generation variability surface plot*, described in Section 4.1.3.4. These plots give a good indication of how the 5 min variability profiles of PV systems vary throughout the year. Plots of this nature may be useful for the electrical industry in assessing the potential variability in network flows, associated power quality issues, and potential supply-demand challenges associated with significant deployment of these different PV configurations. Figure 4.7 and Figure 4.8 below show these plots for fixed-tilt and dual-axis tracking systems.

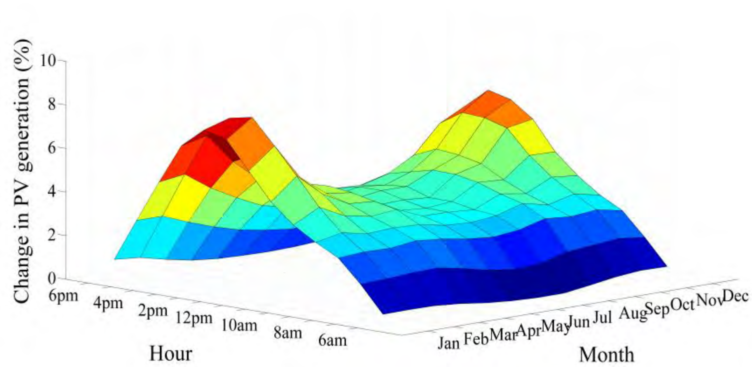

Figure 4.7 Month v hour average generation variability surface plot for fixed-tilt systems

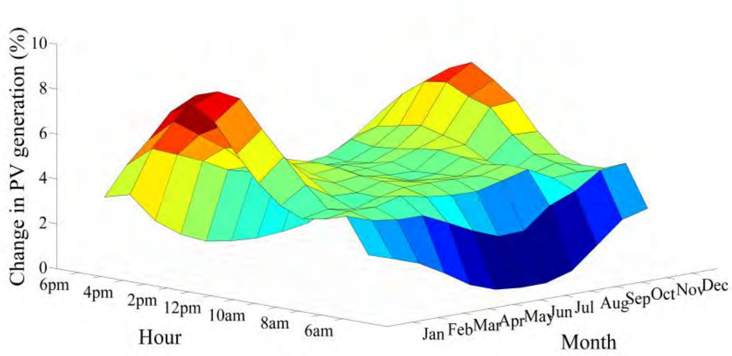

Figure 4.8 Month v hour average generation variability surface plot for dual-axis tracking systems

Examining the above plots, the months of November to February are when Alice Springs receives the most rainfall and therefore has greater cloud cover; this period clearly exhibits greater variability relative to the remainder of the year. At around 2pm the variability (~8%) is almost double that of the April to September months (~4%). These surface plots would vary greatly according to geographical location. Sydney for example has monthly rainfall levels of over 4 inches for 8 months of the year and would give a very different surface plot. It is likely the difference in generation variability throughout the year would not be as obvious as that of Alice Springs which experiences quite pronounced wet and dry seasons. As comparing the two plots is difficult without seeing them from different angles, Figure 4.9 shows the difference in generation variability between fixed and dual for all data points; Figure 4.9 highlights that the dual-tracking system generation is more variable for all data points. The difference isn't large but this could be attributed to the large number of data points used and the smoothing which occurred to better define the climate and time dependent shape of surface plot. Results in a different form presented later are more suited for comparison. From the three figures in can be concluded that the generation of the dual-tracking system is clearly more variable during the mornings and afternoons. It also obvious that the variability at these times increases during the wet season, due to the combination of increased cloud activity and the sun being higher in the sky, and rising earlier and setting later than in the dry season.

	Jan	Feb	Mar	Apr	May	Jun	Jul	Aug	Sep	Oct	Nov	Dec
6 am	2.22	1.84	1.45	0.92	0.37	0.06	0.00	0.01	0.19	0.94	1.79	2.10
7 am	2.57	2.13	1.88	1.84	1.55	1.28	0.99	0.97	1.55	1.90	2.52	2.78
8 am	1.23	1.31	1.33	1.49	1.35	1.43	1.50	1.66	1.65	1.17	1.12	1.34
9 am	0.53	0.53	0.57	0.82	1.12	1.36	1.39	1.23	1.17	0.81	0.80	0.75
10 am	0.32	0.44	0.33	0.50	0.70	0.98	0.90	0.92	0.74	0.38	0.41	0.35
11 am	0.25	0.24	0.13	0.36	0.58	0.89	0.67	0.66	0.55	0.25	0.29	0.27
12 am	0.13	0.11	0.11	0.27	0.53	0.72	0.53	0.59	0.48	0.22	0.26	0.15
1 pm	0.12	0.15	0.22	0.26	0.46	0.53	0.40	0.50	0.34	0.25	0.27	0.16
2 pm	0.44	0.50	0.50	0.39	0.53	0.35	0.40	0.40	0.43	0.41	0.66	0.52
3 pm	0.86	1.13	0.97	0.84	0.66	0.54	0.44	0.45	0.59	0.68	1.20	0.99
4 pm	1.28	1.75	1.78	1.63	1.19	1.01	1.05	1.09	1.35	1.42	1.96	1.55
5 pm	1.91	2.45	2.46	2.40	2.14	2.06	1.96	1.99	2.16	2.43	2.78	2.18
6 pm	2.29	2.31	1.22	0.66	0.28	0.15	0.10	0.16	0.26	0.70	1.53	1.78

	Difference (%)
	< 0.5
	0.5 - 1
	1 - 1.5
	1.5 - 2
	2 - 2.5
	2.5 - 3

Figure 4.9 Average generation variability difference between fixed-tilt and dual tracking systems surface plots

4.1.4.2 Magnitude and Variability by Month and Hour

The next set of results uses the method described in Section 4.1.3.5 *Monthly and hourly generation magnitude and variability* illustrate the 5 min generation variability for the different technologies. Figure 4.10 shows the mean monthly magnitude and 5 min variability for all system types. Note that there is no variability bar for the concentrator system for February; this data point was removed as its variability value was so high that the values in the other months lost resolution. The monthly magnitude values are normalised against the highest value, this being the concentrator system magnitude for August. During the middle of the year the variability is reduced and converges for all systems. This can be explained by the fact that there is very little rainfall during this period and thus no cloud cover to induce a change in PV generation. Where there is more rainfall, during the months of November to February, the difference in variability increases. This difference can be attributed to the morning and afternoon periods when the tracking systems are still orientated towards the sun whilst the fixed tilt systems are not. During these periods there is far less DNI incident on the fixed tilt panels and they are mostly producing power due to diffuse insolation. Diffuse insolation is not impacted as greatly as DNI by a change in cloud cover and so the fixed tilt systems display reduced variability. Tracking systems on the other hand are receiving greater DNI and so a change in cloud cover will result in a change in PV generation resulting in greater variability.

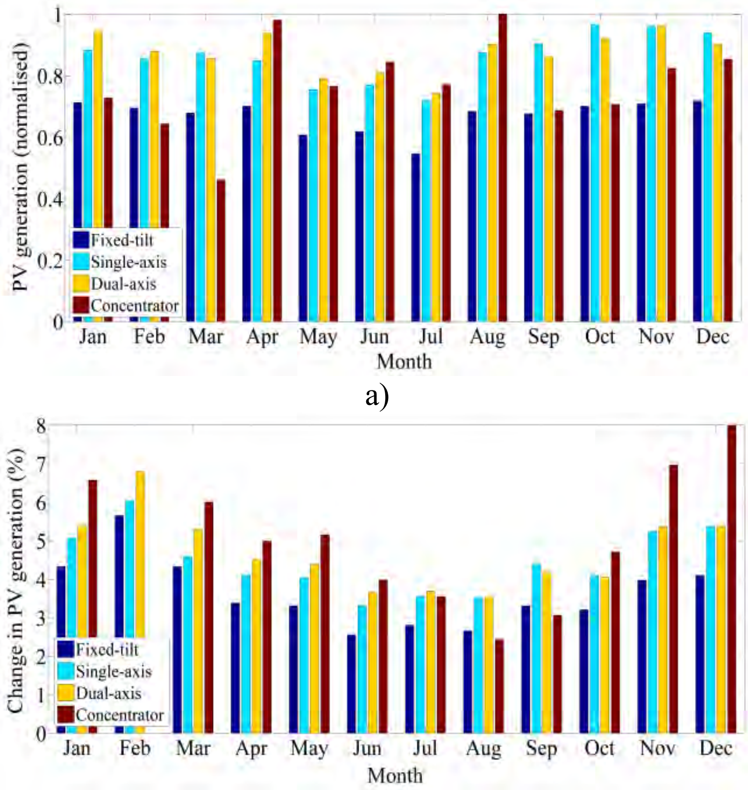

a)

b)

Figure 4.10 Monthly average a) magnitude and b) variability for all technologies

In Figure 4.11, the variability for each of the system types is given by hour. As per Figure 4.10, the hourly magnitude values are normalised against the highest value, the dual-axis system magnitude for 12 pm. 7-8 am and 4-5 pm show the greatest difference in variability, indicating that these are the times where the tracking functionality is making the most significant difference to generation. Higher relative generation will of course give higher relative variability. This is supported by the magnitude bar graph which shows a large difference in PV generation between the tracking and fixed-tilt systems at these times. At 5pm the tracking systems are seeing generation variability of around 5% at a time when generation magnitude is only around 40% of rated capacity. The maximum variability is around 5.5% when generation is close to rated capacity. In comparison the fixed-tilt systems are only exhibiting around 2% (compared to a max of 5.5% at 1pm) variability for an average generation magnitude of approximately 15%.

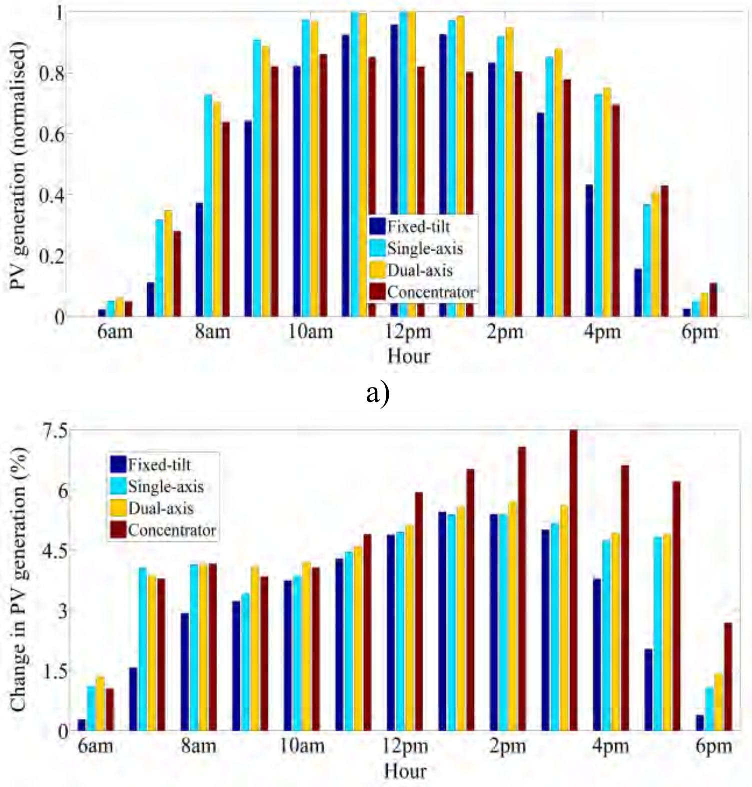

a)

b)

Figure 4.11 Hourly generation a) magnitude and b) variability for all technologies

4.1.4.3 Weekly Scatter Plots with Mean

The following set of results was produced using method *Weekly scatter plot with mean*, described in Section 4.1.3.6. The plots were devised to illustrate the range of possible variability by taking a “slice” of the surface plot to more clearly show how the 5 min variability changes throughout the year. Figure 4.12 is the weekly scatter plot with mean for fixed-tilt systems at 2pm; looking at the scatter aspect we can see variability reaching levels of 80%. The two mean variabilities best illustrate the difference between the wet and dry season with the positive mean moving from around 6% during the dry season (middle) to levels nearing 15% during the wet (ends of the plot); the negative mean also changes from 3% (dry) to 9% (wet). This reflects what one would expect, with only minor negative variability as there are no clouds to force drops in generation.

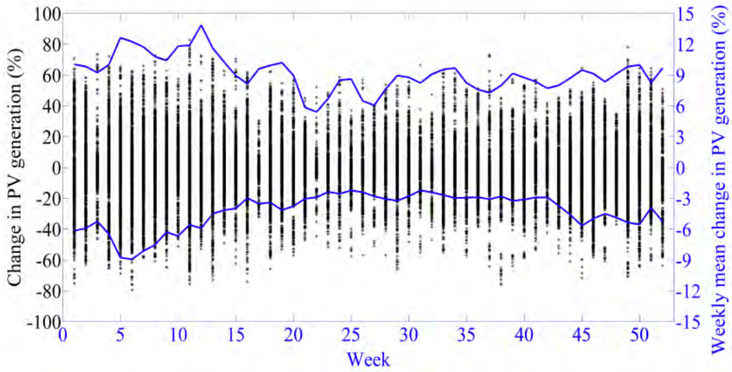

Figure 4.12 Weekly scatter plot for fixed-tilt systems at 2pm

To better show how the difference between fixed-tilt and dual-axis systems a slice at 7pm is taken, Figure 4.13 and Figure 4.14 show these two plots. At this time of day, the difference in variability between the two systems types is quite obvious. The range of possible generation variation for dual-axis is almost triple that of the fixed-tilt, the positive mean is double throughout the year and the negative mean could be said to be triple that of the fixed-tilt during the wet season. The impact of climate is really apparent at 7am, especially in regard to the negative mean. Of concern to the electricity industry would be if these large drops in generation are occurring in the morning when demand is increasing.

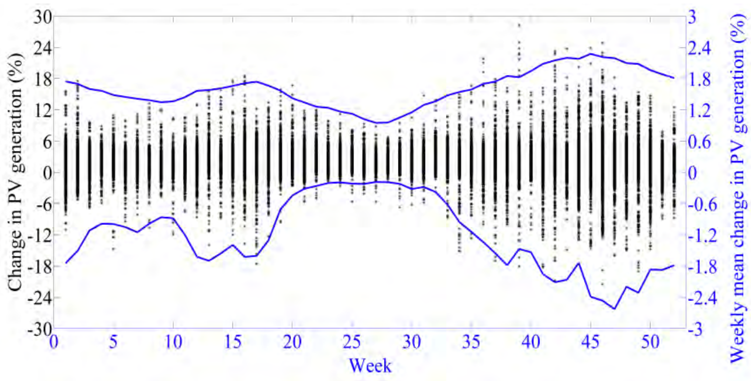

Figure 4.13 Weekly scatter plot for fixed-tilt systems at 7am

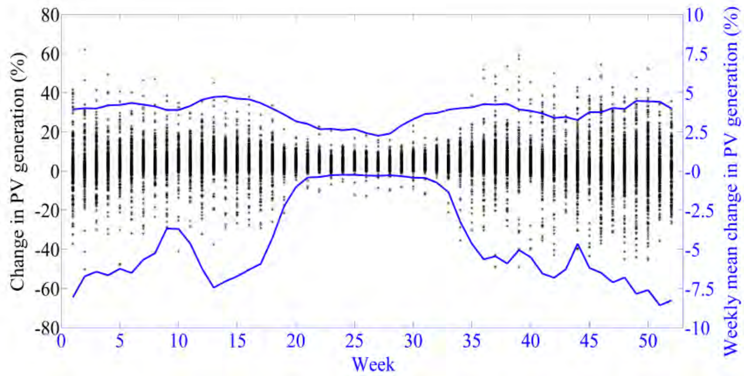

Figure 4.14 Weekly scatter plot for dual-axis systems at 7am

4.1.4.4 Variability Histograms

This next section of results present the final drill down from the original, and least definitive, month v hour surface plot; where the histogram for an individual “cell” of the month v hour surface plot is calculated. The purpose of these histograms is to show the 5 min variability, in a more definitive manner, at a specific time (hour of a month) of the year. These histograms might well be of most use to electricity industry planners and operators as they give the essential detailed information required to take into account the potential impacts of PV system generation variability on the likelihood of negative and positive ramp rates of all magnitudes. The histograms are for both magnitude and variability and for both fixed-tilt and dual-axis. These plots provide answers to questions such as, for example, how frequent and how large are the potential drops in generation during early morning periods of increasing load? Figure 4.15 and Figure 4.16 show the histograms of generation and variability for both fixed and tracking systems at 7am for the June dry season, and February wet season. For June there is little concern that large drops in generation are likely to occur with virtually no negative changes greater than -2.5% for either system; an indication of negligible cloud activity during this period. Even for February when there is maximum cloud activity the chance of a negative change greater than -2.5% is very small.

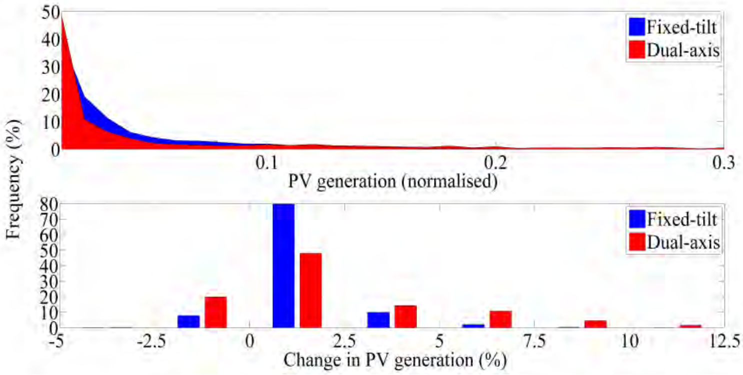

Figure 4.15 Generation magnitude and variability histogram for June 7-8am, fixed-tilt and dual-axis

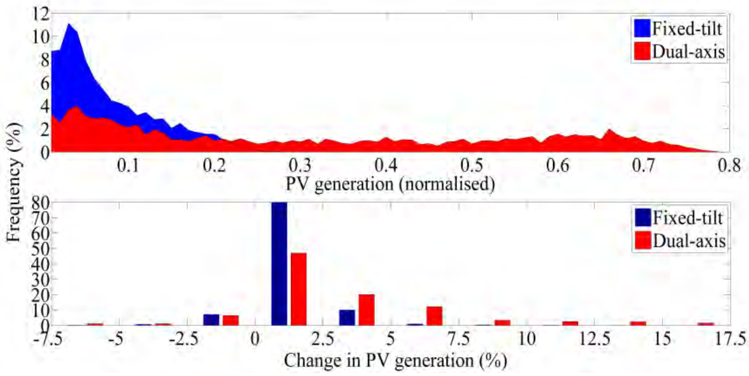

Figure 4.16 Generation magnitude and variability histogram for February 7-8am, fixed-tilt and dual-axis

Comparing the behaviour of the two systems for both time periods we see that in both cases fixed-tilt systems have a far greater percentage of samples in the 0 to 2.5% bin, indicating less variability. Dual-axis has a greater variability spread with values in bin 10 to 12.5% for June and bin 15 to 17.5% for February; by comparison fixed-tilt only manages maximum values in bin 7.5 to 10% for June and 10 to 12.5% for February. The magnitude histogram also gives a useful indication of the level of variability: the greater the spread the greater the variability. The magnitude spread for February reaches 0.8 for dual-axis systems while fixed-tilt is restricted to less than 0.3. As expected the majority of the variability is on the positive side and can be attributed to the normal increase in PV generation as the sun rises. Figure 4.15 and Figure 4.16 allow for a variability comparison between the wet and dry season and Figure 4.16 allows for a comparison between fixed-tilt and dual-axis system behaviour. In summary, due to the lack of cloud activity, the majority of the difference in variability between the two systems could be attributed to the dual-axis system having a steeper change in generation gradient. On the other hand in February, the variability for dual-axis systems is substantially greater and cannot be solely due to this steeper gradient. This indicates that increased cloud activity during the mornings and afternoons will result in increased variability for a dual-axis system. The next figure, Figure 4.17, is for 2-3pm in February and shows, as during this period both systems are exposed to a similar amount of insolation, how similar their behaviour despite this being the period of greater cloud activity. It can be seen that the magnitude spread for both systems is similar and in agreement with the variability spread.

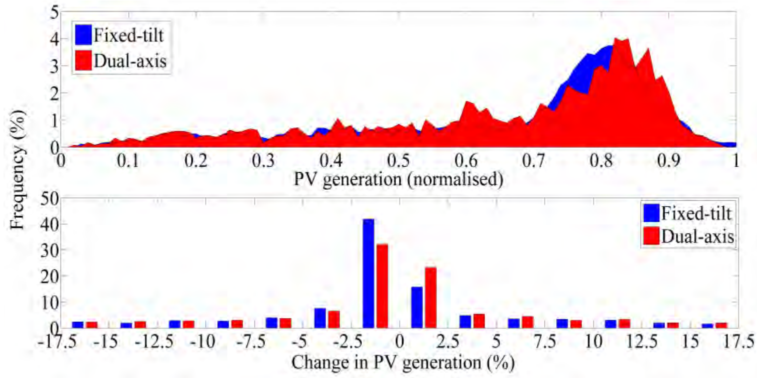

Figure 4.17 Generation magnitude and variability histogram for February 2-3pm, fixed-tilt and dual-axis

The final histogram plot presented, Figure 4.18, is for 2-3pm in June. The purpose of this is to show how predictable the generation for a PV system can be at this time of year: the middle of the dry season (no cloud activity) when the sun is at its peak (minimal change in PV generation). For the fixed-tilt system over 70% of samples are in bin -2.5 to 0% compared to 40% for February, almost double the number of samples. The dual-axis system exhibits similar reductions in variability with an increase in samples from around 30% to over 50%. This low variability is supported by a heavy concentration (as opposed to the large spread seen in Figure 4.17) of samples of normalised generation around 0.7 for fixed-tilt and 0.85 for dual-axis.

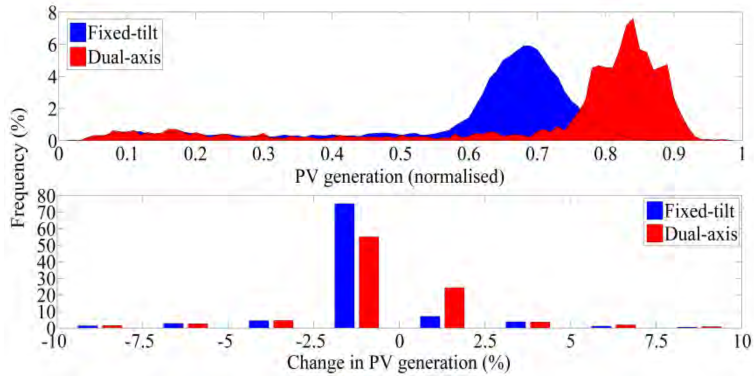

Figure 4.18 Generation magnitude and variability histogram for June 2-3pm, fixed-tilt and dual-axis

4.1.5 Conclusion

Section 4.1 presents a combination of methods to characterise PV generation variability for four different types of PV technologies, all co-located.

The hour versus month variability surface plots highlights how PV generation variability alters over the course of the year, according to season. The weekly scatter plots, which take a “slice” of the month v hour surface plot, gives more detail on PV generation variability for a particular hour across the year. The last type, the histogram illustrates where the PV variability and magnitude probability for an individual “cell” of the month v hour surface plot is presented. Existing studies characterising PV generation variability are often in a histogram format. The drawback of these studies however is that the data input into the histogram covers too large a time period, usually a year. A histogram using a years’ worth of data gives a mean probability distribution, and therefore, for a particular hour of a particular month, the characterisation is unlikely to be truly accurate.

The results of the variability characterisation presented in Section 4.1 justify the necessity of such a method. The first two types, hour v month variability surface and weekly scatter plots, demonstrated a difference in variability season to season, and from hour to hour. This difference in variability is confirmed by the final type, the variability histogram for a particular month and hour. That PV generation variability itself changes from season to season, and hour to hour, and that a comprehensive characterisation would take this into account, is not suggested in the literature.

As stated in Section 3.1.1, the work presented in Section 4.1 addresses characterisation knowledge gaps 1, 2, 5 and 6. The variability characterisation presented in Section 4.1 uses data covering an entire year, this method addresses characterisation knowledge gap 1 which states that a complete characterisation should cover the entire year. The variability characterisation presented in Section 4.1 is also split according hour, this method addresses characterisation knowledge gap 2 which states that it is necessary for a characterisation to be split according to hour to capture the change in PV generation variability which occurs over the course of the day. The data used for the analysis is also from actual PV system measurements, this method addresses characterisation knowledge gap 5 which states that to produce the most accurate characterisation, the PV generation dataset should be obtained from actual PV system measurements. Finally, tracking PV systems are also included in the analysis, this method addresses characterisation knowledge gap 6 which states that the same detail of characterisation described at knowledge gaps 1 and 2 also needs to be applied to tracking PV systems.

4.2 Cluster of Distributed PV Systems

The research presented in Section 4.2 is based on the authors full peer reviewed conference paper "Operational Characteristics of a Cluster of Distributed Photovoltaic Systems", accepted for presentation at the Innovative Smart Grid Technologies Asia (ISGT), Perth 2011 [1].

4.2.1 Introduction

As noted in Section 3.1.2, in Section 4.2 high resolution PV generation data is used to characterise the PV generation variability for a cluster of small-scale PV systems. The characterisation concentrates on variability hour to hour, and also categorises the analysis according to day type. Day type is defined according to cloud cover: sunny, partly cloudy and majority cloud. It also analyses aggregate generation variability. The PV generation data is obtained from actual PV system measurements. The research presented in Section 4.2 addresses characterisation knowledge gaps 2-5 defined in Section 3.1.

According to [113], once PV generation behaviour is understood its impact on regulation and load following operations can be quantified and a dispatch strategy developed. As Australia installed more small scale PV systems on the LV network than Germany in 2010 [114], impacts on the LV network should certainly be the focus. An important question here is the aggregated generation behaviour of clusters of PV systems within particular areas of the electricity network. Also, to accurately characterise PV generation variability, high resolution data is required to capture the fast changes in generation due to cloud transients.

The data set used for the characterisation comes from power measurements of 18 PV systems located in the Hunter Valley, the PV systems are all small scale (< 10 kW) and dispersed over an area approximately 24 km x 30 km. A key aspect of the analysis performed in Section 4.2 is not only the sampling resolution of 10 s but also that it utilises actual PV generation data and so accurately represents PV generation behaviour. The analysis is based on approximately 3 months' worth of data from August to November in 2010.

Section 4.2.2 describes the method of analysis, the results of the analysis are presented in Section 4.2.3 and concluding remarks are made in Section 4.2.4.

4.2.2 Method

Data for all the PV system sites (sites) came as a comma delimited file with 2 columns, timestamp and PV generation. The output current of the inverter is measured through a Current Transformer (CT) and sampled through an Analog to Digital (A/D) converter every second; the A/D converter is connected to a Linux box via a serial link. 10 second averages are logged to the Linux box and then stored on a server located at the CSIRO Energy Centre in Newcastle via the internet. As Figure 4.19 shows, no site logged data continuously over the 3 months with the vertical steps indicate a gap in the sampling. The dashed line is how a plot would look if there was continuous sampling from the earliest sample recorded to the latest.

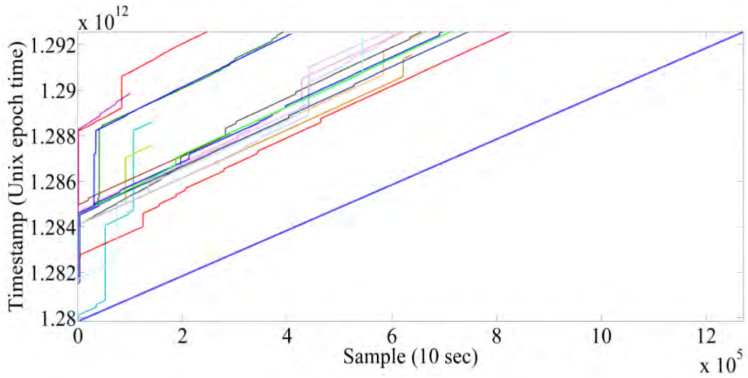

Figure 4.19 Plot showing the continuity of sampling for each site. A vertical jump indicates a time gap in the sampling

This data had to be manipulated to group days and align timestamps before it was ready for analysis – that the data manipulation process was correct was always verified. Figure 4.20 confirms the correctness of a timestamp alignment process for a cluster of sites with the dips in PV generation correlated. The PV generation magnitude for each site used in Figure 4.20 was assigned a different offset to better show the timestamp alignment. The particular value of the data provided by CSIRO is that the high sample resolution enabled the analysis to pick up on the impact of cloud transients. Data manipulation and analysis is executed using Matlab.

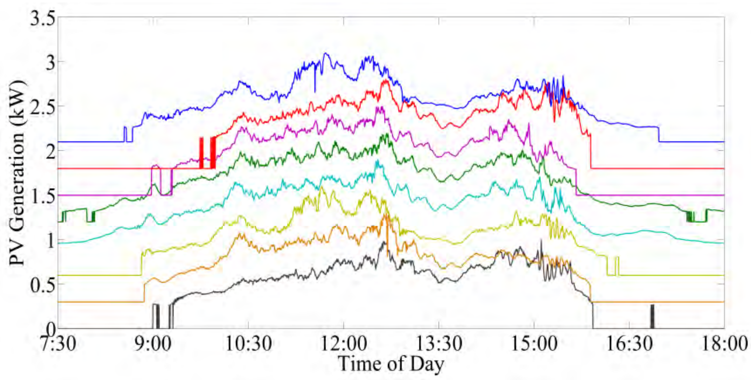

Figure 4.20 PV generation for 8 sites with timestamps aligned

4.2.2.1 Description of Data Manipulation Techniques

Described below is a description of the data manipulation techniques applied to the dataset

- **Split into individual days:** The data for each site was provided as one continuous set across the 3 months and needed to be split into individual days. Start of day was identified as PV generation showing a 10 sample moving average > 0.35 and end of day as 1000 samples of zero output. 99 individual days was the result.
- **Change in PV generation (variability):** Change in PV generation was determined by shifting a normalised PV generation dataset and then taking the absolute difference between the shifted and non-shifted dataset. The result is a ratio: change in PV generation on rated PV generation (4.4). As each sample is 10 s, 1 shift equates to a 10 s time shift comparison, 6 shifts 1 min, 30 shifts 5 min etc. The shift distance is appended onto the front and end of the data set so the first and last section is being compared to zero.

$$Variability = \frac{Change\ in\ PV\ generation\ magnitude}{Rated\ PV\ generation} \tag{4.4}$$

- **Grouped into matching days:** Timestamps for each individual day were compared and matched so days could be grouped. All sites had days with no data with some days being discarded from the analysis due to lack of samples. TABLE 4.2 shows the number of days for each site.

TABLE 4.2: Number of days where PV generation recorded for each site

Site	1	2	3	4	5	6	7	8	9	10	11	12	13	14	15	16	17	18
Days	12	81	77	86	18	73	74	8	90	76	84	36	83	88	34	45	18	8

- **Timestamp aligned:** For each group, the site with the earliest time for which solar insolation occurs is discovered; all other sites then have zeros padded to their PV generation data down to this time. The same is repeated for the latest showing of solar insolation. See Figure 4.21 for an example day after timestamps have been aligned for the group.
- **Hourly split:** Using a dataset which has been *split into individual days* and *timestamp aligned*, this dataset is split further into hourly sections, from 5am to 8pm, giving 15 datasets. To explain further, assuming 10 sites, each with 10 days' worth of data; after an *hourly split* the 5-6am dataset would consist of 100 (10 sites x 10 days) arrays, each containing an hours' worth of data.
- **Day type categorisation:** After being *split into individual days,* each day was then categorised as sunny, partly cloudy or majority cloud using two methods.
    - **BOM split:** The first method, BOM split, uses the fraction of cloud cover classification used by the Australian Bureau of Meteorology (BOM). The BOM classifies cloud cover as the fraction of the sky covered by cloud in units of eighths (8th). The measure ranges from 0 for clear sky up to 8 for full cloud cover. The closest measurement point for cloud cover is Newcastle University where a measurement is taken at 9am and 3pm every day. The BOM eighths method categorises each day as sunny, majority cloud or partly cloudy as per TABLE 4.3. After being *split into individual days,* for all sites, each day was categorised as sunny, partly cloudy or majority according to what was specified by the BOM for that particular day.

TABLE 4.3 Sunny, Majority Cloud, and Partly Cloudy split – BOM split

BOM split (assigned to all sites)	
Sunny	Mean of 9 am and 3 pm measure < 1
Partly cloudy	Mean of 9 am and 3 pm measure > 1 and < 6
Majority cloud	Mean of 9 am and 3 pm measure > 6

- **Non-BOM split:** The second method, Non-BOM split, categorised each day as sunny, partly cloudy or majority cloud according to the conditions described in TABLE 4.4. After being *split into individual days,* each day was categorised as sunny, partly cloudy or majority according to the conditions in TABLE 4.4. The categorisation is done for each site, using each sites PV generation data. As opposed to the BOM-split method which took the day type categorisation from the BOM and applied it to all sites for that day.

TABLE 4.4 Sunny, Majority Cloud, and Partly Cloudy split – Non-BOM split

Non-BOM split	
Sunny	
Mean PV generation for day > Total mean PV generation for site	PV generation variance for day < (Total mean PV generation variance for site - 1 STD of PV generation variance) for site
Majority Cloud	
Mean PV generation for day < (Total mean PV generation - 1 STD of PV generation) for site	PV generation variance for day < Total mean PV generation for site
Partly Cloudy	
Outside both sunny and majority cloud conditions	

Figure 4.21 shows the PV generation for a typical partly cloudy, majority cloud and sunny day. For a partly cloudy day, the majority of the PV generation is due to DNI and diffuse insolation. A partly cloudy day will exhibit occasional downward spikes in PV generation when cloud passes over the PV panels, at this time PV generation is due to diffuse insolation only. Diffuse insolation only results in PV generation between 20 to 40% of DNI and diffuse insolation combined. PV generation can drop up to 80% of rated power within 10 seconds (the sampling resolution of the CSIRO data) as a result. For a majority cloud day, the PV generation is mostly due to diffuse insolation. A majority cloud day will exhibit occasional upward spikes in PV generation when a break in the cloud occurs, at this time PV generation is due to both DNI and diffuse insolation and can increase by up to 80% of rated power within 10 seconds.

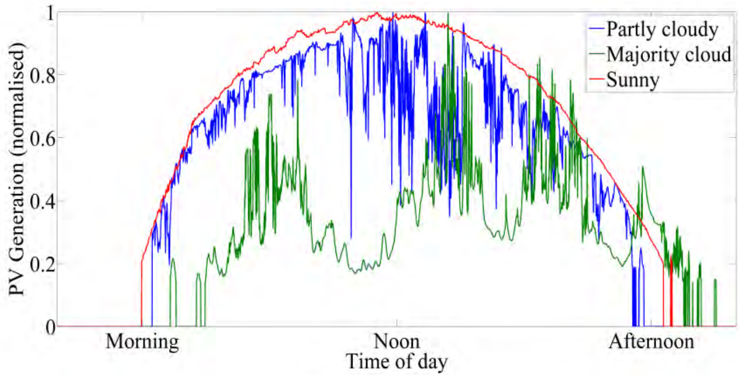

Figure 4.21 PV generation for a typical majority cloud, partly cloudy and sunny day

4.2.2.2 PV Generation Variability Analysis Methods

The following analysis methods were used to describe PV generation variability behaviour: Average PV generation variability, Aggregated PV generation variability, PV generation variability hour to hour, and PV generation variability according to cloud cover.

- **Average PV generation variability:** This analysis takes all data irrespective of day or site after it has been *split into individual days*. The c*hange in PV generation* for this data is then calculated.
- **Aggregated PV generation variability:** Using a dataset which has been *grouped into matching days* and *timestamp aligned*, the resultant dataset then has its PV generation for all matched days summed. The c*hange in PV generation* for this summed PV generation data is then calculated, giving 99 days.
- **PV generation variability hour to hour:** After the *hourly split*, the c*hange in PV generation* for each of these 15 datasets is performed
- **PV generation variability according to cloud cover:** Data is split into 3 categories: sunny, partly cloudy and majority cloud. This is done for both methods, *BOM Split* and *Non-BOM Split*. A *change in PV generation* is performed on the 3 datasets (sunny, partly cloudy and majority cloud). A *change in PV generation* after an *hourly split* of the 3 datasets is also performed for both methods.

4.2.3 Results

4.2.3.1 Presentation of Results

The manner in which data describing the behaviour of PV is presented needs to be in a form useful to those who might utilise it for modelling of DPVG and its impact on voltage and power quality. The histogram is used to describe PV generation variability in Section 4.1, see Figure 4.15 to Figure 4.18, and also in the literature [48]. In [48], the frequency of ramp rates for a single PV system as a percentage of the total capacity of the PV system are presented using a histogram. The majority of the analysis results presented in Section 4.2 are similar in format.

4.2.3.2 Average PV Generation Variability

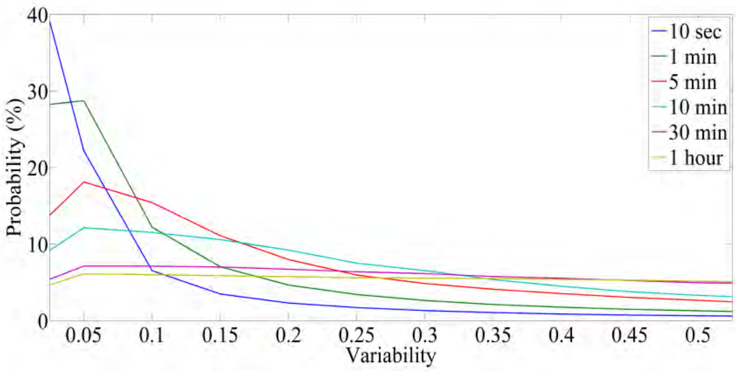

Figure 4.22 Average PV generation variability histogram, for 10 s, 1 min, 5 min, 10 min, 30 min and 1 hour intervals

Figure 4.22 gives the average PV generation variability histogram for 10 s, 1 min, 5 min, 10 min, 30 min and 1 hour intervals. As normalised data was used, the x-axis can essentially be viewed as a percentage change (%), this is the case for all plots of this type in Section 4.2. Each bin has a width of 0.05 (5%) apart for the “0” bin which covers changes in PV generation from 0 – 2.5%, TABLE 4.5 gives the ranges for each bin up to 0.3 to clarify. The PV generation variability is smallest at the 10 s interval with the majority of change in PV generation being less than 0.1 or 10%. With an increase in time interval the plot is “flattened” with an increase in the probability of larger changes in PV generation.

TABLE 4.5 Range of change in PV generation for each bin

Bin	Range of Change in PV generation
0.00	0-0.25%
0.05	2.5-7.5%
0.10	7.5-12.5%
0.15	12.5-17.5%
0.20	17.5-22.5%
0.25	22.5-27.5%
0.30	27.5-32.5%

4.2.3.3 Aggregated PV Generation Variability

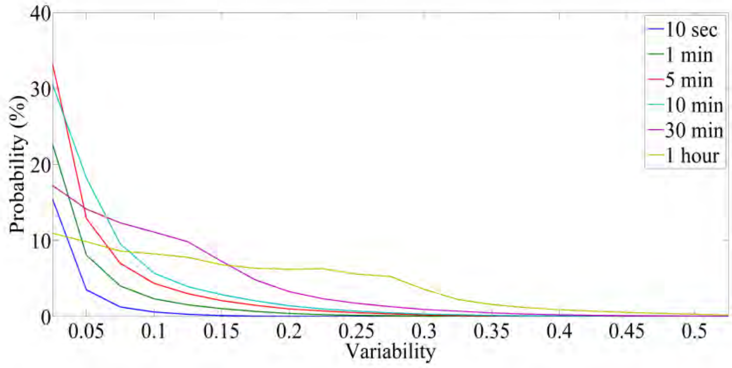

Figure 4.23 Aggregated PV generation variability histogram, for 10 s, 1 min, 5 min, 10 min, 30 min and 1 hour intervals

Figure 4.23 gives the aggregated PV generation variability histogram for 10 s, 1 min, 5 min, 10 min, 30 min and 1 hour intervals. As expected the variability is noticeably less than that of Figure 4.22, the “squashing” (as opposed to “flattening”) of the curves towards the left is an indication of a greater probability of smaller changes in PV generation. Aggregation having a smoothing effect on the total generation variability of multiple PV systems is well appreciated and discussed in a number of existing papers, [115] and [116] for example. However, there has been very limited research at high sampling resolutions as shown here. Considering PV generation variability in aggregate is important; as PV generation will be experienced by the electricity network, at both the system level and the distribution level, in aggregate.

4.2.3.4 PV Generation Variability Hour to Hour

Figure 4.24 and Figure 4.25 depict the average PV generation variability of all sites when broken down by hour. The change in PV generation is calculated at 1 min intervals for Figure 4.24, and 10 min intervals for Figure 4.25. Again, the PV generation variability is less for when the change in PV generation is calculated across a smaller time difference, this is shown by there being a greater probability of a change in PV generation of less than 2.5% for the 1 min chart; averaging around 70% and around 50% for the 10 min chart. Focusing on the 1 min chart, the plot also shows PV generation variability increasing towards the middle of the day with a concave shape present for PV generation changes < 2.5% and a convex shape for PV generation changes > 2.5%.

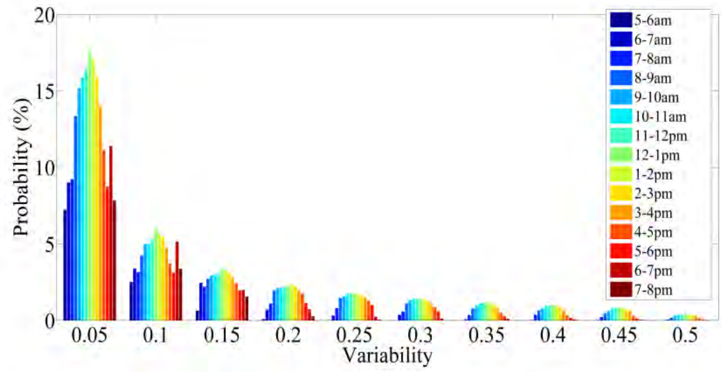

Figure 4.24 Average PV generation variability histogram for all sites broken down by hour, 1 min intervals

Looking closer at the 10 min chart we see small variation in PV generation at the extremes of the day; this could be explained by there being very little PV generation during these times. For the hours of 8-9am and 3-4pm we see PV generation variability is greater than for the middle of the day (indicated by the 2.5 – 7.5% bin), this could be explained by the ramp up in PV generation as the sun rises; more pronounced on the 10 min chart than for the 1 min chart.

It is worthwhile comparing Figure 4.25 and Figure 4.22, Figure 4.22 shows a probability of approximately 12% for a 5% change in PV generation over a 10 min interval. Looking at the 5% bin for Figure 4.25, for a large part of the day, the probability of seeing a 5% change in PV generation is actually quite higher, almost 30% between 8am and 9am.

Figure 4.26 and Figure 4.27 depict the aggregate PV generation variability for all sites when broken down by hour. When compared to Figure 4.24 and Figure 4.25 the reduction in PV generation variability is clear. For 1 min intervals, Figure 4.26, there is only a 2.5% probability of a 10% change in PV generation, and only 1% for a 15% change in PV generation. The probability for change in PV generation larger than 15% is virtually zero. For an individual PV system, Figure 4.24, a probability of a 50% change in PV generation in a 1 min interval is possible. This indicates considering PV systems in aggregate results in nullification of the large changes in PV generation exhibited by individual PV systems. The same observation can be made when comparing the PV generation variability at 10 min intervals, Figure 4.25 and Figure 4.27.

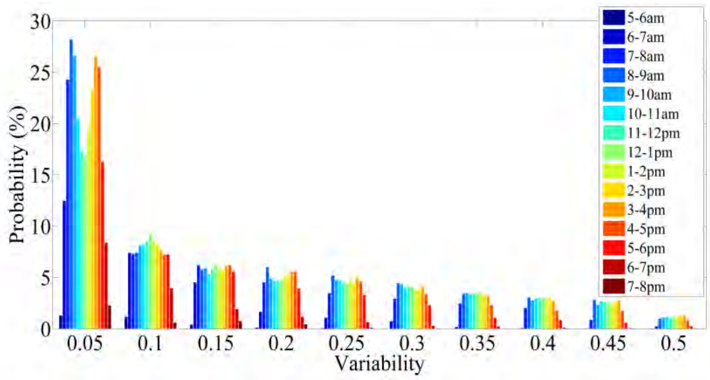

Figure 4.25 Average PV generation variability histogram for all sites broken down by hour, 10 min intervals

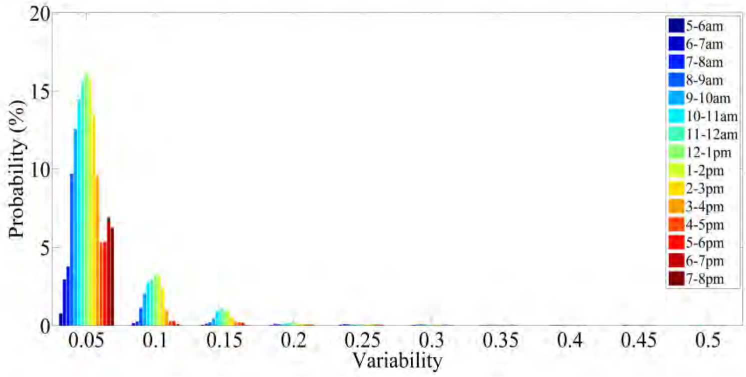

Figure 4.26 Aggregated PV generation variability histogram for all sites broken down by hour, 1 min intervals

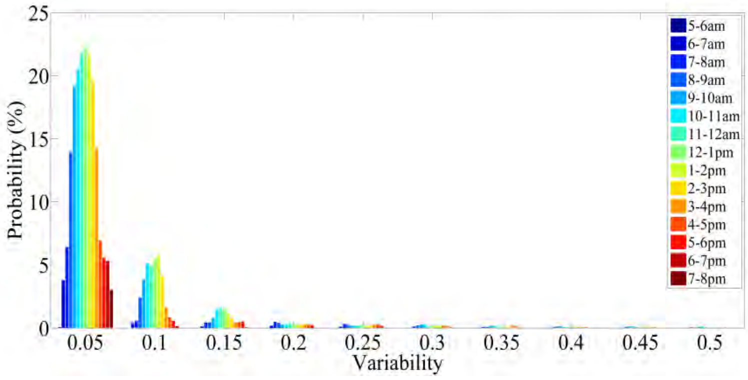

Figure 4.27 Aggregated PV generation variability histogram for all sites broken down by hour, 10 min intervals

4.2.3.5 Variability According to Cloud Cover

The next figure, Figure 4.28, is an observation on the different PV generation variability to be expected for different levels of cloud cover. Figure 4.28 a) uses *BOM-split* method to categorise the days and the *Non-BOM split* method is used for Figure 4.28 b). The *BOM-split* method splits the days according to the mean of two cloud measurements by the BOM (9am and 3pm) made at one location (Newcastle University). The average distance the PV sites are away from Newcastle University is 15 km, with seven sites over 20 km away. This distance may mean the cloud cover measured at the university is different to the cloud cover at the PV site. Also, two cloud cover measurements at 9am and 3pm may not be representative of the average cloud cover for the day. Considering this, the *Non-BOM split* method was developed. This method uses the actual PV generation data at each site to categorise the day type, and is likely to more accurately categorise the day type. The results for both methods are included.

Both charts show that on sunny days PV systems exhibit far less generation variability with a probability of smaller changes in PV generation. Interestingly, majority cloud and partly cloudy days exhibit similar PV generation variability. This indicates that the magnitude and frequency of occurrence of a negative spike in PV generation due to cloud covering the panels in an otherwise sunny sky, for a partly cloudy day, is similar to that of a positive spike in PV generation due to a break in the clouds on an otherwise cloudy day, for a majority cloud day.

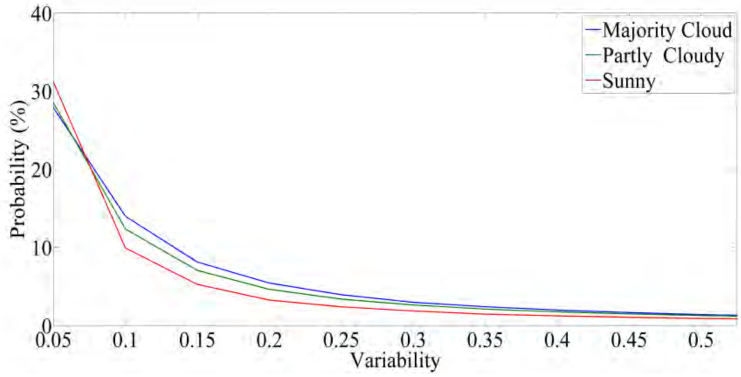

a)

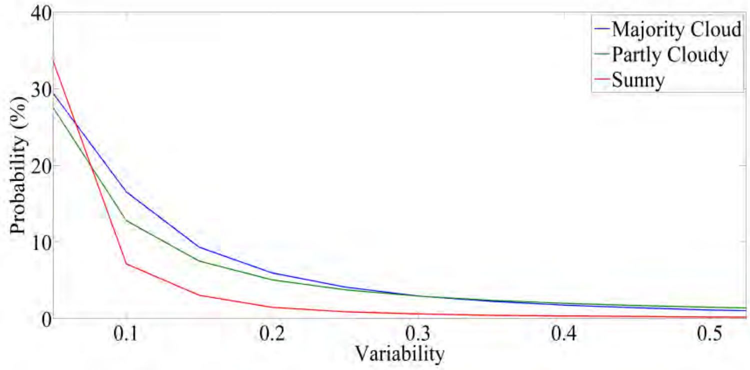

b)

Figure 4.28 PV generation variability histogram for all sites for all sites after being split into sunny, partly cloudy and majority cloud. a) Uses *BOM split* method and the *Non-BOM split* method is used for b). Change in PV generation is calculated at 1 min intervals

Figure 4.29 to Figure 4.31 shows 5 min PV generation variability by the hour for majority cloud, partly cloudy and sunny days using the *Non-BOM split* method. The results for both methods are similar so only one is shown.

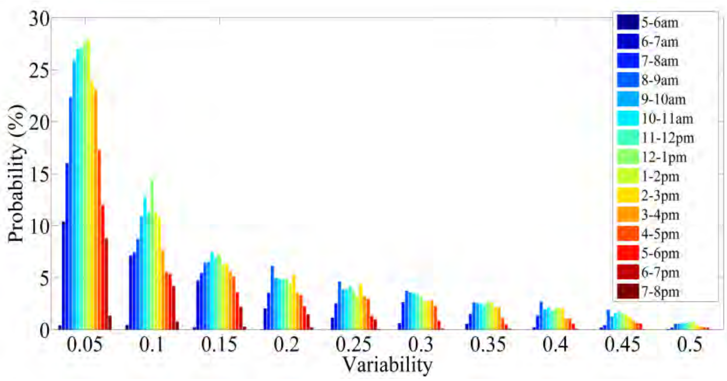

Figure 4.29 *Non-BOM split* - majority cloud, hourly split. Change in PV generation calculated 5 min intervals

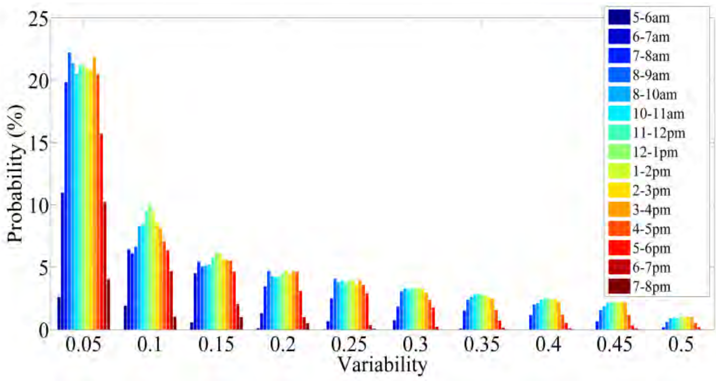

Figure 4.30 *Non-BOM split* - partly cloudy, hourly split. Change in PV generation calculated at 5 min intervals

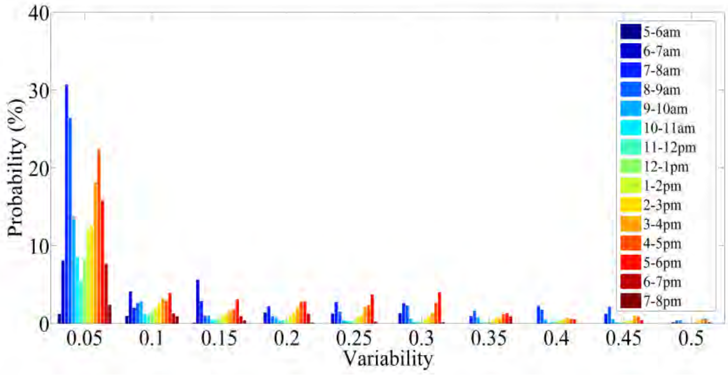

Figure 4.31 *Non-BOM split* – sunny, hourly split. Change in PV generation calculated 5 min intervals

Figure 4.29 to Figure 4.31, compared to Figure 4.28, more clearly shows the PV generation variability behaviour for majority cloud, partly cloudy and sunny days. As per Figure 4.28, the PV generation variability for majority cloud and partly cloudy days is again similar. Partly cloudy days experience a slightly higher number of larger changes in PV generation (>30%) compared to majority cloud days but the difference is minimal. The bar graph at each variability bin imitates the shape of a typical daily PV generation profile, ramping up in the mornings into midday and ramping down from midday into the afternoon. This indicates that PV generation variability at each hour of the day is dependent upon the PV generation magnitude for that hour of the day. A sunny day exhibits the opposite PV generation behaviour compared to a partly cloudy and majority cloud day. The morning and afternoon is when the majority of the change in PV generation occurs, for all variability bins. During the middle of the day there is very little PV generation variability. This indicates that PV generation variability is due to the typical ramping up and down of PV generation in the morning and afternoon and not cloud.

Looking at Figure 4.22, with day type and hour to hour variability not taken into consideration, a 15% probability for a 10% change in PV generation in 5 min is expected. Looking at Figure 4.31, a sunny day, the probability of a 10% change in PV generation in 5 min is actually around 5%. Therefore, a prediction which doesn't take into account day type and hour to hour variability would have an error of 10% for the entire day. This illustrates the importance of breaking up PV generation variability analysis hour to hour and according to day type.

4.2.4 Conclusion

The research presented in Section 4.2 presents a variability characterisation of a cluster of small scale distributed PV systems. The majority of the literature analyses PV variability for time frames of 1 min or more, thus missing very fast changes in PV generation due to cloud transients. The data set used in this study has a sample resolution of 10 s, sufficiently high to pick up changes in generation due to cloud transients; it is also sourced from actual PV system measurements, ensuring greater accuracy of analysis.

This study assesses to an hourly level and also categorises each day according to a type - majority cloud, partly cloudy and sunny. The hourly characterisation, as also conducted in Section 4.1, highlights how variability differs throughout the day. This has potentially significant network implications. Breaking down the characterisation into day type highlights how expected variability will depend significantly on the particular weather patterns experienced on a day to day basis. Forecasts of future weather might therefore be able to guide electricity industry participants in the potential future behaviour and variability of distributed PV. For example, known variability boundary conditions associated with an upcoming day type could be used to plan appropriate network and system-level management strategies.

As stated in Section 3.1.1, the work presented in Section 4.2 addresses characterisation knowledge gaps 2-5. The variability characterisation presented in Section 4.2 is also split according hour, as per in Section 4.1, this method addresses characterisation knowledge gap 2 which states that it is necessary for a characterisation to be split according to hour to capture the change in PV generation variability which occurs over the course of the day. The data set used for the characterisation has a sample resolution of 10 s, sufficiently high to capture changes in PV generation due to cloud transients, this addresses characterisation knowledge gap 3.4. Also, this study analyses clusters of small-scale PV systems where their generation variability is considered in aggregate, this addresses characterisation knowledge gap 3. Finally, as per Section 4.1, the data used for the analyses is from actual PV system measurements, this method addresses characterisation knowledge gap 5.

5 MPVG Estimation Methods

Original research by the authors presented in this chapter addresses the MPVG knowledge gaps defined in Section 3.2.

5.1 A MPVG Estimation Method for Evenly Distributed PV Generation and Load

The research presented in Section 5.1 is based on the authors journal paper “Method for Determining a PV Generation Limit on Low Voltage Feeders for Evenly Distributed PV and Load”, published in Energy Procedia [4].

5.1.1 Introduction

As noted in Section 3.2.3, in Section 5.1 an examination into the relationship between MPVG, feeder characteristics and load conditions is conducted. General relationships are identified through examination of power flow results. Assuming a number simplifying conditions, a method is developed for deriving the MPVG. The research presented in Section 5.1 is a first step attempt to address MPVG knowledge gaps 1-4 and limitations 5-8 in current DNO PV installation assessment processes defined in Section 3.2.

The purpose of this study is to establish a generalised relationship between feeder impedance, load and MPVG for a group of residential feeder types within the network of a DNO servicing a 24,500 km square area in the Australian city of Sydney’s Greater West region. MPVG is defined as the level of PV generation a feeder can accommodate before the upper voltage limit is exceeded for a given load along the feeder. Using the feeder models provided by the DNO, for a range of feeder characteristics and load conditions, results are obtained through power flow calculations conducted in DIgSILENT. The study assumes a number of simplifying conditions including evenly distributed PV generation and load, cable reactance of zero and load and PV system operating at unity power factor.

Section 5.1 is structured as follows; Section 5.1.2 presents the method, the DIgSILENT feeder model and the approaches undertaken towards the development of a generalised relationship between feeder impedance, load and MPVG. Section 5.1.3 presents the findings from the methods described in Section 5.1.2 and in Section 5.1.4 the merits of the generalised relationship are discussed, as well as how it might be improved. Section 5.1.5 gives concluding comments.

5.1.1.1 Nomenclature

The nomenclature listed here applies to Section 5.1 only.

Ω	Ohms
R	Resistance
X	Reactance
kW	Kilowatt
P	Voltage-dependent real power
P_{ref}	Power at V_{ref}
V	Voltage (rms)
V_{ref}	Reference voltage, 230 V
$maxPVh_{offset}$	MPVG/household when load/household equals 0 kW
$maxPVph_{offset}$	MPVG/phase when load/phase equals 0 kW
$maxPVphfl$	(MPVG/phase) * feeder length

5.1.2 Method

5.1.2.1 Model

The DIgSILENT model provided by the DNO is a generalised example of an urban residential feeder; Figure 5.1 below gives a schematic of the model. The DTx steps down the voltage from 11 kV to 400 V and is rated at 500 kVA. The 11 kV voltage source is assumed to be stiff and does not change with power flow. The DTx has a positive and zero sequence impedance of 4%, the tap setting is such that the phase to neutral voltage at its terminals is 249.7 V. A setting between 245 V and 255 V is typical for the DNO, to account for the expected drop in voltage at peak load. The 400 V line is three phase, four wire, rated at 180 A with R=0.707 Ω/km and X=0.284 Ω/km, type 7/3 AAC. The 400 V line is one typically used by Endeavour Energy, a DNO servicing Greater Western Sydney. Supply is at 50 Hz. A terminal is the point on the feeder where the household is connected; each terminal has 2 households connected. The household connections are single phase, two wire, rated at 90 A with impedances of R=1.49 Ω/km and X=0.097 Ω/km. The length of these connections is 20 m. This example feeder model has 3 terminals, each with 2 households connected. Each household is assumed to have a PV system and household loads and PV are distributed evenly across the 3 phases over the feeder as a whole. The time-varying behaviour of household load and PV generation is not modelled in this study so the relationship being sought can be thought of as the MPVG injected into the network for a given coincident load. Simulations are performed at 20^{0}C. This feeder model is a template, and in the attempt to establish a generalised relationship between feeder impedance, load and MPVG, the number of terminals and distance between terminals (terminal distance) was varied. Changing the distance between terminals gives the required change in feeder impedance. In Section 5.1, the terms "feeder length" and "terminal distance" can be inferred to mean "impedance". The X/R ratio of the feeder cable impedance, single phase household connection impedance and the DTx impedance and tap setting is not altered in this study. Voltage measurements are made at the feeder terminals.

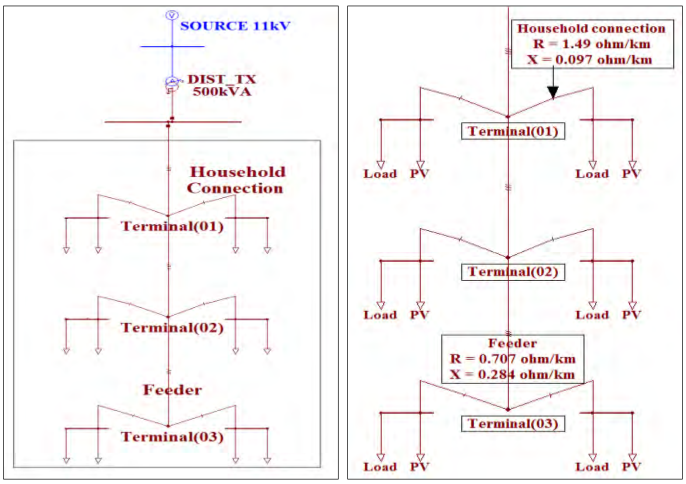

Figure 5.1 (a) DIgSILENT model of three terminal feeder; (b) Boxed section of (a)

All loads are modelled as constant impedance with a power factor of 1. Constant impedance means power drawn is proportional to voltage squared, (5.1).

$$P = P_{ref}(\frac{V}{V_{ref}})^2 \tag{5.1}$$

PV generation is modelled as negative load, generating with a power factor of 1, injecting constant power. Constant power means current injected in inversely proportional to voltage (5.10).

$$P = P_{ref} \tag{5.2}$$

5.1.2.2 DIgSILENT Scripting Language

The DIgSILENT Scripting Language (DSL) allows for multiple power flow calculations to be performed for a feeder model. Feeder parameters can also be altered for each calculation thus allowing for the execution of multiple power flow calculations which cover a large range of feeder parameters. DPL cannot update the number of terminals so models were created with terminal counts of 3, 6, 9, 12 and 15. These terminal counts ensured PV and load were balanced across 3 phases. 15 terminals gave the maximum number of nodes that DIgSILENT allows in the software version available for the study.

5.1.2.3 Voltage Profile

A DPL script was written which updated the load (kW) and PV generation (kW) per household and terminal distance for each power flow calculation, the ranges for these values being

- Load: 0-10 kW with 1 W step size.
- PV Generation: 1-50 kW with 1 kW step size.
- Terminal distance: 5-50 m with 5 m step size.

For each calculation, the voltage magnitude is recorded for each terminal, giving the voltage profile for the feeder. The voltage data was then imported into Matlab. For each load and terminal distance variation Matlab identifies the first breach of the upper voltage limit (according to AS61000.3.100 this is 253 V, +10% of the nominal 230 V). With the DTx at 249.7 V, this is a change of 3.3 V. The PV generation magnitude and voltage profile at this breach point is then analysed. Scrutiny of these results revealed that the highest voltage point always occurred at the end of the feeder. Knowing the voltage at the end of the feeder would always reach 253 V first, this voltage was then used as the voltage reference in the next step to identify a relationship between load, feeder length and MPVG.

5.1.2.4 Investigation into the Relationship between MPVG and Load

With the voltage at the end of feeder determining the MPVG, further research involved plotting the MPVG/household for a range of household loads (0-10 kW), terminal distance (5-50 m) and number of terminals. The terminal distance is the distance between poles, from which households are connected to the feeder via a single-phase cable. Terminal counts were 3, 6, 9, 12 and 15. This research revealed the same linear relationship between MPVG/household and load/household for all terminals counts.

5.1.2.5 Investigation into the Relationship between MPVG/Phase, Terminal Count and Feeder Length

To see how MPVG/phase varied according to terminal count, MPVG/phase plots were developed for each terminal count (3, 6, 9, 12 and 15) with load kept constant at 10 kW/phase while feeder length was increased from 50 m to 1000 m. Figure 5.2 gives the MPVG/phase (kW) curve for each terminal count for 10 kW load/phase. Feeder length range is from 50 m to 1000 m with 10 m increments.

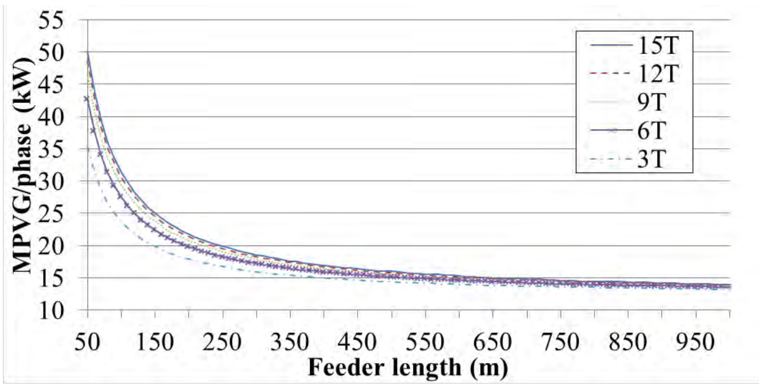

Figure 5.2 Curves for each terminal count showing the MPVG/phase (kW) for 10 kW load/phase. Feeder length ranges from 50 m to 1000 m in 10 m increments. The top curve is 15 terminals (15T) while the bottom curve is for 3 terminals (3T)

An increase in feeder length is achieved by increasing the terminal distance. For example, a feeder length of 1000 m gives an interval distance of 333 m (1000/3) for a 3 terminal feeder and an interval distance of 67 m (1000/15) for a 15 terminal feeder. As expected the shorter the terminal interval length the higher the MPVG/phase. The lower impedance due to the reduced length gives less voltage rise (power flowing towards the DTx) allowing more PV to be installed. For the MPVG/household and MPVG/phase curve, which is plotted for a given number of terminals, if the curve is known for one particular number of terminals, the curve for any number of terminals can be derived, for a particular feeder. How the 15T MPVG/household and MPVG/phase curve is derived from the 3T curve is demonstrated in Section 5.1.3.1.

5.1.3 Results

5.1.3.1 Relationship between MPVG/Household and Load/Household

For a 15T feeder, Figure 5.3 shows the relationship between load/household (0-10 kW) and MPVG/household for a given feeder length (50-500 m) required for the end of the feeder to reach the voltage limit of 253 V, a 3.3 V change.

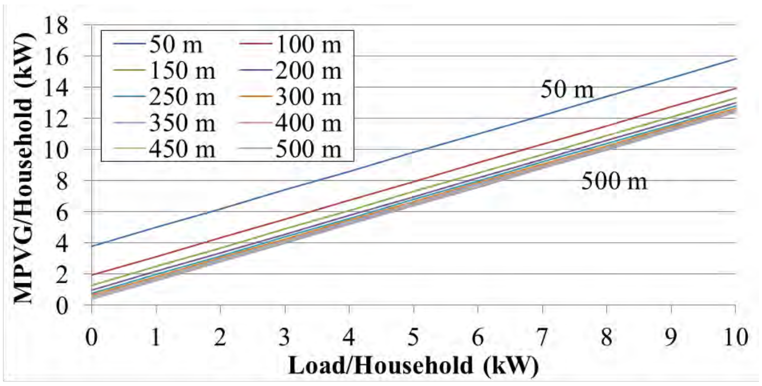

Figure 5.3 MPVG/household (kW) versus load/household (kW) for a 15 terminal feeder with feeder length ranging from 50 m to 500 m in 50 m increments. The top line is for 50 m and the bottom for 500 m

The linear relationship between MPVG/household and load/household for all terminal counts (3T to 15T) is the same, where

$$C_v = {MPVG/Household}/{(load/household)} \tag{5.3}$$

The value of C_v will vary with feeder impedance, for this case study C_v is calculated to be 1.2. The relationship takes the following simple form (5.4).

$$MPVG/Household = C_v * (load/household) + maxPVh_{offset} \tag{5.4}$$

Where $maxPVh_{offset}$ is the MPVG/household when load/household equals 0 kW. Note that the relationship (5.4) holds for MPVG/phase and load/phase, giving (5.5)

$$MPVG/phase = C_v * (load/phase) + maxPVph_{offset} \tag{5.5}$$

Where $maxPVph_{offset}$ is the MPVG/phase when load/phase equals 0 kW.

5.1.3.2 Relationship between MPVG/phase, Terminal count and Feeder Length

To further develop the method it was necessary to determine a relationship between MPVG/phase and terminal count. Referring to Figure 5.2, the relationship between the curves is non-linear with respect to feeder length. It was discovered that multiplying each curve by feeder length produces a linear plot, see Figure 5.4. From Figure 5.4, for each plot (3T to 15T), the relationship between feeder length and *maxPVphfl* has the form (5.6)

$$maxPVphfl = C_{vfl} * \left(feeder\ length - FL_{offset}\right) + maxPVphfl_{offset} \tag{5.6}$$

Where FL_{offset} is the feeder offset length (in this case 50 m) and $maxPVphfl_{offset}$ is *maxPVphfl* at FL_{offset}.

The linear relationship between feeder length and *maxPVphfl* for all terminal counts (3T to 15T) is the same, where

$$C_{vfl} = {}^{maxPVphfl}\!/_{feeder\ length} \tag{5.7}$$

As per C_v, the value of C_{vfl} will vary with feeder impedance, for this case study C_{vfl} is calculated to be 12.

The curves (3T to 15T) in Figure 5.4 also have a relationship which relates terminal count to *maxPVphfl* and is independent of feeder length. Figure 5.5 is simply Figure 5.4 with feeder length and terminal count switched and shows that the *maxPVphfl* curves for each feeder length are of the same form. The offset between each curve can be calculated using (5.6). The curves in Figure 5.5 have the form (5.8)

$$f(x) = C(1 - e^{-kx}), k > 0 \tag{5.8}$$

This is the same as discovered in [6] that with increasing village participation (equivalent to terminal count) MPVG increased as per an increasing decaying exponential. Referring to Figure 5.5, a curve fitting using the form of (5.8) was attempted on the 50 m curve in Figure 5.5.

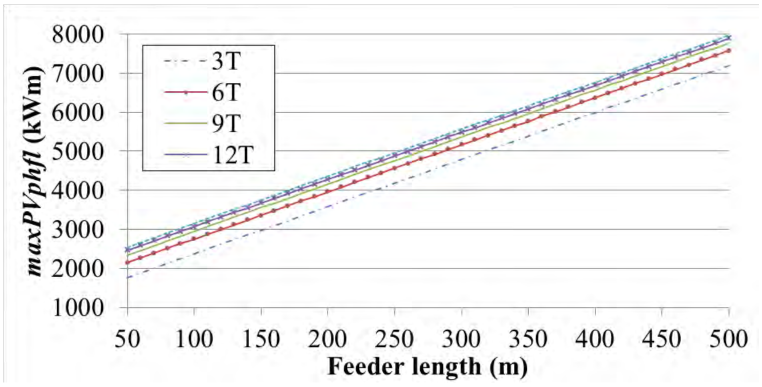

Figure 5.4 (MPVG/phase)*feeder length (maxPVphfl) versus feeder length for terminal count 3 to 15. This plot is a linearised version of Figure 5.2. The top plot is for 15 terminals and the bottom for the 3 terminals case

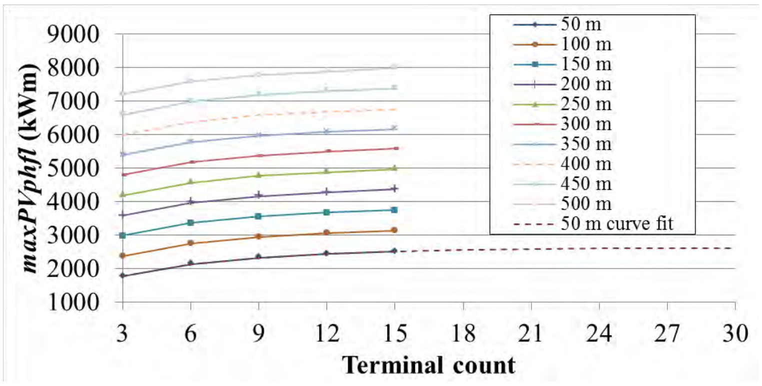

Figure 5.5 maxPVphfl versus terminal count. Figure 5.4 with feeder length and terminal count switched. Included is the 50 m curve fit. The curves range from 50 m (bottom) to 500 m (top) in 50 m increments

The fit was poor so a variation on the increasing decaying exponential was used instead (5.9), giving a superior fit.

$$f(x) = C_L(1 - e^{-kx}) - C_{offset}, k > 0 \tag{5.9}$$

Equation (5.10) gives the fit for the 50 m curve from Figure 5.5.

$$maxPVphfl = 6800\left(1 - e^{-0.52\left(\left(\frac{tc}{3}\right)+3\right)}\right) - 4180 \tag{5.10}$$

Where tc is the terminal count. Through (5.10) it is possible to determine the

MPVG/phase for all terminal counts for a feeder length of 50 m. When combined with (5.6) it is possible to calculate the *maxPVphfl* for any feeder length. Dividing *maxPVphfl* by feeder length then gives the MPVG/phase at that feeder length for a 10 kW load/phase.

Using (5.6) and (5.10), the 15T MPVG/phase curve (refer to Figure 5.2) for 10 kW load/phase was derived. Figure 5.6 shows how the derived curve compares with the actual 15T curve. The error between the two curves is below 1.2% for all feeder lengths.

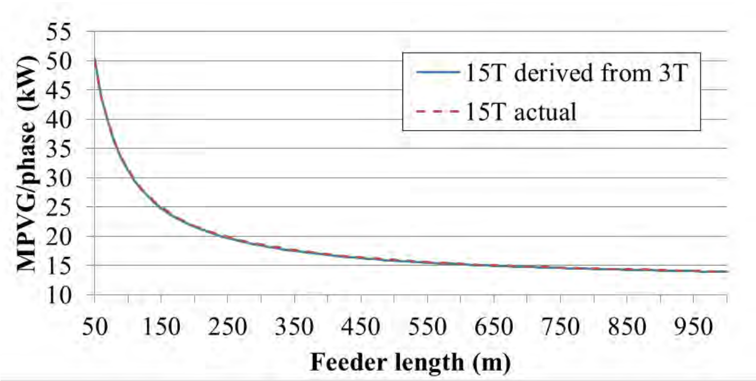

Figure 5.6 Curve derived from 3T and original 15T curve. Curves give MPVG/phase (kW) for 10 kW load/phase. Feeder length ranges from 50 m to 1000 m with 10 m increments

5.1.3.3 Estimation of MPVG/Phase

Using (5.5), (5.6) and (5.10) it is possible to determine the MPVG/phase for any load/phase, feeder length and terminal count, given the network configuration and cable assumptions used for this study. For example, in order to estimate the MPVG/phase for a 15 terminal feeder, with 75 kW load/phase and a length of 200 m the DNO would first use (5.10) to determine the *maxPVphfl* for 15 terminal, 50 m long feeder with 10 kW load/phase, getting 2520 kWm. We then use (5.6) to get the *maxPVphfl* at 200 m, 4320 kWm, and then divide by feeder length (200 m) to get the MPVG/phase, 21.6 kW. Finally, (5.5) is used to determine the MPVG/phase for 75 kW load/phase, giving 99.6 kW. In DIgSILENT; a power flow calculation for a 200 m long, 15 terminal feeder with 99.6 kW PV/phase and 75 kW load/phase gives an end of feeder voltage of approximately 252.98 V, confirming the estimation method.

5.1.4 Discussion

As shown in Section 5.1.3, the method by which the MPVG/phase is estimated is accurate given the assumptions involved. Note, however, that the assumption of evenly distributed PV and load has parallels with the use by DNOs of an After Diversity Maximum Demand (ADMD) metric when determining network capacity. ADMD is essentially the average demand per household and is used by DNOs for network planning. The load/household and PV/household parameters might, in this context, be considered the average load/household and average PV/household.

5.1.5 Conclusion

In Section 5.1, the voltage profile was obtained through power flow simulations for a large range of feeder configurations and PV and load profiles. The derivation of a relationship between MPVG, terminal count, total feeder impedance and load was obtained through analysis of these voltage profiles. It is assumed that all load and PV are evenly distributed along the feeder and that load and PV are at unity power factor. The X/R ratio of the feeder cable is kept constant. Under these assumptions, it was discovered that the upper voltage limit breach always occurred at the end of the feeder. A method was then developed using the end of feeder voltage as the voltage reference. It was demonstrated that the method effectively and accurately determined the MPVG for a given feeder impedance, terminal count and load.

The method is considered a tool, albeit a simple one, which DNOs could use to make MPVG estimates for their LV feeders. The method however, due to its simplified conditions, does have limited application under realistic network conditions. The research presented in Section 5.2 presents a more sophisticated method that overcomes these limitations.

5.2 A Comprehensive MPVG Estimation Method for Residential LV Feeders

The research presented in Section 5.2 is based on the author's journal paper "Maximum PV Generation Estimation Method for Residential Low Voltage Feeders", published in Sustainable Energy, Grids and Networks [7].

5.2.1 Introduction

As noted in Section 3.2.3, a method derived through analytical means for estimating the MPVG for LV feeders is presented in Section 5.2. The method is more sophisticated that that presented in Section 5.1 and can potentially be applied to a DNOs entire distribution network. It more completely addresses MPVG knowledge gaps 1-4 and limitations 5-8 in current DNO PV installation assessment processes defined in Section 3.2.

The research in Section 5.2 presents a MPVG estimation method (MPVGEM) which can be used to estimate the MPVG for all LV (11 kV/400 V) feeders within the LV network of a DNO. The MPVGEM does not require power flow analysis software, and can be implemented in standard spreadsheet software. The MPVGEM aims to provide a more sophisticated approach than that currently employed by Australian DNOs when assessing new PV installation applications (see Section 5.2.6 for discussion on this point) whilst still relieving them of the need to perform dedicated power flow calculations.

The MPVGEM is presented in Section 5.2, along with a comparison of its results against those calculated by power flow analysis software package DIgSILENT. Section 5.2 is structured as follows. Section 5.2.2 defines the Nomenclature, Section 5.2.3 describes the method and results are presented in Section 5.2.4. Section 5.2.5 investigates the application of the MPVGEM with imbalanced load and PV generation and Section 5.2.6 discusses the utility of the MPVGEM. Section 5.2.7 gives a derivation of the MPVGEM equation (5.12) and in Section 5.2.8 an example application of the MPVGEM is demonstrated. Section 5.2.9 provides concluding comments.

5.2.2 Nomenclature

The nomenclature listed here applies to Section 5.2 only.

V_{ul}	Upper voltage limit. Assigned to the *last PV household*
V_{lvp}	Voltage at the LV point
V_m	Mean voltage estimate, see equation (5.31)
$R_{b,lvp}$	Resistance between bus *b* and the LV point
$X_{b,lvp}$	Reactance between bus *b* and the LV point
n	Number of households on each phase
m	Number of households with PV systems on each phase
R_{cc}	Resistance of the household connection of the *last PV household*
X_{cc}	Reactance of the household connection of the *last PV household*
P_b	Real load at bus *b*
Q_b	Reactive load at bus *b*
P_l	Real load for the *last PV household*
Q_l	Reactive load for the *last PV household*
P_{PV}	MPVG real power estimate for each PV system
Q_{PV}	MPVG reactive power estimate for each PV system
η_b	Number of PV systems connected at bus *b*
$\alpha_{i,b}$	Normalised value for data point *i* of the generation time-series applied to the PV system at bus *b*
$P_{b,+120}$	Refers to equation (5.20), and is the PV generation at bus *b* from the +120° phase line
$P_{b,-120}$	Refers to equation (5.20), and is the PV generation at bus *b* from the -120° phase line
X_m	refers to equation (5.20), and is the mutual inductance between phases in Ω/km.
R_s	refers to equation (5.20), and is the line series resistance in Ω/km

5.2.3 Method

For a LV feeder, the 11 kV line is 3-wire and 400 V line three-phase, four-wire. The neutral wire is multigrounded, with the resistance between the neutral and earth assumed to be zero. The 400 V line can therefore be analysed as three-wire [38]. Testing is conducted under balanced load and PV generation and mutual coupling between phases can therefore be neglected. The MPVGEM presented in this section, consequently, does not take into account mutual coupling between phases. When load or PV generation is imbalanced mutual coupling between phases may need to be taken into account. The impact on MPVGEM estimation accuracy due to imbalanced load or PV generation, when mutual coupling is not taken into account, is discussed in Section 5.2.5. A supplementary method which does take into account mutual coupling when PV generation is imbalanced is presented in Section 5.2.5.3.

The MPVGEM calculates the MPVG for one phase at a time. When determining the MPVG for one phase, the conventional power flow equation (5.11) can be used.

$$V_x = \left[\frac{V_y^2 + R_{x,y}P_y + X_{x,y}Q_y}{V_y}\right] + j\left[\frac{X_{x,y}P_y - R_{x,y}Q_y}{V_y}\right] \tag{5.11}$$

To be able to solve for the MPVG analytically, the imaginary component of (5.11) needs to be removed. This will only have a minor effect on the MPVG estimation, accuracy as the real component of (5.11) is much larger than the imaginary component. See Section 5.2.9 for evidence justifying this simplification.

Equation (5.11) is applied between two known voltage points, in our case the Low Voltage Point (LVP), with a voltage of V_{lvp}, and the *last PV household*, assigned the upper voltage limit (V_{ul}). The *last PV household* is the household with a PV system installed where the impedance between itself and the LVP is the largest. When equation (5.11) is applied between two known voltage points on a LV feeder consisting of PV generation and loads, equation (5.12) can be derived. See Section 5.2.7 for derivation.

$$V_{lvp} = \frac{V_m V_{ul} + \left(P_l R_{cc} + \sum_{b=1}^{n} P_b R_{b,lvp}\right) + \left(Q_l X_{cc} + \sum_{b=1}^{n} Q_b X_{b,lvp}\right) - \left(P_{PV} R_{cc} + \sum_{b=1}^{m} \eta_b P_{PV} R_{b,lvp}\right)}{V_m} \tag{5.12}$$

Equation (5.12) is made up of three components, $Load_P$ (5.13), $Load_Q$ (5.14) and Solar$_P$ (5.15).

$$Load_P \equiv P_l R_{cc} + \sum_{b=1}^{n} P_b R_{b,lvp} \tag{5.13}$$

$$Load_Q \equiv Q_l X_{cc} + \sum_{b=1}^{n} Q_b X_{b,lvp} \tag{5.14}$$

$$Solar_P \equiv P_{PV} R_{cc} + \sum_{b=1}^{m} \eta_b P_{PV} R_{b,lvp} \tag{5.15}$$

P_{PV} is the MPVG real power estimate for every PV household. Equation (5.12) is re-arranged to make P_{PV} the subject. The MPVGEM has only been tested where PV systems operate at unity power factor; therefore $Solar_Q$ (5.16) is not included in (5.12). Section 5.2.3.1 explains how PV systems operating at non-unity power factor can theoretically be included in the MPVGEM. If (5.12) were to include $Solar_Q$ it would still solve for P_{PV} with Q_{PV} calculated afterwards using (5.17). As PV systems operating at non-unity power factor are not considered in this research, henceforth any reference to the MPVG is a reference to the MPVG real power, P_{PV}. For a given set of feeder and load characteristics, the MPVGEM estimates only one value of P_{PV}. For $Load_P$ and $Load_Q$, if the bus is located beyond the bus of the *last PV household* then $R_{b,lvp}$ and $X_{b,lvp}$ is equal to the resistance and reactance between the bus of the *last PV household* and the LVP. The estimated MPVG is the maximum each PV system can generate, the rated power. If any of the PV systems are not generating rated power then the upper voltage limit will not be reached.

5.2.3.1 Non-unity Power Factor PV Generation

Non-unity power factor PV generation can theoretically be incorporated into the MPVGEM, by adding the component $Solar_Q$ (5.16) to (5.12).

$$Solar_Q \equiv Q_{PV} X_{cc} + \sum_{b=1}^{m} \eta_b Q_{PV} X_{b,lvp} \tag{5.16}$$

This is for a known, static, PV system power factor (pf_{PV}), the relationship between Q_{PV} and P_{PV} is defined by (5.17).

$$Q_{PV} = P_{PV}\sqrt{\frac{1-pf_{PV}^{2}}{pf_{PV}^{2}}} \tag{5.17}$$

An MPVG for inverters with *Q(V)* control could also be incorporated. A theoretical approach is presented below

It would be a 2 step process. The first step calculates the MPVG assuming no *Q* from each inverter and the voltage at each household then calculated using the first step MPVG. Once an estimated voltage is known the pu Q value can then be estimated, according to the *Q(V)* characteristics of each inverter. From the Q-P relationship of the PV inverter the pu P value can then be calculated and thus the total allowable capacity of the PV system. This will give a different MPVG estimation for each household as the Q value at each household will be different

This extension has not yet been tested but could be an avenue for future research. To the author's knowledge, no research has been conducted in this area.

5.2.3.2 Time-series Analysis

Time-series load and generation data can be input to the MPVGEM, with the MPVG calculated at each data point. The smallest calculated MPVG for the time-series is selected as the final MPVG estimate. The generation data set, either of insolation or actual PV generation, would be normalised. The normalised value ($\alpha_{i,b}$) scales P_{PV} for the MPVG calculation at each data point (5.18).

$$Solar_P \equiv P_{PV}R_{cc} + \sum_{b=1}^{m}\alpha_{i,b}\eta_b P_{PV}R_{b,lvp} \tag{5.18}$$

5.2.4 Results

The significant voltage changes on a LV feeder occur at the 400 V level, therefore the accuracy of the MPVGEM is tested at the 400 V level. A case study is presented in Section 5.2.4.7 where the MPVG estimation also includes an 11 kV section of a LV feeder. Note that for the case study, all PV systems are connected at the 400 V level

5.2.4.1 400 V Line Template

A 400 V line DIgSILENT template provided by a DNO servicing Greater Western Sydney is used for testing. An example of a six terminal 400 V line is given in Figure 5.7. A terminal is the point on the line where the household is connected; each terminal has 2 households connected. The household connection (R_{cc}, X_{cc}) is single phase and connects the household to a terminal on the 400 V line. For the purposes of applying equation (5.12) to a 400 V line, a terminal is equivalent to a bus *b*. PV generation and load for each household is represented by a *P*, *Q* value. When applying the MPVGEM to a 400 V line, the LVP is at the DTx and V_{lvp} is equal to the voltage on the LV side of the DTx under zero load conditions.

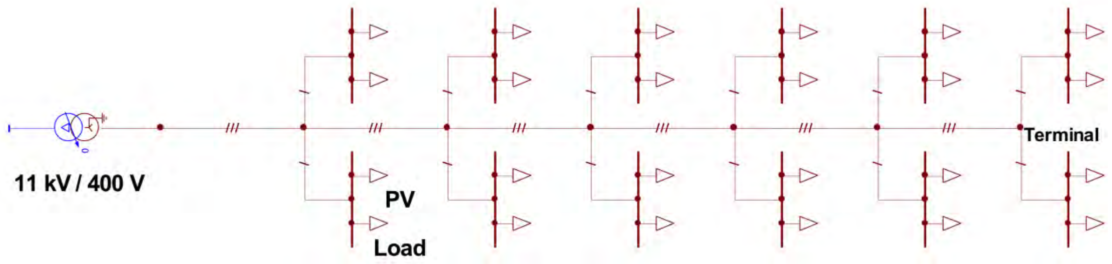

Figure 5.7 Example of a six terminal 400 V line

5.2.4.2 Testing Method

The MPVGEM is implemented in standard spreadsheet software (for our research, MS Excel). For every test case, load conditions and line characteristics are entered into the spreadsheet and the MPVG estimated. Following this, the same load conditions and line characteristics are setup in DIgSILENT using the template described in Section 5.2.4.1. Each PV system is then set to the MPVG estimated by the MPVGEM. A power flow calculation is then executed and the voltage for the *last PV household* recorded. The Newton-Raphson method is used in DIgSILENT to conduct the power flow calculation. Under balanced load conditions, determining the MPVG for one phase is equivalent to determining the MPVG for all phases.

The MPVGEM MPVG estimation error is the recorded voltage at the *last PV household* minus the upper voltage limit, V_{ul}. A positive estimation error occurs when the MPVGEM overestimates the MPVG and vice-versa.

5.2.4.3 400 V Uniform Line Testing

A 400 V *uniform* line has the following characteristics: every household has a PV installed, every household has the same load and the impedance between each terminal is the same.

Testing of 400 V *uniform* lines allows for the MPVG estimation accuracy for a large number of load conditions and line characteristics to be determined. The influence of load conditions and line characteristics on the MPVG estimation accuracy can then be assessed.

The accuracy of the MPVG estimate was tested for DTx voltages (V_{lvp}) of 249.7, 243 and 236 V and under the set of load conditions and line characteristics specified in TABLE 5.1. These voltages represent 3 different tap settings on the DTx; each change in tap gives a 2.5% change in voltage. For many Australian DNOs, the regulation voltage range is 230V+10%/-6%, or 216-253 V. The upper voltage limit (V_{ul}) is therefore set to 253 V for all test cases. For the DNO who provided the 400 V line template, the average 400 V line resistance is around 0.5 Ω/km (approximately 70 mm^2 cross-section for aluminium conductor) and a mean *X/R* ratio around 0.5. Varying the distance between terminals is equivalent to altering the impedance between terminals and the total impedance for the line. The range of line reactance values tested, 0.125 to 0.375 Ω/km, give line *X/R* ratios of approximately 0.25 to 0.75 for a line resistance of 0.5 Ω/km. This range of *X/R* ratios approximately equates to the range of *X/R* ratios for the different 400 V cable typically used by Endeavour Energy. Around 0.5 kVA is a typical household mean midday load [117]. The typical load input to the MPVGEM would be a mean or minimum midday load.

TABLE 5.1 Load conditions and line characteristics used for testing MPVG estimation accuracy for 400 V *uniform* lines

Terminal count (t)	**Distance between terminals (m)**	**Line reactance (Ω/km)**
3,6,9,12,15	10, 20, 30, 40, 50	0.125, 0.25, 0.375
Line resistance (Ω/km)	**Load (kVA)**	**Load pf**
0.5	0, 0.5, 1	0.85, 0.9, 095

Figure 5.8 gives the results of this testing. Results show that the estimation error range is between -0.1 V and 0.5 V. The bias of the estimation error towards the positive indicates that the MPVGEM tends to overestimate the MPVG.

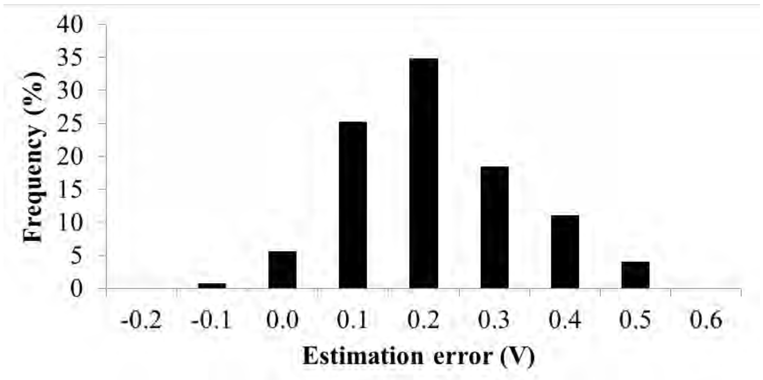

Figure 5.8 Histogram of MPVG estimation accuracy, DTx voltage set to 249.7, 243 and 236 V, 400 V *uniform* line for load conditions and line characteristics presented in TABLE 5.1

TABLE 5.2 below gives an example of the MPVG for a DTx voltage set to 236 V, an upper voltage limit of 253 V, a distance between each terminal of 30 m, and a line resistance of 0.5 Ω/km and X/R ratio of 0.25.

TABLE 5.2 Example MPVG calculations for a range of customers with DTx voltage set to 236 V, a distance between terminals of 30 m, line resistance 0.5 Ω/km and *X/R* ratio of 0.25

Customers	2	4	6	8	10
MPVG (kW)	41.45	16.52	8.81	5.56	3.92

5.2.4.4 Dependency of MPVGEM Estimation Accuracy

The results of the 400 V *uniform* line testing were examined to ascertain how load conditions and line characteristics influenced estimation accuracy. Significant variation in estimation error was found to occur with changes in DTx voltage and line *X/R* ratio whilst estimation error did not vary significantly with terminal count, distance between terminals or load.

Further investigation is required to determine why estimation error increases for lines with higher *X/R* ratio and with decreasing DTx voltage. Figure 5.9 gives the change in estimation error with decreasing DTx voltage. The lower the DTx voltage the greater the difference in voltage between V_{lvp} and the upper voltage limit (V_{ul}). Figure 5.9

shows that the estimation error becomes more positive, indicating an increase in overestimation, for line *X/R* ratios of 0.25 and 0.5 with decreasing DTx voltage, whilst the estimation error becomes more negative, indicating an increase in underestimation, for a line *X/R* ratio of 0.75. The increase in overestimation and underestimation with decreasing DTx voltage is approximately linear for all line *X/R* ratios. Figure 5.9 indicates that the MPVGEM overestimating the MPVG tends to increase with decreasing line *X/R* ratio. An *X/R* ratio < 1 is typical for a 400 V line, where the resistance is typically much larger than the reactance.

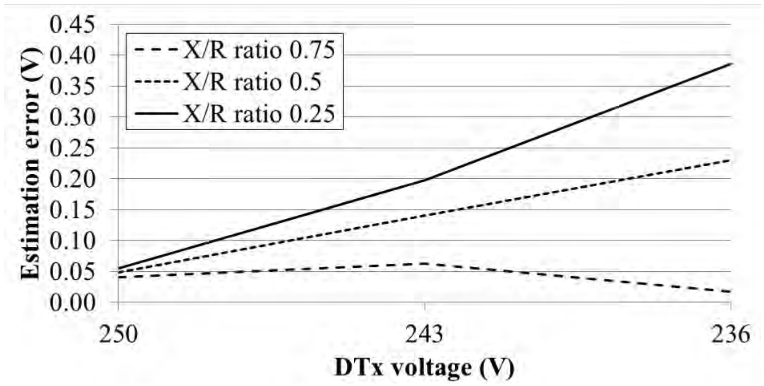

Figure 5.9 Estimation error with decreasing DTx voltage for a given line *X/R* ratio.

Estimation error results for Figure 5.10 through to Figure 5.13 are for a DTx voltage of 236 V; the variation in estimation error is greatest at 236 V. Results will therefore more clearly illustrate the dependence of estimation accuracy on different line characteristics and load conditions.

Figure 5.10 gives the change in estimation error with increasing terminal count for a given line *X/R* ratio and shows that estimation error remains relatively constant with increasing terminal count (*t*) for each line *X/R* ratio. Testing of the MPVGEM in DIgSILENT was limited to fifteen terminals. Estimation error remaining steady with increasing terminal count indicates the MPVGEM estimation accuracy will likely be maintained for lines with a terminal count greater than fifteen.

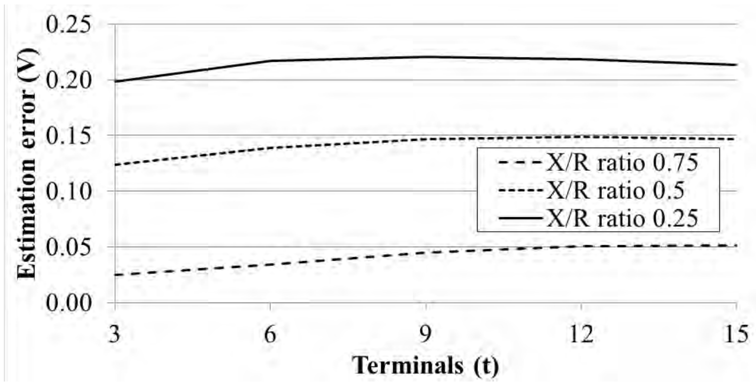

Figure 5.10 Estimation error with increasing terminal count (t) for a given line X/R ratio, DTx = 236 V

Figure 5.11 shows the change in estimation error with increasing distance between terminals for a given line X/R ratio. An increase in the distance between terminals is equivalent to an increase in line impedance. Figure 5.11 shows that estimation error becomes only slightly more negative with increasing distance between terminals for each line X/R ratio, confirming that estimation error variation is independent of line impedance.

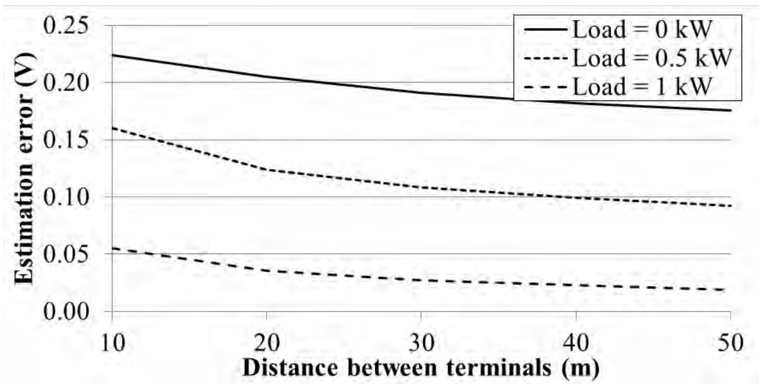

Figure 5.11 Estimation error with increasing distance between terminals for a given line X/R ratio, DTx = 236 V

Figure 5.12 and Figure 5.13 show the change in estimation error with increasing load and increasing load power factor for a given line X/R ratio. Both figures show that estimation error remains relatively constant with increasing load and load power factor. These final two figures confirm that estimation error varies only with DTx voltage and line X/R ratio.

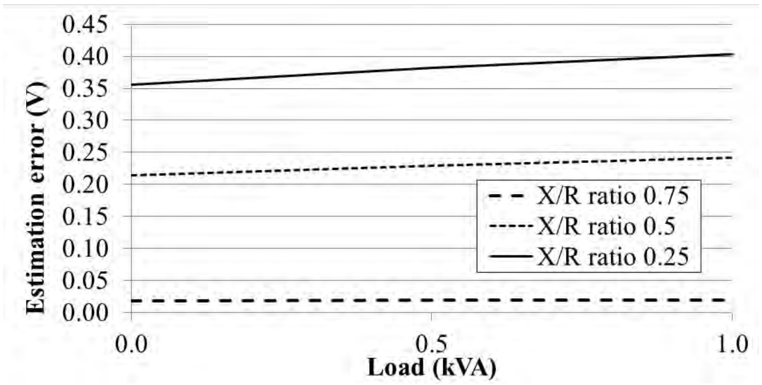

Figure 5.12 Estimation error with increasing load (kVA) for a given line *X/R* ratio, DTx = 236 V

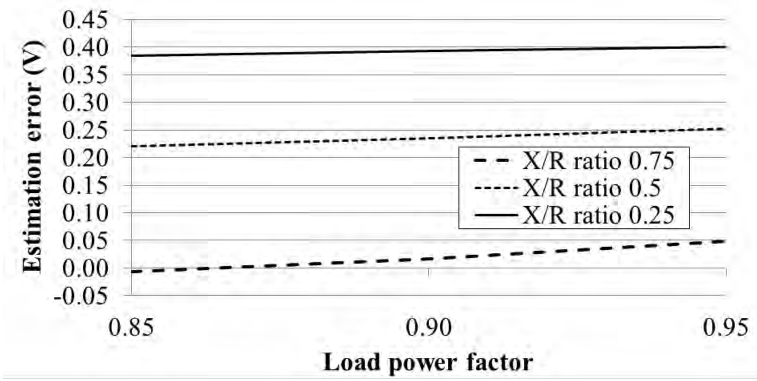

Figure 5.13 Estimation error with increasing load power factor for a given line *X/R* ratio, DTx = 236 V

5.2.4.5 400 V Non-uniform Line Testing

Non-uniform lines have different distances between terminals, loads are different, not all households have PV systems installed and the line type is not the same for the length of the line.

The first chosen scenario tests the accuracy of the MPVGEM with varying load and varying line types, using a 400 V 15 terminal line. Two line types are used: type 1 has a resistance of 0.2 Ω/km and reactance zero and type 2 has a resistance of 0.5 Ω/km and a reactance of 0.5 Ω/km. The DTx is set to 249.7 V. Note that a 400 V line with zero reactance is not realistic; is it used here as a boundary test. The line is arranged in two ways, type 1 for the front half and type 2 for the back half and vice versa. All loads have a power factor of 0.9 but either increase linearly from 0.25 to 0.75 kVA with distance from the DTx or decrease linearly from 0.75 to 0.25 kVA. The varying load allocation combined with two line types and arrangements gives four test scenarios. The MPVG estimation proved to be as accurate as it was for 400 V *uniform* lines with the estimation error within 0.1 V for all scenarios. This test demonstrates that variation in load and variation in line type has little impact on the accuracy of the MPVGEM.

The final set of tests conducted also use a 400 V fifteen terminal line. For a large number of tests, the line was randomly allocated line characteristics and load conditions from TABLE 5.1. Individual households are assigned different load sizes and power factors, load is balanced across phases; distances between terminals differed and *X/R* ratios were varied along the length of the line. Finally, only select households have a PV system installed. Note, however, that PV generation is still balanced across phases; therefore if Household 10 is selected as having a PV system installed then the 10th household on each phase has a PV system installed. Figure 5.14 represents the arrangements of PV household allocation tested where a shaded block indicates that PV is installed at that household. Note that a 400 V fifteen terminal line has ten households on each phase. Testing is conducted for DTx voltages of 249.7, 243 and 236 V.

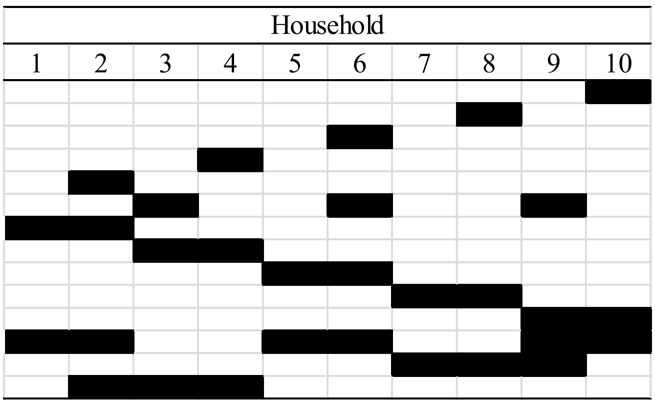

Figure 5.14 Arrangements of selected households with PV systems installed. A shaded mark indicates a PV system is installed at that household

Figure 5.15 gives the results of the testing. Results show that the estimation error ranges from -0.6 to 0.7 V and confirm that the MPVGEM can accurately estimate the MPVG for *non-uniform* lines where only select households have a PV system installed.

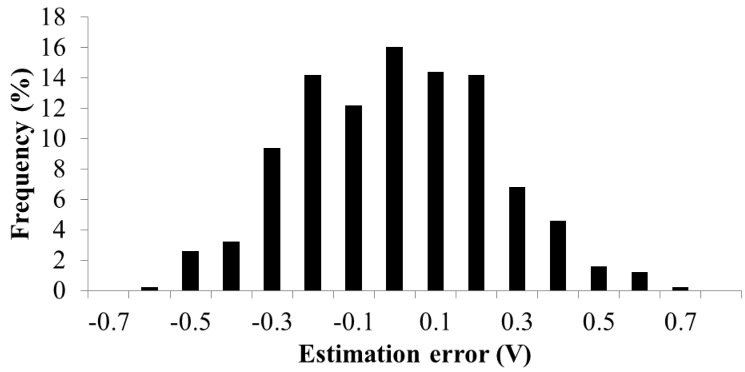

Figure 5.15 Histogram of MPVG estimation accuracy for a 400 V fifteen terminal *non-uniform* line. DTx voltages 249.7, 243 and 236 V. PV systems are arranged as described Line characteristics and load conditions are randomly selected from TABLE 5.1

5.2.4.6 MPVGEM at Higher Terminal Counts

Also of importance for the broader applicability of MPVGEM, is how it might perform at higher terminal counts. As per Figure 5.10, the argument that the estimation error will remain within similar bounds for higher terminal counts is supported by Figure 5.16 which shows that, by fifteen terminals, the difference between the estimated MPVG and the MPVG calculated by DIgSILENT has reduced from 1 kW to less than 0.1 kW for all cases. Assuming this trend continues with increasing terminal count, the estimation accuracy will also remain high.

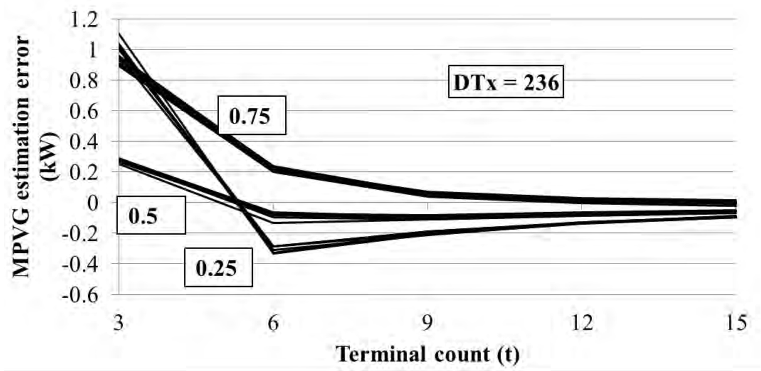

Figure 5.16 MPVG estimation error, DTx voltage = 236 V, line *X/R* ratio of 0.25, 0.5, 0.75

5.2.4.7 Case Study

The MPVGEM is used to estimate the MPVG for the section of an actual LV feeder [38] which includes both the 11 kV and 400 V lines, see Figure 5.17. The feeder is considered a typical Australian semi-rural feeder. The feeder is 80 km long and includes three voltage regulators. The voltage regulators split the feeder into four sections. The MPVGEM is applied to one section at a time, between a voltage regulator and the *last PV household* for the section. In this case the MPVG for the final section is calculated, downstream of the voltage regulator located at bus 27. Figure 5.18 shows this section of the feeder, including the 400 V line in detail. The distance between each bus is 500 m, using a typical 11 kV overhead line. Each 400 V line is assumed to have the same configuration, load is set to zero, each household has a PV system installed, and households are evenly distributed across the three phases. Under these conditions the *last PV household* will be located at the end of the 400 V line connected at bus 32, the impedance between itself and the voltage regulator is the highest. The MPVGEM is calculated under static conditions; therefore a static voltage at the output of the regulator needs to be assumed. The voltage regulator is assumed to maintain voltage at 11 kW, 1pu. The regulator is assumed to be zero for the case study. Although the impedance of the voltage regulator can be incorporated into the MPVGEM by including it in the variables $R_{b,lvp}$ and $X_{b,lvp}$. The DTx is set to a neutral tapping. This tap setting is arbitrary and does not influence the accuracy of the MPVGEM. If a non-neutral DTx tap setting is selected, then the step change (ΔV_{dtx}) needs to be included in equation (5.12), see equation (5.19) below.

$$V_{lvp} = \frac{\Delta V_{DTx} + V_m V_{ul} + \left(P_l R_{cc} + \sum_{b=1}^{n} P_b R_{b,lvp}\right) + \left(Q_l X_{cc} + \sum_{b=1}^{n} Q_b X_{b,lvp}\right) - \left(P_{PV} R_{cc} + \sum_{b=1}^{m} \eta_b P_{PV} R_{b,lvp}\right)}{V_m} \tag{5.19}$$

With the *last PV household* located at the end of bus 32, the “trunk” path of the LV feeder runs from the voltage regulator to *the last PV household*. The MPVGEM equations are applied to the trunk to calculate the MPVG. All “non-trunk” paths, side branches, have their real and reactive power aggregated; this power is considered at the point of connection with the trunk. Using bus 28 as an example; P_b and Q_b will be the aggregate of the real and reactive power for busses 28 and 55 to 58, and $R_{b,lvp}$ and $X_{b,lvp}$ will be the impedance between bus 28 and the voltage regulator, and η_b is the number of

PV systems located on the side branch. Note that for the 400 V line, each terminal is regarded as a bus, with η_b equal to 1.

The estimated MPVG by the MPVGEM is **20 kW**. When tested in DIgSILENT as described in Section 5.2.4.2, the estimation error is 0.004 pu, or 1 V.

If the MPVG for the second section of the LV feeder were to be calculated, downstream of the voltage regulator at bus 9 and upstream of the voltage regulator at bus 17, then the MPVG for the both the third section and the last section would need to be calculated first. The sections beyond bus 17 can then be represented by the aggregate PV generation (the number of PV systems multiplied by the MPVG) and the aggregate load of the third and last sections. The simplified test conditions used are sufficient to show the capability of the MPVGEM to determine the MPVG for a section of a LV feeder which includes both the 11 kV and 400 V lines. It is not necessary to test the MPVGEM further under various configurations as the significant voltage rise occurs at the 400 V level. For this case study, with a MPVG of 20 kW, the voltage rise along the 11 kV trunk is only 0.005 pu, while the voltage rise along the 400 V line is 0.1 pu. The voltage rise along the 400 V line is therefore 20 times that of the 11 kV line. The generation from PV systems installed on the 400 V line will be curtailed due to upper voltage constraints well before high voltages are experienced on the MV network. This is also the reason why MV equipment such as STATCOM's are not considered in the study.

Whilst significant PV (solar farms) installed at 11 kV would certainly increase voltage levels in the MV network, at this point in time the majority of solar is installed at the 400 V level, and therefore the research focus has been at the 400 V level. A higher 11 kV voltage can be accounted for however by simply adjusting V_{lvp} upwards.

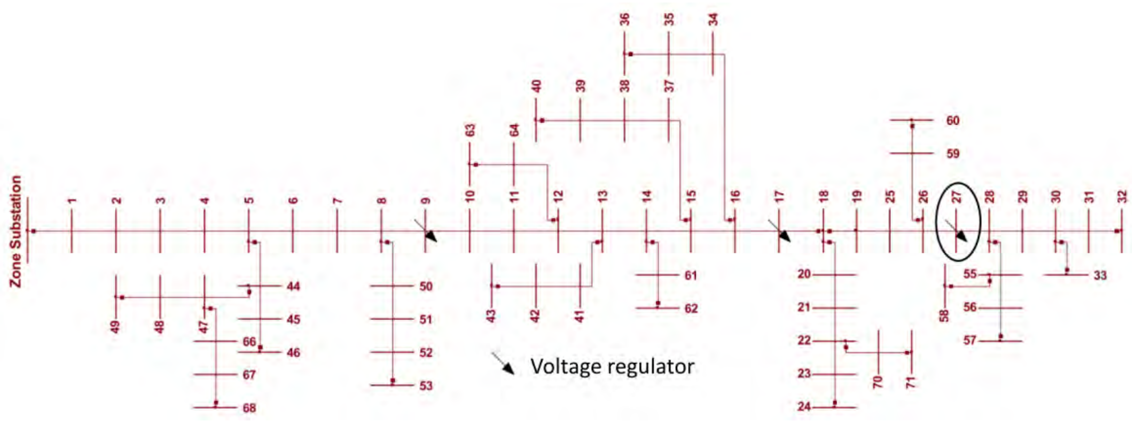

Figure 5.17 Case study LV feeder [38], Bus 27 is highlighted.

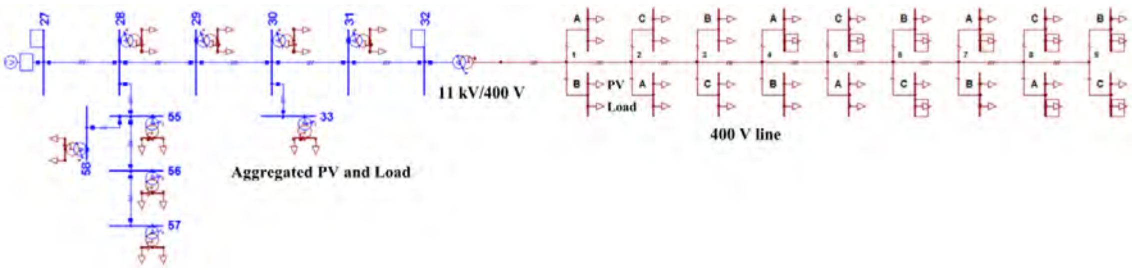

Figure 5.18 Case study LV feeder – downstream of bus 27

5.2.5 MPVGEM with imbalanced load or PV generation across phases

The MPVGEM presented in Section 5.2.3 does not take into account the mutual coupling between phases. This introduces some error into the estimated MPVG when load or PV generation is imbalanced. This section examines the impact of imbalanced load and PV generation on MPVGEM accuracy when mutual coupling is not taken into account, and also presents a supplementary method which does take into account mutual coupling.

5.2.5.1 Imbalanced Load

The typical, conservative, load input to the MPVGEM would be a mean or minimum midday load, possibly zero. Either way the load will be low, typically less than 0.5 kVA, given that there will be circumstances where the PV is generating at near rated output while household loads are low – typically on working weekdays which are sunny but not so hot that household air-conditioning is run. Under such circumstances, even if load is imbalanced across phases, the effect of this imbalance will also be low. Therefore, when the installed PV is the MPVG as per estimated by the MPVGEM under the condition of balanced load, there will be little deviation in the maximum voltage from the upper voltage limit. It is worth knowing however, the extent to which imbalanced load influences the voltage at the *last PV household* voltage.

The test line is a 400 V *uniform* line with fifteen terminals, distance between terminals is 20 m, line resistance is 0.5 Ω/km and line reactance is 0.25 Ω/km. The mutual inductance between phases is set to 0.3 Ω/km. This value of 0.3 Ω/km was taken from DIgSILENT, which calculates the mutual inductance between phases when a 3-phase overhead line is created. The distance between each phase was assumed to be 1 m. DTx is at 249.7 V and 0.5 kVA ± 25% at 0.9 pf is randomly assigned to each household, generating imbalanced load across phases.

1000 power flow calculations were conducted in DIgSILENT where each PV household is assigned the MPVG estimated under balanced load (0.5 kVA) but households are assigned an imbalanced load of 0.5 kVA ± 25%. Figure 5.19 presents a histogram of the introduced estimation error due to imbalanced load. The estimation error range under the same test conditions but with balanced load is ±0.1 V, an estimation error range of -0.2 V to 0.3 V for imbalanced load is only a slight increase.

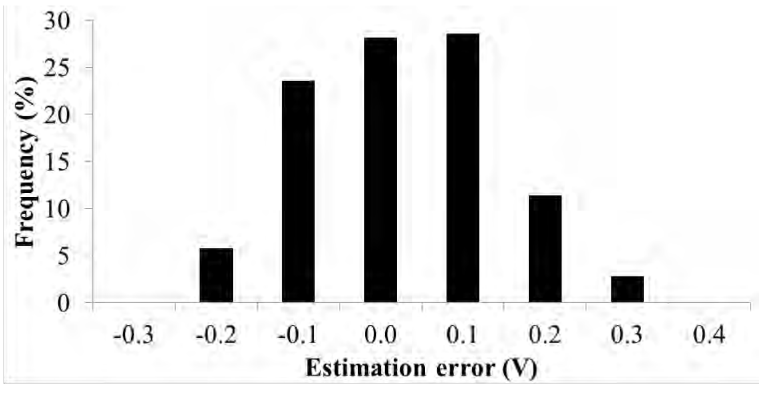

Figure 5.19 Introduced estimation error due to imbalanced load

5.2.5.2 Imbalanced PV Generation

The test line for imbalanced PV generation is the same as used for imbalanced load above, with the exception that load is set to zero and three levels of DTx voltage are tested, 249.7 V, 243 V and 236 V.

A worst case scenario is tested, where PV systems are only installed on two of the three phases. PV systems are randomly assigned to houses on the two phases. The MPVGEM would first estimate the MPVG for each phase. Using DIgSILENT; the estimated MPVG value is then assigned to the PV systems on the two phases. A power flow calculation is conducted and the voltage at *the last PV household* for each phase measured and the estimation error calculated. Estimation error results are presented in Figure 5.20, represented by the dark bar. Included in Figure 5.20 are the results for when equation (5.20) is incorporated into the MPVGEM, the light bar.

As evident in Figure 5.20, the impact of PV generation imbalance on MPVGEM accuracy can be substantial. The biggest error occurs at the lowest DTx voltage, 236 V, as the PV generation is the largest.

It is unlikely that a DNO would calculate MPVG values for a feeder with the intention of allowing excessive PV generation imbalance. To be fair to all future PV system owners, a reasonable approach would be that a DNO would calculate the MPVG under the condition that all homes will eventually have a PV system installed, with PV systems added gradually over time. For each new installation, the DNO would set the phase of the household to minimise imbalance. The results of Figure 5.20 illustrate the importance of this. If the size of each new PV installation is restricted to the MPVG calculated under the condition that all homes have a PV system installed, and phase imbalance is minimised as new installations are added, there is no risk of the upper voltage limit being exceeded.

5.2.5.3 Mutual Coupling

This section presents additional method to account for mutual coupling between phases, to be used in the case where PV generation imbalance is unavoidable. The first step is to calculate the MPVG for each phase using equation (5.12). The MPVG for each phase is then re-calculated, incorporating equation (5.20) below.

$$MC \equiv \sum_{b=1}^{n} \left(\frac{X_m}{R_s} \right) (P_{b,-120} - P_{b,+120}) R_{b,lvp} \tag{5.20}$$

For ease of calculation, at each bus, the PV systems installed on the other phases have their power referred across to the phase being re-calculated via the ratio of mutual inductance to series impedance (X_m/R_s). The light bar of Figure 5.20 shows the impact on MPVGEM accuracy when (9) is incorporated into the MPVGEM, the error spread is reduced significantly from -3.5 to 2 V to -1 to 0.75 V.

Whilst the estimated MPVG for each phase gives similar maximum voltage levels at the *last PV household* for each phase, PV generation will still be imbalanced across the phases, potentially producing imbalanced reverse power flow out of the 400 V line. Imbalanced generation can also come from larger 3-phase systems, due to PV panels not being evenly distributed across the three phases as well as partial shading [118]. To reduce the power imbalance flowing into the MV section a voltage sensitivity analysis and network re-configuration solution such as suggested in [36] could be considered.

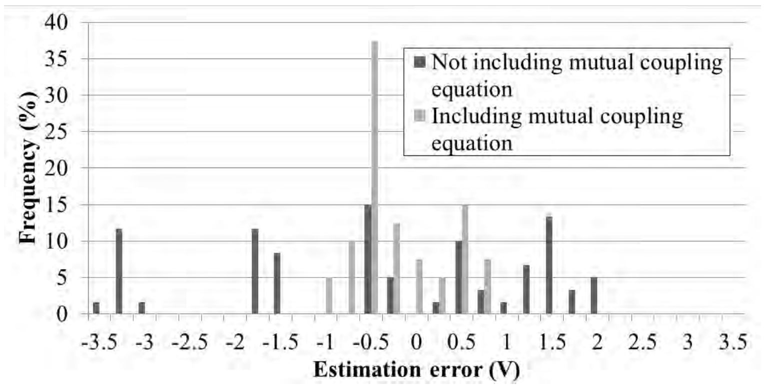

Figure 5.20 Estimation error with and without the mutual coupling equation

5.2.6 Utility of the MPVGEM

In Australia, the assessment process DNOs undertake when a new PV installation application is received varies. Some allow PV installations only up to a set limit [99] while others set a limit based on DTx capacity [100], [101]. DNO's experiencing greater PV penetration levels are more thorough, Ausgrid for example assesses each PV system to determine if "the contribution of the proposed PV installation to the steady state voltage rise on the LV distribution mains between the PCC and the DTx is greater than 1% of the nominal voltage, and if the steady state voltage rise on the distributor due to all embedded generation connected is greater than 2% of the nominal voltage"

[65] and if so network augmentation will be required. Ergon also undertakes a network impact assessment, but only if the PV system size is greater than 3.5 kVA [66].

Setting a hard limit or not assessing PV systems under a certain size has a number of shortcomings; it does not take into account the number of systems installed, their location on the LV feeder or the feeder characteristics. It can either result in excessive voltage rise or an under-utilisation of the LV feeders PV hosting capacity. Setting a limit based on transformer capacity is also not ideal; DTx sizing is calculated using load demand, not DG. The approach used by Ausgrid also has its limitations; a set percentage voltage rise does not take into account the DTx tap setting, a key factor when determining PV system size limits based on voltage rise. It is also iniquitous, allowing residents closer to the DTx to have larger systems compared to residents located further from the DTx, and favours early installers of PV systems.

Australian DNO's using the above rules for setting PV system size limits indicate that power flow analysis software is not, prior to a technical impact analysis, routinely used. As such, the MPVGEM could replace the above methods to give more accurate PV system size limits. In regard to planning: A DNO's LV network typically consists of a wide range of feeders with diverse characteristics, hence configuring power flow analysis software to determine PV generation limits for all cases where PV is being deployed would be a resource-intensive exercise. The same exercise could be accomplished far more quickly and easily using the MPVGEM.

The MPVGEM produces realistic high-penetration PV generation values for a LV network, values which could then be incorporated into a system wide bulk grid analysis. It is also suitable for researchers without access to, or the technical ability to use, power flow analysis software. The MPVGEM could also be used by DNOs in developing countries that may also not have access to power flow analysis software.

5.2.7 Derivation of MPVGEM Equation

A three bus feeder is used to derive equation (5.12). The voltage at the end of the feeder, bus 3, is assigned the upper voltage limit (V_{ul}), and the voltage at the start of the feeder, bus 1, is assigned the value V_{lvp}. Both V_{ul} and V_{lvp} are known values. It is assumed that a real (P) and reactive (Q) load and a PV system (P_{PV}) are located at busses 2 and 3. Using equation (5.11) and starting at bus 3 we have

$$V_2 = \frac{V_{ul}^2 + (R_{cc} + R_{2,3})P_3 + (X_{cc} + X_{2,3})Q_3 - (R_{cc} + R_{2,3})P_{PV3}}{V_{ul}} \tag{5.21}$$

The PV system at bus 3 is the *last PV household*; therefore the household connection (R_{cc}, X_{cc}) is included at this stage. Breaking the powers of (5.21) into their voltage and current components gives

$$V_2 = \frac{V_{ul}^2 + (R_{cc} + R_{2,3})\left(\frac{V_{ul}}{V_n}\right)^2 I_{r3} + (X_{cc} + X_{2,3})\left(\frac{V_{ul}}{V_n}\right)^2 I_{i3} - (R_{cc} + R_{2,3})V_{ul}I_{PV3}}{V_{ul}} \tag{5.22}$$

Where I_{r3} and I_{i3} is the real and imaginary current of P_3 and Q_3, I_{PV3} is the real current of P_{PV3} and V_n is the nominal voltage. Loads are modelled as constant impedance and PV systems are modelled as constant power. Dividing top and bottom by V_{ul} gives

$$V_2 = V_{ul} + (R_{cc} + R_{2,3})\frac{V_{ul}}{V_n^2}I_{r3} + (X_{cc} + X_{2,3})\frac{V_{ul}}{V_n^2}I_{i3} - (R_{cc} + R_{2,3})I_{PV3} \tag{5.23}$$

Examining bus 2 gives

$$V_{lvp} = \frac{V_2^2 + R_{1,2}\left(\frac{V_2}{V_n}\right)^2 I_{r2} + X_{1,2}\left(\frac{V_2}{V_n}\right)^2 I_{i2} - R_{1,2}V_2I_{PV2}}{V_2} + \left(R_{1,2}\frac{V_{ul}}{V_n^2}I_{r3} + X_{1,2}\frac{V_{ul}}{V_n^2}I_{i3} - R_{1,2}I_{PV3}\right) \tag{5.24}$$

Dividing top and bottom of the first part of (5.24) by V_2 gives

$$V_{lvp} = V_2 + \left(R_{1,2}\frac{V_2}{V_n^2}I_{r2} + X_{1,2}\frac{V_2}{V_n^2}I_{i2} - R_{1,2}I_{PV2}\right) + \left(R_{1,2}\frac{V_{ul}}{V_n^2}I_{r3} + X_{1,2}\frac{V_{ul}}{V_n^2}I_{i3} - R_{1,2}I_{PV3}\right) \tag{5.25}$$

V_2 is then replaced with equation (5.23), giving

$$V_{lvp} = V_{ul} + \left(R_{cc} + R_{2,3}\right)\frac{V_{ul}}{V_n^2} I_{r3} + \left(X_{cc} + X_{2,3}\right)\frac{V_{ul}}{V_n^2} I_{i3} - \left(R_{cc} + R_{2,3}\right) I_{PV3} + \left(R_{1,2}\frac{V_2}{V_n^2} I_{r2} + X_{1,2}\frac{V_2}{V_n^2} I_{i2} - R_{1,2} I_{PV2}\right) + \left(R_{1,2}\frac{V_{ul}}{V_n^2} I_{r3} + X_{1,2}\frac{V_{ul}}{V_n^2} I_{i3} - R_{1,2} I_{PV3}\right) \tag{5.26}$$

Grouping the right hand side gives

$$V_{lvp} = V_{ul} + I_{r3}\frac{V_{ul}}{V_n^2}\left(R_{cc} + R_{2,3} + R_{1,2}\right) + I_{i3}\frac{V_{ul}}{V_n^2}\left(X_{cc} + X_{2,3} + X_{1,2}\right) + R_{1,2}\frac{V_2}{V_n^2} I_{r2} + X_{1,2}\frac{V_2}{V_n^2} I_{i2} - I_{PV3}\left(R_{cc} + R_{2,3} + R_{1,2}\right) - I_{PV2} R_{1,2} \tag{5.27}$$

The right hand side is then multiplied through by a mean voltage (V_m) and V_2 and V_{ul} for the load and PV components also replaced with V_m

$$V_{lvp} = \frac{V_m V_{ul} + R_t \frac{V_m^2}{V_n^2} I_{r3} + X_t \frac{V_m^2}{V_n^2} I_{i3} + R_{1,2}\frac{V_m^2}{V_n^2} I_{r2} + X_{1,2}\frac{V_m^2}{V_n^2} I_{i2} - R_t V_m I_{PV3} - R_{1,2} V_m I_{PV2}}{V_m} \tag{5.28}$$

Where

$$R_t = R_{cc} + R_{1,2} + R_{2,3} \tag{5.29}$$

And

$$X_t = X_{cc} + X_{1,2} + X_{2,3} \tag{5.30}$$

This is equivalent to scaling the PV generation and load components by V_m, as opposed to their actual bus voltages; V_b. Scaling by V_m introduces some error but is necessary as the bus voltages between V_{lvp} and V_{ul} are unknown. Load values entered into the MPVGEM by the user are scaled up by V_m/V_n from V_n. And the actual maximum rating of the PV systems to be installed will be the MPVG estimate (P_{PV}) scaled down from V_m by V_n/V_m.

The voltage profile of a feeder in the presence of PV pushing the voltage up from V_{lvp} to V_{ul} takes the form of an increasing decaying exponential [16], and 2/3 of the voltage spread is a reliable estimate of the mean voltage for the feeder.

$$V_m = V_{lvp} + \frac{2}{3}\left(V_{ul} - V_{lvp}\right) \tag{5.31}$$

Re-writing (5.28) in power form gives

$$V_{lvp} = \frac{V_m V_{ul} + \left(P_3 R_t + P_2 R_{1,2}\right) + \left(Q_3 X_t + Q_2 X_{1,2}\right) - \left(P_{PV3} R_t + P_{PV2} R_{1,2}\right)}{V_m} \tag{5.32}$$

Equation (5.32) presented in the form of equations (5.13) to (5.15) gives

$$Load_P \equiv P_l R_{cc} + \sum_{b=1}^{n} P_b R_{b,lvp} \equiv P_3 R_{cc} + P_3\left(R_{2,3} + R_{1,2}\right) + P_2 R_{1,2} \tag{5.33}$$

$$Load_Q \equiv Q_l X_{cc} + \sum_{b=1}^{n} Q_b X_{b,lvp} \equiv Q_3 X_{cc} + Q_3\left(X_{2,3} + X_{1,2}\right) + Q_2 X_{1,2} \tag{5.34}$$

$$Solar_P \equiv P_{PV} R_{cc} + \sum_{b=1}^{m} \eta_b P_{PV} R_{b,lvp} \equiv P_{PV3} R_{cc} + P_{PV3}\left(R_{2,3} + R_{1,2}\right) + P_{PV2} R_{1,2} \tag{5.35}$$

As the MPVGEM estimates the MPVG where all PV systems are the same size, (5.35) becomes

$$Solar_P \equiv P_{PV} R_{cc} + \sum_{b=1}^{m} \eta_b P_{PV} R_{b,lvp} \equiv P_{PV} R_{cc} + P_{PV}\left(R_{2,3} + R_{1,2}\right) + P_{PV} R_{1,2} \tag{5.36}$$

For all testing presented in Section 5.2, loads are modelled as constant impedance and PV systems as constant power; as modelled by the provider of the DIgSILENT model. The full derivation for constant impedance loads and constant power PV systems is therefore given. The MPVGEM presented could also estimate the MPVG with loads and PV systems modelled differently; only requiring a different scaling of the load inputs and the final rating of the PV systems to be installed.

5.2.8 Example Application of the MPVGEM

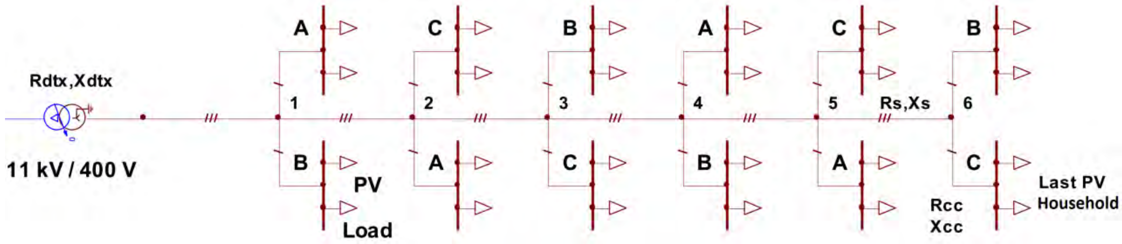

Figure 5.21 Example six bus 400 V line

This section gives an example application of the MPVGEM using a six bus 400 V line, as shown in Figure 5.21. Each household has a PV system installed and each has a real load 0.5 kW (P_l) and reactive load 0.1 kVAr (Q_l). Mutual coupling between phases can be neglected as load and PV generation is closely balanced across phases. The MPVG (P_{PV}) will be calculated for phase-C.

The 400 V line cable is 7/3 AAC, resistance 0.707 Ω/km and reactance 0.284 Ω/km. 7/3 is the stranding of the cable (7 strands with a diameter of 3 mm), AAC means All Aluminium Conductor. The distance between each bus is 20 m; the resistance between each bus is therefore 0.014 Ω (R_s), and reactance 0.006 Ω (X_s). The household connection cable has a cross-section of 25mm^2, resistance 1.49 Ω/km and reactance 0.097 Ω/km. The household connection for *the last PV household* (the household connected on phase-C at bus 6) is 20 m long, giving a resistance of 0.03 Ω (R_{cc}) and reactance 0.002 Ω (X_{cc}). The DTx has a resistance of 0.0003 Ω (R_{dtx}) and reactance 0.0125 Ω (X_{dtx}). This impedance is typical for a DTx within Endeavour Energy's Lv network.

The upper voltage limit (V_{ul} = 253 V) is assigned to the *last PV household*, the LV point (V_{lvp} = 250 V) is set to the high voltage side of the DTx. Using equation (5.31), V_m is calculated to be 252 V.

Applying equations (5.13), (5.14) and (5.15) to the example 400 V line gives

$$\begin{aligned} Load_P &\equiv P_l(R_{cc}+6R_s+R_{dtx})+P_l(5R_s+R_{dtx}) \\ &+P_l(3R_s+R_{dtx})+P_l(2R_s+R_{dtx})=128 \end{aligned}$$

$$Load_Q \equiv Q_l(X_{cc} + 6X_s + X_{dtx}) + Q_l(5X_s + X_{dtx})$$
$$+ Q_l(3X_s + X_{dtx}) + Q_l(2X_s + X_{dtx}) = 15$$
$$Solar_P \equiv P_{PV}(R_{cc} + 6R_s + R_{dtx}) + P_{PV}(5R_s + R_{dtx})$$
$$+ P_{PV}(3R_s + R_{dtx}) + P_{PV}(2R_s + R_{dtx}) = 0.26P_{PV}$$

Inserting the above values into equation (5.12) gives

$$V_{lp} = \frac{V_m V_{ul} + 128 + 15 - 0.26P_{PV}}{V_m}$$

Inserting values for voltages V_{ul}, V_{lvp} and V_m gives

$$250 = \frac{63756 + 128 + 15 - 0.26P_{PV}}{252}$$

The above equation is then re-arranged to make P_{PV} the subject, P_{PV} is then calculated to be 3.5 kW.

When implementing the MPVGEM in spreadsheet software, it does only require a small number of inputs, specifically

- V_{ul} Upper voltage limit. Assigned to the last PV household
- V_{lvp} Voltage at the LV point
- $R_{b,lvp}$ Resistance between bus b and the LV point
- $X_{b,lvp}$ Reactance between bus b and the LV point
- R_{cc} Resistance of the household connection of the *last PV household*
- X_{cc} Reactance of the household connection of the *last PV household*
- P_b Real load at bus *b*
- Q_b Reactive load at bus *b*

It can be applied to any radial feeder anywhere in the world. In terms of scaling, the larger the feeder, and the more PV systems and households, the more data entry required. This would also be the case for any power flow analysis software

5.2.9 Proof - Imaginary Component of Conventional Equation is Negligible

By not taking into account the imaginary component of equation (5.9), the MPVGEM is essentially attempting to estimate the MPVG based on the real component (a voltage value) of equation (5.9). The impact of this is that the upper limit voltage V_{ul} set in equation (5.10) is interpreted by the equation as the real component of the V_{ul}, instead of the complex value. The impact of this on the MPVGEM estimation accuracy can be determined by examining the difference between the voltage (real component) and the complex voltage along the length of the feeder.

Figure 5.22 shows the voltage angle at each terminal along the length of a 15 terminal test feeder. The test feeder length ranges from 100 m to 500 m; the cable has an *X/R* ratio of 1. The load for each household is 0.5 kW with power factor 0.9. Figure 5.22 shows how little the voltage angle changes, just 1.6 deg, by terminal 15 for the 500 m long feeder.

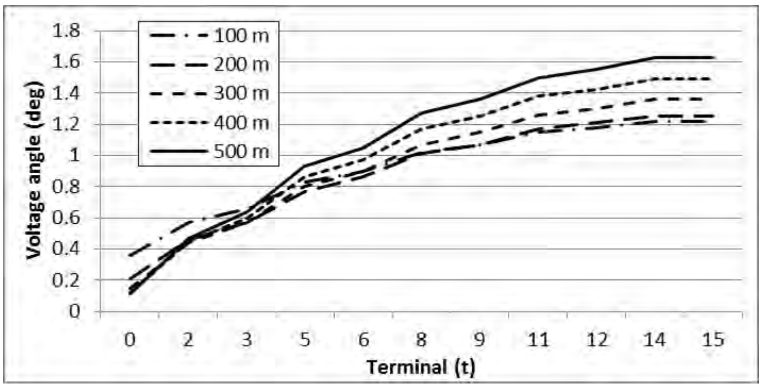

Figure 5.22 Change in voltage angle at each terminal

The following figure, Figure 5.23, shows how the change in voltage angle translates to a difference between the real voltage and complex voltage at each terminal. It can be seen that by terminal 15, the difference between the real voltage and complex voltage is just 0.1 V. Were the MPVGEM be applied to the 500 m long feeder to estimate the MPVG, this indicates that the MPVGEM is attempting to estimate the MPVG using a V_{ul} (real voltage) that is 0.1 V higher than it should. This small difference has negligible impact on the accuracy of the MPVGEM.

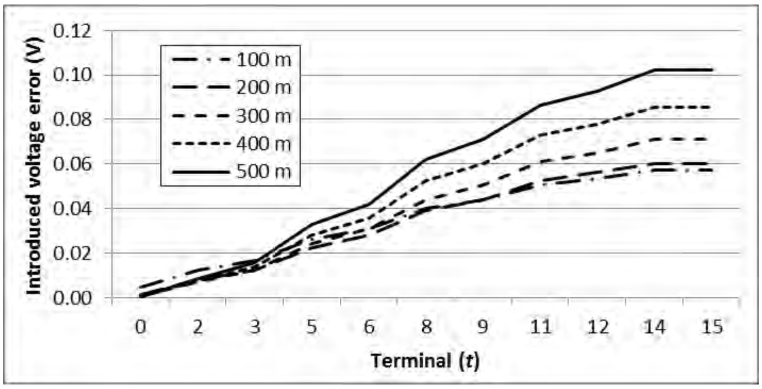

Figure 5.23 Difference between real voltage and complex voltage at each terminal

5.2.10 Conclusion

Section 5.2 presents a method for estimating the MPVG that can be installed on a LV feeder without breaching the upper voltage limit. The MPVG estimation for all test cases is close to those modelled using DIgSILENT.

Results show the MPVG estimation error for 400 V *uniform* lines is less than 0.5 V under a broad range of test conditions. The MPVGEM was also tested against a 400 V fifteen terminal *non-uniform* line with two varying load allocations and two line types and arrangements, giving four test cases. The end of voltage estimation error was within 0.1 V for all test cases. For the final test, a 400 V *non-uniform* line was randomly allocated line characteristics and load conditions from a large range of possibilities, with only select households with a PV system installed, the estimation error for this testing ranged between -0.6 to 0.7 V. A case study demonstrates that the MPVGEM can be applied to the section of a LV feeder which includes both the 11 kV and 400 V lines.

PV systems are assumed to operate at unity power factor, but it is shown that PV systems operating at non-unity power factors can theoretically be incorporated in the MPVGEM. The majority of testing is under balanced load conditions, but sensitivity analysis on the impact of imbalanced load on MPVGEM estimation accuracy when balanced load is assumed is shown to be minimal. Finally, the impact of imbalanced PV generation on MPVGEM estimation accuracy when mutual coupling is not taken into account is shown to potentially be significant, but that modelling the effects of mutual inductance into the MPVGEM reduces this estimation error substantially.

The MPVGEM can be easily implemented in standard spreadsheet software without the need for power flow analysis software. It is considered a tool with the potential to be used by DNOs to quickly and easily estimate the MPVG on all feeders within their LV network.

6 New Distributed Voltage Management Techniques

Original research by the author presented in this chapter addresses the voltage management knowledge gaps defined in Section 3.3.

6.1 A Balanced Approach to Distributed Voltage Management

The research presented in Section 6.1 is based on the authors' full peer reviewed conference paper "Voltage Probability Analysis – PV and Load in Low Voltage Networks", accepted for presentation at the Asia Pacific Solar Research Conference (APSRC), Brisbane 2015 [5].

6.1.1 Introduction

As noted in Section 3.3.3, a high-penetration PV case study is presented in Section 6.1, where a probabilistic voltage analysis at the household level is conducted for a number of PV and demand scenarios and voltage management options. No additional communication infrastructure is required for any of the voltage management options whose objective is the minimisation of voltage excursion, either above or below regulated standards. The results of the analysis are examined to select the most appropriate voltage management solution to minimise voltage excursion as a whole. The study demonstrates a balanced approach to distributed voltage management. The research presented in Section 6.1 addresses the voltage management knowledge gaps 1-3 defined in Section 3.3.1.

An extensive data set is used for the study, consisting of a year's worth of actual half-hourly load and PV data for 300 residences in Sydney, Australia [117]. Voltage probability data is obtained by running power flow calculations in DIgSILENT for a typical LV feeder with high penetrations of PV.

Section 6.1 is structured as follows. Section 6.1.2 describes the case study, including a description of the data set, the LV feeder model and the method used to simulate the different voltage management options. Section 6.1.3 presents the results and Section

6.1.4 suggests the most appropriate voltage control options through examination of the results. Section 6.1.5 provides concluding comments.

6.1.2 Case Study

6.1.2.1 Dataset

The dataset used for the voltage analysis is provided by Ausgrid, Australia's largest (by household) DNO. Ausgrid operates an electricity network in NSW, Australia, including Sydney. The data is sourced from 300 solar households in Ausgrid's electricity network between 1 July 2010 and 30 June 2011, offering a years' worth of household load and PV data [117]. Individual readings of the kilowatt hours (kWh) of electrical energy consumed by the household load and generated by the installed PV system were recorded at 30 min intervals. A years' worth of half hour household load and PV generation data is considered here as a load and PV profile respectively, where each profile has 17520 chronological measurements.

The PV generation correlation between all 300 households was calculated and found that for 290 of the 300 households the mean correlation ranged between 0.8 and 0.9. This is similar to the correlation calculated for 25 households located in the same suburb, an area of approximately 1 km^2. Therefore, it is reasonable to use the PV generation data for all 300 households in a voltage analysis of a LV feeder, as their level of correlation is representative of a cluster of PV systems located on the same LV feeder.

6.1.2.2 Feeder Model – DIgSILENT

The characteristics of the feeder used for analysis are those typically used by Endeavour Energy. Endeavour Energy is the DNO servicing Greater Western Sydney. The impedance of the overhead line is 0.707 Ω/km (R) and 0.284 Ω/km (X) and the impedance of the household connection is 1.49 Ω/km (R) and 0.097 Ω/km (X). The DTx steps down the voltage from MV (11 kV) to LV (400/230 V). Australia's residential LV network operates at 230 V. The DTx tap setting gives 250 V on the low side, a setting typical for LV residential feeders in Endeavour Energy's network which serves a region adjacent to Ausgrid (details on Ausgrid's DTx tap settings were not available). The feeder line is three-phase, four-wire. Voltage standards for both Endeavour and Ausgrid are 230+10%/-6%. This gives an upper voltage limit of 253 V and a lower voltage limit of 216 V. Households are evenly distributed across the phases. Each household consists of a load and PV system. Figure 6.1 presents the DIgSILENT schematic of the feeder. A 400 m long feeder with 20 terminals hosting 40 households is used for the study, a typical urban feeder. The majority of Australia's residential LV network consists of overhead line.

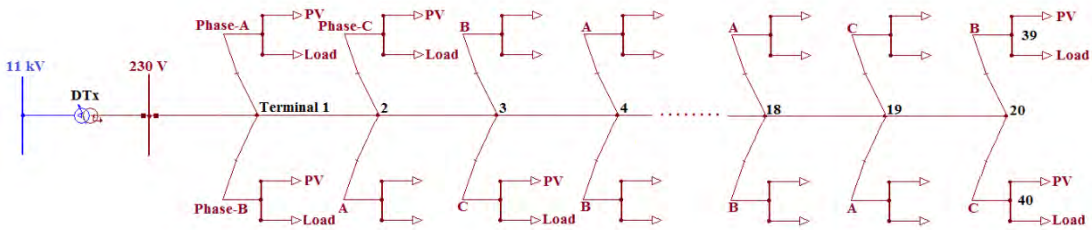

Figure 6.1 Schematic of DIgSILENT feeder model

6.1.2.3 Method

A yearlong load and PV profile is selected randomly from the data set. To simulate each voltage management option (scenario), the data set is altered and a voltage control method applied if required.

Using DIgSILENT, a power flow calculation is performed at hourly intervals across the year between the times of 10 am and 10 pm. For each power flow calculation the voltage for each household is recorded. The random selection of load and PV profile is implemented a further nineteen times and the power flow calculations repeated. This gives a total of 87,600 power flow calculations and 175,200 voltage recordings. The probabilistic voltage impact analysis is generated from these recordings. Using hourly intervals and a restricted time frame reduces the number of power flow calculations required without impacting on the key findings of the analysis. For the situation where households are affected, a household impact analysis is also conducted.

Described below is how the data set is altered for each scenario. Where one is applied, the voltage control method is also described. A reference scenario is also used as part of the case study, this scenario leaves the load and PV profiles unaltered and implements no control.

DSM: In this scenario DSM is modelled. The load datasets are altered such that the top 5% of household load samples are decreased by between 10% and 50%. Whilst a 50% decrease in load appears significant, the top 5% of load samples for all households is, on average, approximately three times their mean evening peak load and in some cases it is over ten times. Therefore a 50% decrease in the top 5% of load samples still results in a load significantly greater than their evening peak mean, and therefore can be considered potentially realistic. The aim of this simulation is determine the potential effectiveness of DSM. A reduction of this extent should not require complex control systems and could be achieved through appropriate tariffs in combination with in-house displays [119].

PV generation to reduce peak load demand: In this scenario the PV generation for each PV system is increased from 1 pu to 1.5 pu in 0.1 pu steps. The method described in Section 6.1.2.3 is repeated for each per unit step. The aim of this simulation is to identify the correlation between PV generation and peak load demand. A significant correlation between PV generation and peak load demand results in peak load shaving and a reduction in low voltage excursion.

PV inverter tripping on high voltage: In this scenario PV inverter tripping on high voltage is modelled. This is the present technical requirement for PV inverter settings in many jurisdictions including Australia. After each power flow calculation, the voltage at each household is examined, moving sequentially from the end of the feeder towards the DTx. If over-voltage is detected at a household then their PV system is tripped off and the power flow calculation repeated. This process is repeated until no over-voltage is detected; a tripped PV system will remain tripped. Once no more over-voltages are detected the voltage profile and the households with tripped PV systems are then recorded. Prioritising the tripping of PV systems towards the end of the feeder is representative of what currently happens to PV systems installed on the LV network in Australia as there are currently no Australian LV networks which formally coordinate control of PV systems on a feeder. The PV downtime due to tripping and the resultant loss in energy generation is then calculated. For an increase in PV system size, 1 pu to 1.5 pu in 0.1 pu steps, the number of PV trip events for each household was recorded and the lost generation calculated. The aim of this is to quantify the relationship between increased PV penetration levels and the household impact of required PV generation curtailment. The voltage trip point is set to the upper voltage limit, 253 V. At the time of this study the new standard for grid-connected PV inverters [67] had not yet been released. To minimise voltage rise, the new standard specifies *Q(V)* and *P(V)* droop control of the PV inverter whilst the previous version of the standard specified a voltage set point trip the PV inverter. The majority of PV inverters in Australia would still operate in accordance with the old standard at this time and it therefore remains appropriate to simulate PV inverter voltage control in this fashion.

Appliance tripping on low voltage: In this scenario load tripping on low voltage is modelled. The load tripping process is the same as for PV inverter tripping, the only difference being that the tripping of the load occurs when a voltage less than 216 V is detected. The average PV system size is 1.7 kW in the Ausgrid data set, so a reasonable comparison in the downtime between appliance and PV can be made, 1.7 kW is the amount of load “tripped” when a voltage lower than 216 V is detected. It is envisaged that load tripping would occur at a specific appliance level, air-conditioning is an example of such an appliance being a common driver of network peak demand, and having a typical electrical demand in the 2-3kW range [120]. It is worth noting that one Australian DNO currently has an air-conditioner demand management program [106].

Re-orientation of PV systems from north to west facing: In this scenario the PV systems are reoriented westwards. PV generation data from the DKASC is used for this conversion. At DKASC there is a “*solar compass”* with four otherwise identical systems facing north, east, west and south. The DKASC PV systems are located close to each other so all experience the same meteorological conditions. The generation profiles of the north and west facing systems were used to estimate an hourly multiplier for converting generation from a north-facing system to a west facing one. This conversion is applied to the PV generation dataset, resulting in a transformed dataset representing generation from PV systems with a west-facing orientation. The aim of this scenario is to quantify the effectiveness off re-orientated PV systems at reducing peak load demand. A reduction in peak load demand results in a reduction in low voltage excursion.

Battery Storage: In this final scenario, households own battery storage to ensure voltages are maintained above a lower voltage limit.

- *Battery sizing method:* After each load flow calculation, the voltage of the two households at the end of the feeder is recorded. If the voltage for either household is under the lower voltage limit (230 V, 220 V or 216 V) then the load of every household is incrementally reduced until the voltage is within the limit. For each day, the amount of energy required to ensure the voltage remains above the limit is recorded. This analysis produces probabilistic battery storage capacity requirements to keep voltages above a set lower limit. This approach is considered a novel battery sizing strategy; it can also be used for determining load shifting requirements. This work is similar to that presented in [121]. The probabilistic capability of PV generation to meet the daily energy requirements is also determined, simulating the action of PV generation charging the battery during the day.
- *Assumed charging operation:* During the day, PV real power is transferred to the battery until battery capacity is reached.
- *Assumed discharging operation:* The battery is discharged, until depleted, when the household voltage is below the lower voltage limit.

6.1.3 Results

The largest voltage excursions are the most important for the analysis. The end of the feeder is where the lowest voltage occurs during peak load times. Towards the end of the feeder is also where the highest voltage is likely to occur. This may not always occur on actual feeders, if for example there is a large load located at the end of the feeder and PV systems are not installed at all households. In this study it is likely to be the case though, as all households have a PV system installed and for residential feeders, high PV generation tends to coincide with lower demand. Voltage impact analysis results are therefore presented for voltages recorded at the last household on each phase.

6.1.3.1 Reference Scenario

The voltage histogram for the reference scenario is presented in Figure 6.2. The DTx no-load voltage is 249.67 V, as noted earlier a common setting for Endeavour Energy.

TABLE 6.1 gives a statistical summary of Figure 6.2 highlighting how much greater the impact of load is on voltage spread compared to PV generation. Load produces a voltage spread of 49 V, over three times that of PV at 14 V. The total percentage of voltage recordings below 216 V is only 0.7%, showing how a small number of high load periods have a large impact on voltage spread. When assessing the seasonal results of Figure 6.2 as expected, the largest number of voltage recordings below 216 V occurs during summer and winter due to additional cooling and heating loads respectively. Interestingly a large portion of the voltage recordings above 253 V occur in spring and autumn, not just summer. This is due to demand dropping more than PV generation during the day for season's autumn and spring, relative to summer levels of demand and PV generation.

To provide a point of comparison with the reference scenario, Figure 6.3 and Figure 6.4 give the voltage histograms for zero PV generation and zero load respectively. For zero PV generation, the tail on low voltage excursions remains and the voltage occurrences greater than 250 V due to PV generation are no longer present. The low voltage tail remains the same for Figure 6.2 and Figure 6.3. This is due to there being no significant correlation between PV generation and peak load. If there was correlation there would be a greater percentage of recordings in the low voltage tail in Figure 6.3 compared to Figure 6.2.

For zero load, Figure 6.4, the majority of voltage recordings occur between 249 V and 258 V. Without the midday load to offset peak PV generation, the maximum recorded voltage increases from 264 V to 269 V. This confirms that even at zero load, the impact of PV generation on voltage excursion is still well below that of load, at less than 20 V compared to almost 50 V. In practice the PV inverters will generally turn the PV systems off well before these voltages are reached.

TABLE 6.1 Summary statistics for Figure 6.2

	Description	
Load	Lowest voltage (V)	201
	Voltage spread due to load (V)	49
	Samples < 216 V (%)	0.7
PV	Highest voltage (V)	264
	Voltage spread due to PV (V)	14
	Samples > 253 V (%)	7.6

6.1.3.2 DSM

The next scenario examines the impact of gradually decreasing peak load demand on upper voltage excursion. There have been DSM trials conducted in Australia with moderate success [122]. A key success of the Energex programs is an increased awareness by consumers of their electricity consumption behaviour on prices. Figure 6.5 gives the voltage histogram for when the top 5% of load samples are reduced by 50%. Comparing Figure 6.5 to Figure 6.2 clearly illustrated is the reduction in the extent of the low voltage tail.

Figure 6.6 shows the impact of decreasing peak load demand on the percentage of voltage recordings below 216 V, the regulation lower voltage limit, and low voltage excursion (< 250 V). The linear decrease in peak load results in a rapid decrease in voltage recordings less than 216 V so is effective at reducing low voltage excursion. The number of recordings below 216 V falls to zero for a 50% decrease in the top 5% of load samples. The low voltage excursion also improves from 49 V to 33 V, increasing the minimum voltage from 201 V to 217 V.

According to Figure 6.6, only a 20% curtailment in the top 5% of load samples is required to substantially reduce the number of voltage recording below 216 V. The percentage of recording below 216 V reduces from 0.7% to 0.1% for a 20% drop in the top 5% of load samples. A 20% drop is not excessive, and realistically should not impact too greatly on household services but is extremely effective at improving the voltage regulation of the households during peak load periods. The majority of the top 5% of load samples occur during summer and are a consequence of increased air-conditioning load.

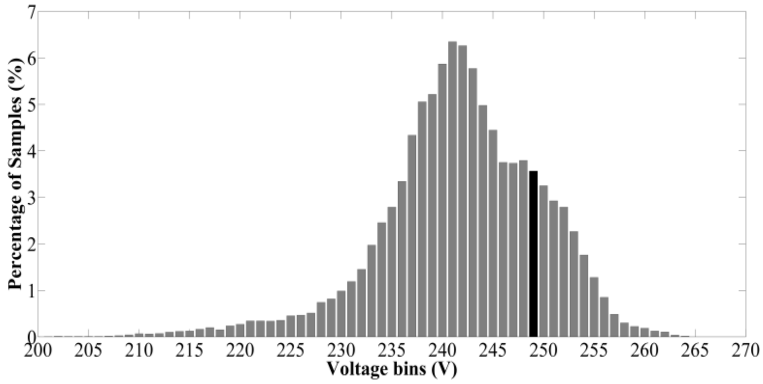

Figure 6.2 Voltage histogram – reference scenario. The highlighted bar indicates the DTx voltage tap setting

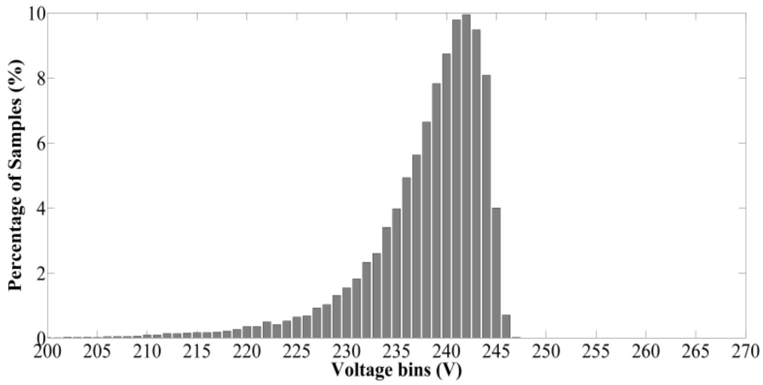

Figure 6.3 Voltage histogram - Zero PV generation

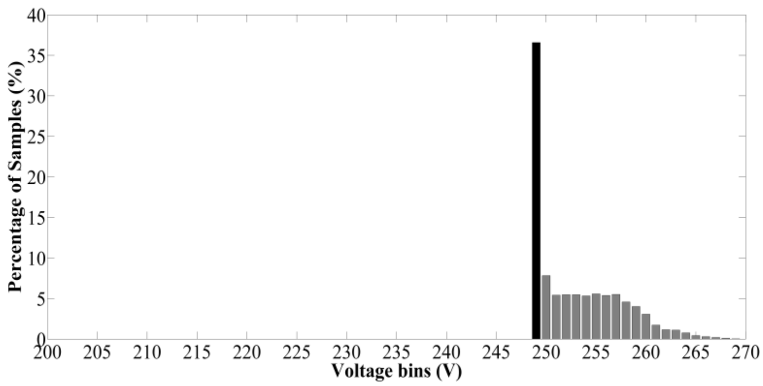

Figure 6.4 Voltage histogram - Zero load

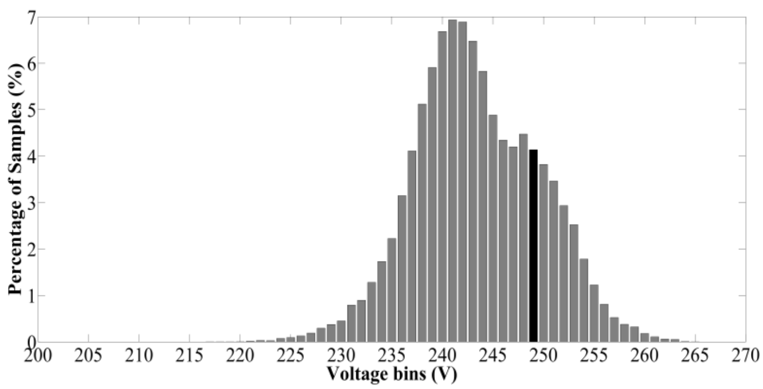

Figure 6.5 Voltage histogram 50% reduction in top 5% of samples

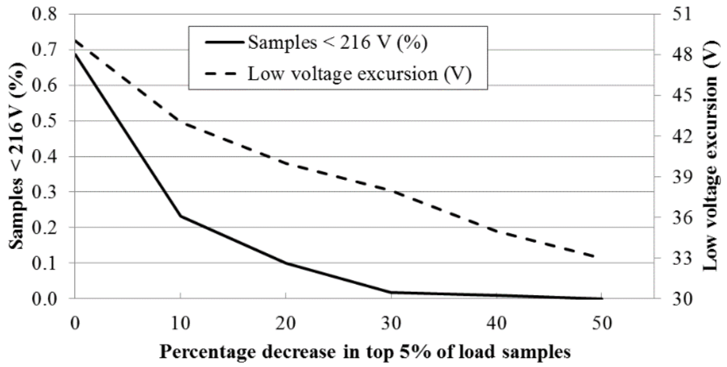

Figure 6.6 Peak load decrease v percentage of voltage recordings less than 216 V and low voltage excursion (< 250 V)

6.1.3.3 PV Generation to Reduce Peak Load Demand

The second scenario examines the coincidence between PV generation and peak load demand; this is the case if an increase in PV capacity results in a corresponding decrease in peak demand. If so, then increasing PV becomes an option to reduce peak load demand and minimise low voltage excursion. Figure 6.7 shows the impact of increasing PV penetration on the percentage of voltage recordings above 253 V and below 230 V. The impact is one sided with the percentage of recordings greater than 253 V increasing from 6% to over 20% whereas the number of recordings below 230 V remains unchanged at around 5%. Therefore increasing PV penetration gives an expected increase in the occurrence of voltage recordings greater than 253 V but not a corresponding decrease in peak load demand. A reduction in voltage recordings less than 230 V is considered a decrease in peak load. These results confirm there is no coincidence between peak PV generation and peak load. This is not an unexpected result, a natural coincidence between PV generation and peak demand is not common, and studies in this area ([74], [75] and [76]) show that a reduction in peak demand generally requires a re-orientation of the panels towards the west.

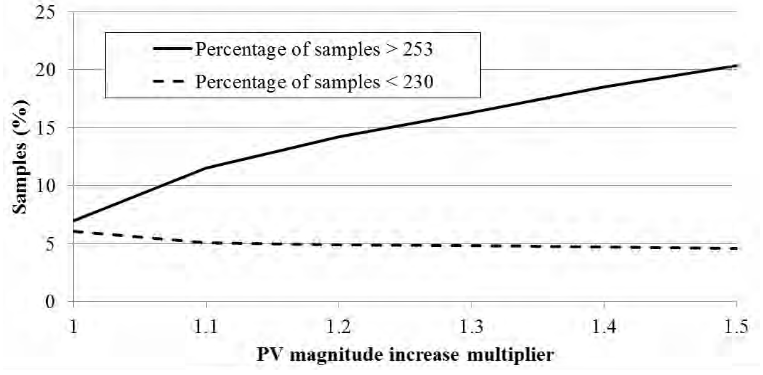

Figure 6.7 PV magnitude increase v percentage of voltage recordings greater than 253 V and less than 230 V

6.1.3.4 PV Inverter Tripping on High Voltage

The next scenario models PV inverter tripping on high voltage. Figure 6.8 shows the voltage histogram, using unaltered PV and load data, but when PV inverters are tripped at the upper-voltage limit. The upper voltage limit is 253 V. When compared to Figure 6.2 the change is obvious, with all the voltage recordings previously above 253 V moving into the 245 V to 253 V voltage range. For households 8, 16, 24, 32 and 40, Figure 6.9 gives the PV downtime as a percentage while Figure 6.10 gives the lost energy generation as a percentage. Both are plotted against a PV multiplier ranging from 1 pu to 1.5 pu. Figure 6.10 shows that PV downtime time for each household increases linearly with PV system size. As expected, it is the household at the end of the feeder which experiences the most PV downtime. This imbalance becomes apparent at a PV multiplier of just 1.1 pu.

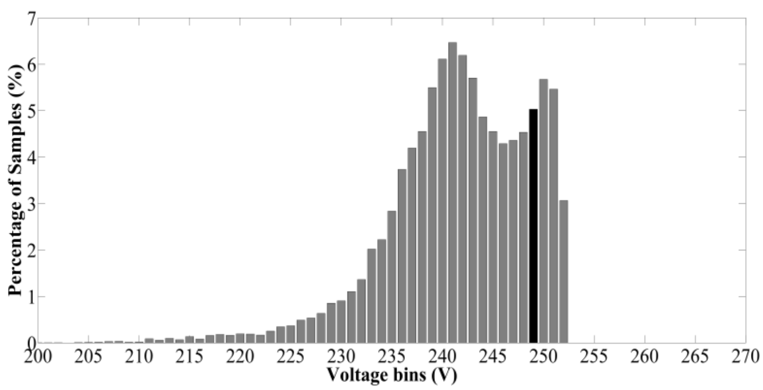

Figure 6.8 Voltage histogram with PV systems capped at upper voltage limit

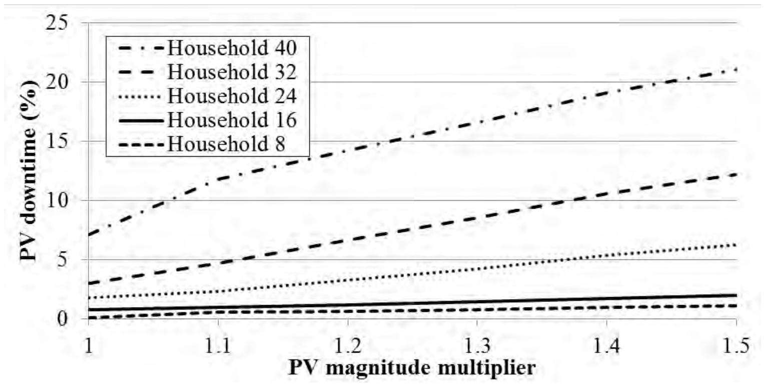

Figure 6.9 PV downtime (%) v increase in PV system size (1 pu to 1.5 pu)

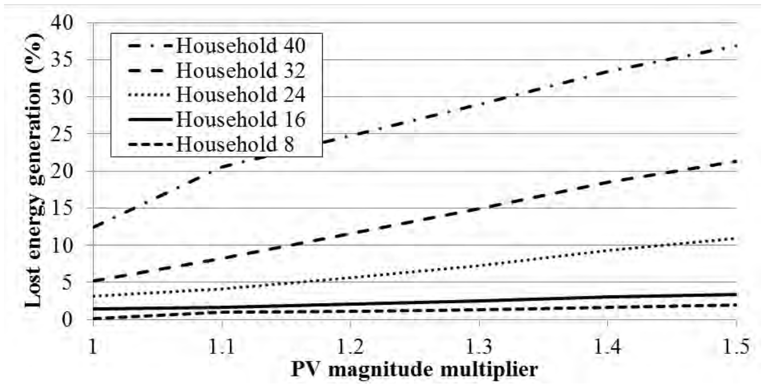

Figure 6.10 Lost generation (%) versus increase in PV system size (1 pu to 1.5 pu)

Referring to Figure 6.10, of interest here is how lost generation increases with an increase in PV system size. For household 40, lost generation increases from around 12% to over 35% for a 0.5 pu increase in PV system size. At 1.5 pu their PV system, due to tripping on over-voltage, is only generating approximately 10% more generation than at 1 pu. The loss in generation does decrease for households closer to the DTx. For households 8 and 16, loss in generation for PV systems at 1 pu and 1.5 pu, as a percentage, is the same. For PV systems at 1 pu, these results show that LV feeders do have the capacity to accommodate PV without breaching upper voltage limits. This accommodation is possible without the need for systems which control and coordinate PV inverters to ensure this; an appropriately set trip-voltage is all that is required. With an increase in PV system size the loss in generation for households, especially for those situated towards the end of the feeder, becomes significant.

For a DTx setting of 243 V, one tap setting lower than is typical for the DNO Endeavour Energy according to their models, the reduced peak load dataset and the PV system tripping at the upper voltage limit were combined. The PV downtime is reduced dramatically; for PV system size at 1.5 pu, Household 40 only experienced 3.6% downtime, compared to over 20% at a DTx voltage of 249 V. With peak load reduction, breaches of the lower voltage limit are mitigated. For a 50% reduction in the top 5% of load samples there are still recorded voltages below 216 V, but these only constitute 0.07% of the total. The lowest recorded voltage was 209 V, still 9 V higher than the lowest recorded voltage for the reference scenario (Section 6.1.3.1).

It is likely that customers who have their PV generation curtailed would be compensated. Results from an impact analysis such as this, and the significance of this impact on customers, would enable the DNO to determine the economic feasibility of this type of DSM relative to other voltage management measures.

Whilst *Q(V)* droop control is considered a more sophisticated form of voltage control, changes to Australian grid-connected inverter standards (AS4777 [67]) specifying *Q(V)* droop control were only introduced in 2015. As such, the majority of PV inverters in Australia still self-manage voltage using a trip set-point, *Q(V)* droop control is therefore not considered in this study but is considered future work.

6.1.3.5 Appliance Tripping on Low Voltage

The next scenario examined tripping load at the lower voltage limit. Excessive load occurs during extreme temperatures and a load tripping event could be viewed as a tripping of the heating/cooling system, and as noted in Section 6.1.2.3 under the sub-heading *"Appliance tripping on low voltage",* the air-conditioning unit is considered a suitable appliance to trip. At a DTx voltage of 249.7 V the number of load trip events is negligible, only six and four trip events in winter and summer respectively. For households 8, 16, 24, 32 and 40, Figure 6.11 gives the seasonal cumulative number of trip events when the DTx voltage is at 243 V. As expected, results show that the majority of load tripping occurs for the household at the end of the feeder, household 40, and drops quickly for households closer to the DTx. For household 40, Figure 6.12 plots the percentage of trip events against trip duration, and shows that the majority of trip events are one hour or less in duration. Referring back to Figure 6.12, in winter, household 40 would experience 32 load trip events. This is approximately one every three days, the majority being one hour or less in duration.

It is likely that customers who have their air-conditioning units tripped would be compensated. Results from an impact analysis such as this, and the significance of this impact on customers, would enable the DNO to determine the economic feasibility of this type of DSM relative to other voltage management measures.

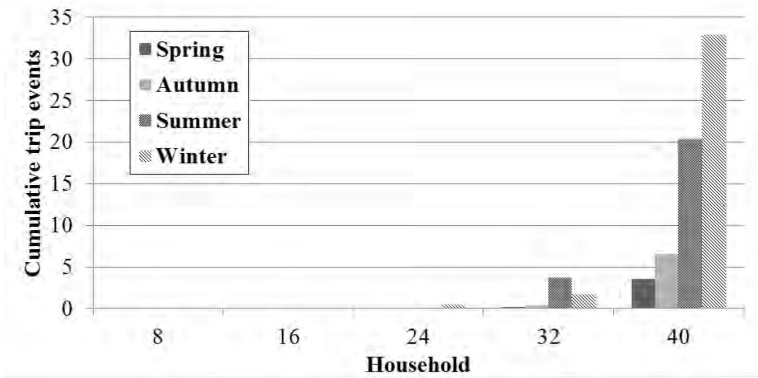

Figure 6.11 Seasonal average daily load trip duration for households 8, 16, 24, 32 and 40. DTx voltage at 243 V.

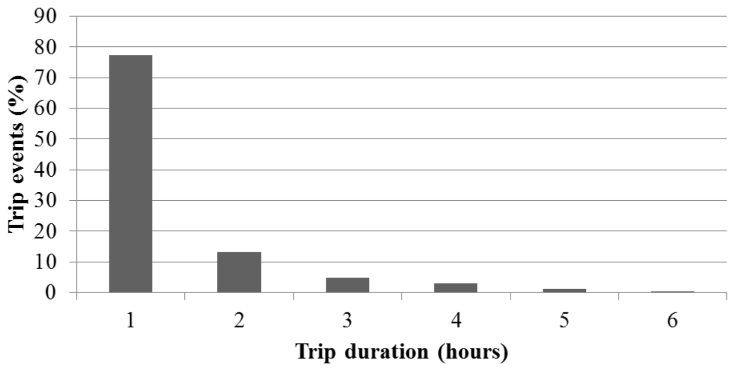

Figure 6.12 Percentage of trip events v trip duration for household 40

6.1.3.6 Re-orientation of PV Systems from North to West Facing

The next scenario examined is the impact of orientating PV towards the west has on reducing breaches of the lower voltage limit, and also reducing peak load. Figure 6.13 gives the percentage of voltage recordings below 216 V and 230 V for a PV dataset altered to represent generation for a west-facing orientation. A reduction in the percentage of voltage recordings below 230 V is indicative of a reduction in peak load. PV magnitude is increased from 1 to 1.5 pu to observe how the results are affected by increasing PV size. The reference value (ref) is the result for the unaltered PV dataset.

Results show that orientating a PV system in Sydney towards the west does little to reduce breaches of the lower voltage limit, with only a 0.12% reduction in voltage recordings below 216 V at 1.5 pu PV. The reduction in low voltage excursion is also insignificant, with only a 1% reduction, from 5.8% to 4.8%, in voltage recordings below 230 V. This shows that re-orientation of PV systems towards the west is also ineffective at reducing peak load.

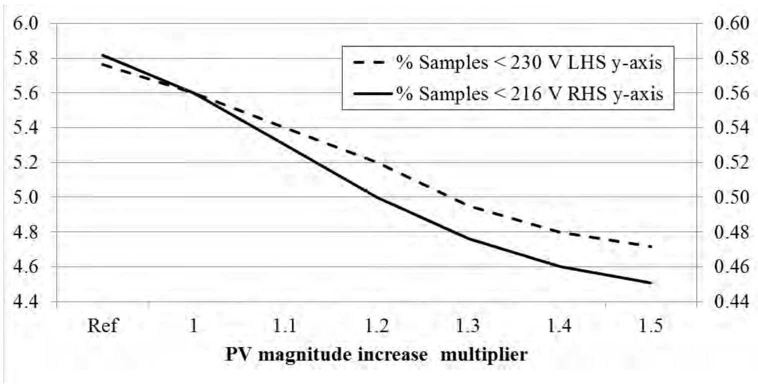

Figure 6.13 Impact of western-facing PV on peak reduction

It is likely that customers who have their panels re-orientated, thus reducing their generation, would be compensated. Results from an impact analysis such as this, and the significance of this impact on customers, would enable the DNO to determine the economic feasibility of this type of DSM relative to other voltage management measures.

6.1.3.7 Battery Storage

The final scenario simulated households equipped with battery storage to ensure voltages are maintained above a lower voltage limit. Also examined is the capability of the household PV system to charge the battery to ensure energy requirements are met. The method for this analysis is described under the sub-heading *Battery Storage* at Section 6.1.2.3. Figure 6.14 is a histogram presenting the probable amount of energy required to ensure voltage levels are maintained above 230 V, 220 V and 216 V during the peak demand period. Figure 6.14 shows the storage capacity required per household ensure voltage levels are maintained. Probabilistically, 2 kWh of storage will ensure voltage levels remain above 216 V for all days, above 220 V for 99% of days and above 230 V for 98% of days. Figure 6.15 then illustrates the capability of a 1 kW PV system to charge the battery so the energy required to maintain voltage levels during the peak demand period is met.

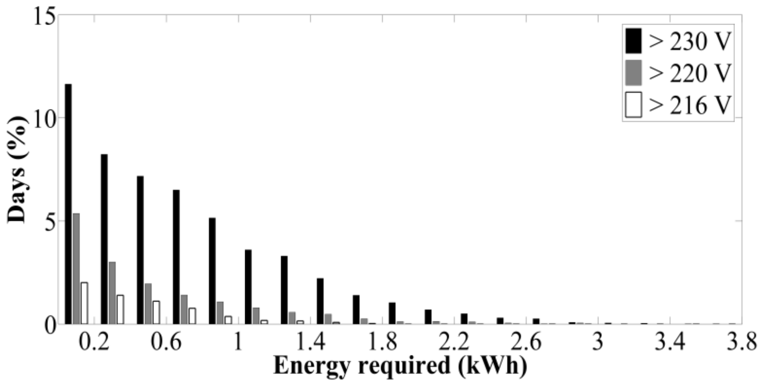

Figure 6.14 Histogram of energy required to ensure voltage stays above 230, 220 and 216 V during the peak demand period

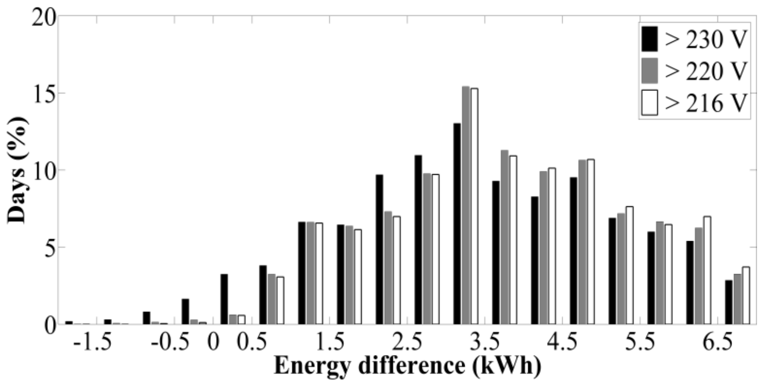

Figure 6.15 Histogram of difference in energy between energy generated by a 1 kW PV system during the day and energy required to ensure voltage stays above 216, 220 and 230 V.

Figure 6.15 shows that PV generation is able to charge the battery sufficiently to maintain voltages above 216 V and 220 V for virtually all days and only falls short at maintaining voltages above 230 V for approximately 4% of days. A positive energy difference bin equates to when the PV system generates more energy than is required during the peak demand period to ensure a given voltage level and vice versa for negative.

6.1.4 Proposed Voltage Management Solution

To determine the most appropriate voltage management solution, an examination of the results for each scenario is undertaken.

- ***DSM:*** Referring to Figure 6.5 and Figure 6.6, for a DTx setting of 249.7 V, the DSM option showed a large reduction in maximum low voltage excursion is possible with infrequent and minor reductions in peak load demand. Whilst the study doesn't calculate the likelihood of households responding to price signals through an in-house display, it does demonstrate the potential if households were responsive.

- ***PV Generation to Reduce Peak Load and Panel Re-orientation***: Referring to Figure 6.7 and Figure 6.13, due to the lack of correlation between PV generation and peak load demand, the option of either increasing PV penetration levels or re-orientating PV system from north to west facing is unlikely to be an effective voltage management option.
- ***PV Inverter Tripping:*** Referring to Figure 6.10, for a DTx setting of 249.7 V, the results for modelling of PV inverter tripping on high voltage show the greatest curtailment is experienced by household 40, with a 12% reduction in generation across the year at 1 pu. This increases linearly with increasing PV size, reaching over 35% at 1.5 pu. However, the average for all households ranges from around 2.5% curtailment at 1 pu to less than 10% at 1.5 pu. So whilst the curtailment for the last household is significant, the average across all households could be much less. For a DTx setting of 243 V, curtailment is negligible for all households, even at 1.5 pu.
- ***Appliance Tripping:*** Referring to Figure 6.11 and Figure 6.12, for a DTx setting of 243 V, the results for modelling of load tripping on low voltage shows household 40 experiences by far the majority of load tripping events. Load tripping experienced by other households is insignificant in comparison. Load tripping at a DTx setting of 249.7 V is negligible for all households.
- ***Battery Storage:*** Referring to Figure 6.14, results show that a 2 kWh battery is sufficient to ensure that voltages are maintained above 216 V 100% of the time. Figure 6.15 shows that a 1 kW PV system is required to charge a 2 kWh battery each day.

Through examination of the results it is suggested that the best voltage management solution combines PV inverter tripping and load tripping with DSM or PV inverter tripping combined with battery storage. Lowering the DTx tap setting to 243 V is also an option as it would reduce loss in PV generation while low voltage excursions are still managed using load tripping and DSM. Load tripping is considered the second option behind DSM for ensuring lower voltage limits aren't exceeded. It is expected that DSM will keep voltages above the lower voltage limit for the majority of the time, and on occasions where they aren't, load tripping will ensure this. As the majority of impact is likely to be experienced by households at the end of the feeder, it is suggested that these households receive some type of concession from the DNO.

A tap setting of 243 V is one tap lower than is typical for Australian DNO's. A reduction in DTx tap settings is supported by a recent report by Energex [98]. This study is directed primarily at Australian DNO's, which currently bias voltage management towards load (a typically high tap setting is evidence of this). It is expected that this study will demonstrate that voltage problems are not purely due to PV and that when examining potential voltage management solutions, distributed techniques should be considered a viable option. The other aim of the study is to argue that minimising voltage excursion in general should be the goal.

Note that this is a suggestion only, for a DNO conducting this analysis, a full cost analysis would be required and the practicality of each measure would also need to be considered. The significance of customer impacts for customer end control (DSM, PV tripping and panel re-orientation) would also need to be assessed. The aim of this case study is only to present the types of analysis that might be conducted when considering distributed voltage management techniques.

The battery storage analysis is conducted without considering either load tripping or DSM, it therefore considered an alternative to load tripping with DSM. The difference between the two is cost; the installation of a 2 kWh battery in each household would cost more than implementing load tripping with DSM. A full cost benefit analysis would be required to determine whether such an investment is worthwhile. The benefit of installing battery storage over load tripping with DSM is reduced household impact. The battery is charged by the PV system during the day thus reducing the likelihood of PV inverter tripping at high voltage, and the battery is discharged during the evening offsetting the need for load shedding.

The actual implementation of the suggested distributed voltage management techniques in Australia appears to still be some time off but progress is being made. A number of DNO's now examine the impact of distributed PV generation on peak load [123], [124] and [125]. Also, there are DNO's investigating distributed generation and battery storage for voltage management, still primarily at the trial/pilot stage. An example of load control at the residential level in Australia is the Energex program in Queensland [119], where the key success of the program was an increased awareness by consumers of their electricity consumption behaviour on prices. Trials on battery storage are more common, a residential example includes the Smart Grid, Smart City residential PV and battery storage trial by Ausgrid [126]. Two other trials ([127] and [128]) are currently underway but equipment (battery storage and distributed generation) is installed at the MV level, not at the residential level.

6.1.5 Conclusion

In Section 6.1, for a case study with high PV penetration, a probabilistic voltage and household impact analysis is conducted for a number of voltage management options. The results of the analysis are examined to select the most appropriate voltage management solution to minimise voltage excursion as a whole.

For the case study presented, analysis of the results revealed that the most appropriate voltage solution is a combination of PV inverter tripping and either DSM combined with load tripping or battery storage. It is also suggested that the DTx tap setting is lowered. The aim of the study is to demonstrate a general approach to distributed voltage management in a high PV penetration environment. It is suggested that this type of approach be used by DNO's when examining voltage management issues and potential solutions within their network.

6.2 A Practical Distributed Voltage Control Method to Ensure Efficient and Equitable Intervention of Distributed Devices

The research presented in Section 6.2 is based on a paper currently under review at the journal IEEE Transactions on Power Delivery.

6.2.1 Introduction

As noted in Section 3.3.3, in Section 6.2 an original distributed voltage control method is proposed. The method controls PV inverters to ensure an upper voltage limit is not exceeded, and controllable loads to ensure a lower voltage limit is not exceeded. Air-conditioning units are considered an appropriate controllable load. The method uses both a voltage and a power set point for control to ensure both the minimisation and fair distribution of intervention among PV inverters and controllable loads. Also, local measurements only are required to implement the control method. The research presented in Section 6.2 addresses the voltage management knowledge gaps 4-8 defined in Section 3.3.2.

In relation to distributed voltage control methods, the approach is taken that the intervention of distributed devices for distributed voltage control should operate under the principles described below. The term "intervention" refers to PV system real power curtailment and reactive power absorption, and activation of controllable loads.

- Control methods should not require measurements beyond that which can be taken locally, meaning no communication infrastructure is required.
- Intervention should be accurate, meaning the control method should intervene such that the final voltage is close to the voltage limit.
- Intervention should be efficient, the less intervention required to ensure voltage limits are not exceeded, the more efficient the control method.
- Intervention should also be fairly allocated among households, according to their net load contribution.

The distributed voltage control method presented in Section 6.2 follows the above principles. The method first determines the voltage sensitivity of each household; from this a voltage and net real power set point is calculated for both the PV system and the controllable load. Air-conditioning units are considered an appropriate controllable load given they are a common driver of network peak demand and can operate under a range of power modes. Using voltage sensitivities to manage the control of DG, installed to meet load demand, and provide voltage and frequency support, are also proposed in [129] and [130]. The PV system set points, along with voltage sensitivity, are compared to the locally measured voltage and power to control PV system generation to ensure an upper voltage limit is not exceeded. The air-conditioning unit set points, again along with voltage sensitivity, are compared to the locally measured voltage and power to control load shedding of the air-conditioning unit to ensure a lower voltage limit is not exceeded. The method is termed the Power Set Point Control (PSPC) plus Voltage Set Point Control (VSPC) method.

The PSPC+VSPC method can be used to control both real power curtailment and/or reactive power absorption of PV systems. For the case study presented, the PSPC+VSPC method is used to control the real power curtailment of PV systems. The method is compared with a PSPC only method, equivalent to that presented in [71]. It is also compared to the AS4777 standard, which uses *P(V)* droop control. This is a voltage set point only method and is similar to the method presented in [72]. All of these methods use local measurements only. Actual load and PV generation data, sourced from Ausgrid [117], is used for testing. Results show the PSPC+VSPC method outperforms both previously reported methods in terms of accuracy and efficiency and in terms of equally allocating intervention among households according to net load contribution.

Section 6.2 is structured as follows. Section 6.2.2 describes the method and a case study is presented in Section 6.2.3. Section 6.2.4 gives the results of the case study and Section 6.2.5 provides concluding comments.

6.2.2 Method

The following is included as part of the method; a description of the process to calculate the voltage and power set points and sensitivities, the definition of the equations used to control intervention, and a description of the steps a DNO would take to configure the devices on a 400 V line to manage voltage using the PSPC+VSPC method.

A case study is presented in Section 6.2.3 to further explain the method.

6.2.2.1 Calculation of Voltage and Real Power Set Points

This section describes how the PV system voltage set points ($V_{ph,h}^{PV}$) for each household (h) and the PV system real power set points (P_{ph}^{PV}) for each phase (ph) are calculated. This process is performed using power flow software DIgSILENT.

The real power set points are used to ensure equal allocation of intervention among households according to their net load contribution. To achieve this, households on the same phase have the same power set points. The steps below describe the process for calculating the set points, $V_{ph,h}^{PV}$ and P_{ph}^{PV}, for PV systems on a selected phase for a 400 V line of interest, termed the *target 400 V line*. The *last PV system* is the PV system furthest from the DTx on the *target 400 V line*.

Step 1a: Increment the real power of all the PV systems (on all phases) on all 400 V lines within the distribution network until the upper voltage limit (V_{ul}) is reached at the *last PV system*.

Step 1b: Record the voltage at each household ($V_{ph,h}^{PV-u}$). This set of voltage set points is the *upper bound* set.

Step 1c: Record the power set point (P_{ph}^{PV-u}); it will be the same for every PV system. This power set point is the *upper bound* set point.

Step 2a: Increment the real power of the PV systems (on all phases) located on the *target 400 V line* until the upper voltage limit (V_{ul}) is reached at the *last PV system*.

Step 2b: Record the voltage at each household ($V_{ph,h}^{PV-l}$). This set of voltage set points is the *lower bound* set.

Step 2c: Record the power set point (P_{ph}^{PV-l}); it will be the same for every PV system. This power set point is the *lower bound* set point.

Step 3: Calculate the final set of voltage set points for each household on ($V_{ph,h}^{PV}$) and the final power set point (P_{ph}^{PV}) for the phase using equations (6.1) and (6.2) respectively.

$$V_{ph,h}^{PV} = \frac{V_{ph,h}^{PV-u} + V_{ph,h}^{PV-l}}{2}, h \in 1,..., H_{ph}; ph \in A,B,C \tag{6.1}$$

$$P_{ph}^{PV} = \frac{P_{ph}^{PV-u} + P_{ph}^{PV-l}}{2}, ph \in A, B, C \tag{6.2}$$

Where H_{ph} is the number of houses on phase *ph*. The PV generation outside the *target 400 V line* influences the voltage at the DTx of the *target 400 V line*, and therefore its voltage rise window. This needs to be taken into account when determining the set points. The *upper bound* set points are calculated for the instance where all PV systems in the distribution network are generating at rated values. The *lower bound* set points are calculated for the instance where only the PV systems for the target 400 V line are generating. The average of both sets is then used. Note that this process assumes that all other 400 V lines have the same DTx tap setting.

The process for calculating the air-conditioning voltage set points ($V_{ph,h}^{AC}$) and real power set points (P_{ph}^{AC}) for each phase is the same for air-conditioning units with two differences. Load is incremented instead of PV generation (PV generation is assumed to be zero) and the *lower bound* set points are calculated when all air-conditioning units in the distribution network are operating and the *upper bound* set points is calculated when only the air-conditioning units of the *target 400 V line* are operating.

6.2.2.2 Calculation of Sensitivities

Sensitivities for each household on each phase ($S_{ph,h}$) are determined using the PV voltage and power set point values already calculated. These are input into (6.3). The household sensitivity is the ratio of change in household voltage to the change in real power for the phase. Sensitivities are calculated using power flow software, where the change in voltage is observed at each household for an incremental change in real power at the household.

$$S_{ph,h} = \frac{V_{ph,h}^{PV}}{P_{ph}^{PV}}, h \in 1,\ldots,H_{ph}; ph \in A, B, C \tag{6.3}$$

6.2.2.3 Curtailment and Load Shedding Control

Equations (6.4) to (6.7) define the intervention control process, through which PV systems have their real power curtailed and air-conditioning units activate load shedding.

Equation (6.4) calculates $C_{ph,h}^{PV-P}$, the required change in PV system real power curtailment according to the power set point. Equation (6.5) calculates $C_{ph,h}^{PV-V}$, the required change in PV system real power curtailment according to the voltage set point. Equation (6.6) calculates $C_{ph,h}^{AC-P}$, the required change in air-conditioning load shedding according to the power set point. Equation (6.7) calculates $C_{ph,h}^{AC-V}$, the required change in air-conditioning unit load shedding according to the voltage set point.

PV system real power curtailment is used to explain the process. For each instance that the local voltage ($V_{ph,h}$) and net power ($P_{ph,h}^{net}$) of the household is measured, two change in curtailment amounts, $C_{ph,h}^{PV-P}$ and $C_{ph,h}^{PV-V}$, are calculated. The real power curtailment of the PV system is changed by the minimum of the two. Note that when $P_{ph,h}^{net}$ is less than P_{ph}^{PV} and $V_{ph,h}^{PV}$ is less than $V_{ph,h}$ a negative change in curtailment will be calculated. In this case the curtailment of the PV system will be reduced, not increased. The PV system curtailment can be reduced to a minimum of zero. The process is the same for air-conditioning units.

$$C_{ph,h}^{PV-P} = P_{ph,h}^{net} - P_{ph}^{PV} \tag{6.4}$$

$$C_{ph,h}^{PV-V} = S_{ph,h}\left(V_{ph,h} - V_{ph,h}^{PV}\right) \tag{6.5}$$

$$C_{ph,h}^{AC-P} = P_{ph,h}^{net} - P_{ph}^{AC} \tag{6.6}$$

$$C_{ph,h}^{AC-V} = S_{ph,h}\left(V_{ph,h}^{AC} - V_{ph,h}\right) \tag{6.7}$$

Equations (6.6) and (6.7) are equivalent to those used in [131]. In [131] the local voltage is compared to a reference voltage, a sensitivity measure (*dV/dP* and *dV/dQ*) is then used to adjust the real and reactive power output of a wind turbine to regulate the voltage to the reference value. The PSPC+VSPC method expands on that of [131] for application to distributed voltage controlled devices on the LV network. This is done through the inclusion of a power set point for each household, to ensure an improved distribution of intervention. The PSPC+VSPC method also calculates a voltage and power set points for each household such that the upper voltage limit (V_{ul}) is reached at the last PV system. In [131] no method for determining a voltage set point is provided, an assumed voltage set point of 1 pu is used.

6.2.2.4 Application

The steps taken by a DNO to setup a *target 400 V line* to use the PSPC+VSPC method to manage voltage are as follows

1. Using power flow software, calculate the voltage and power set points for each PV system and air-conditioning unit on the *target 400 V line* using the method described in Section 6.2.2.1.
2. Using power flow software, calculate the sensitivities for each household on the *target 400 V line* using the method described in Section 6.2.2.2.
3. The above values are input into the control hardware of each PV inverter and air-conditioning unit.
4. Program the control hardware of each PV inverter and air-conditioning unit as per the method described in Section 6.2.2.3.

6.2.3 Case Study

The following case study is used to demonstrate the PSPC+VSPC method. The following operating conditions are assumed for the case study, under which the PSPC+VSPC method is described.

- PV real power curtailment and air-conditioning unit real power load shedding is used by the PSPC+VSPC method for voltage control.
- As real power only is controlled, the voltage sensitivity for each household is calculated using the ratio of change in real power to change in voltage.
- PV systems and load are assumed to operate at unity power factor.

Changes to grid-connected inverter standards AS4777 [67] have been introduced to help mitigate voltage rise due to high-penetration PV. These include volt-watt, volt-VAR and a characteristic power factor curve for cos(ϕ) as a function of real power. PV inverters operating under AS4777 standards will absorb reactive power and increase network losses. The absorption of reactive power also undermines one of the advantages of installing a PV system, reduction in CO_2 emissions. The reactive power needs to be supplied by another generating source, in Australia this is likely to be coal fired or local reactive power compensators. Using coal fired generation to supply the reactive power undermines the key environmental benefit of installing PV, a reduction in CO_2 emissions; real power curtailment is therefore preferred over reactive power absorption.

PV real power curtailment is used in the case study. The author is not suggesting that inverter reactive power control have no role in distributed voltage management, only that the drawbacks of its use be considered.

In the case where the PSPC+VSPC method is used to control PV reactive power absorption, the voltage sensitivity calculated for each household is the ratio of change in reactive power to change in voltage. Otherwise, the method is the same as when using PV real power curtailment.

No network based solutions (DTx tap control or STATCOM for example) are considered for this study. Most DTx's in Australia are fixed; it is therefore realistic to not consider a DTx automatic tap-changer. Also, the majority of voltage rise occurs on the 400 V lines (the reason for this is explained towards the end of Section 5.2.4.7) and therefore a STATCOM or other voltage control devices will have little influence in a situation where a PSPC+VSPC method is implemented. The study is comparing efficiency, equity and accuracy against methods proposed in the literature. Including a DTx tap changer or STATCOM would influence the performance of all methods equally and would not affect the performance comparison. Finally, the study is purely a technical one, with no discussion on the impacts/penalties to customers. This is also the case for the studies to which this work is compared.

6.2.3.1 Test feeder

The voltage control method is tested using the same LV distribution feeder as described in Section 5.2.4.7, which includes both 11 kV and 400 V lines. The feeder is 80 km long and includes three voltage regulators. The voltage regulators split the feeder into four sections. The distance between each bus is 500 m, using a typical 11 kV overhead line. A 400 V line is connected to each bus, each assumed to have the same characteristics. The characteristics of the 400 V line are those typically used by Endeavour Energy, a DNO servicing Greater Western Sydney. The overhead line is three-phase, four-wire with impedance 0.707 Ω/km (*R*) and 0.284 Ω/km (*X*) and is 240 m long. The impedance of the household connection is 1.49 Ω/km (*R*) and 0.097 Ω/km (*X*). Each household connection is 20 m long. There are 6 households on each phase. The DTx steps down the voltage from 11 kV to 400/230 V. Australia's residential LV network operates at 230 V. The DTx tap setting is set to give 250 V on the low side during zero net load, a setting typical for 400 V lines in Endeavour Energy's network. Voltage standards for Endeavour (and Ausgrid) are 230+10%/-6%. This gives an upper voltage limit of 253 V and a lower voltage limit of 216 V. The section used for the case study is downstream of the voltage regulator located at bus 27. The 400 V line connected at bus 32 is selected as the *target 400 V line*, and is used to test the PSPC+VSPC method. Figure 6.16, taken from DIgSILENT, shows this section of the distribution feeder, including the *target 400 V line* in detail.

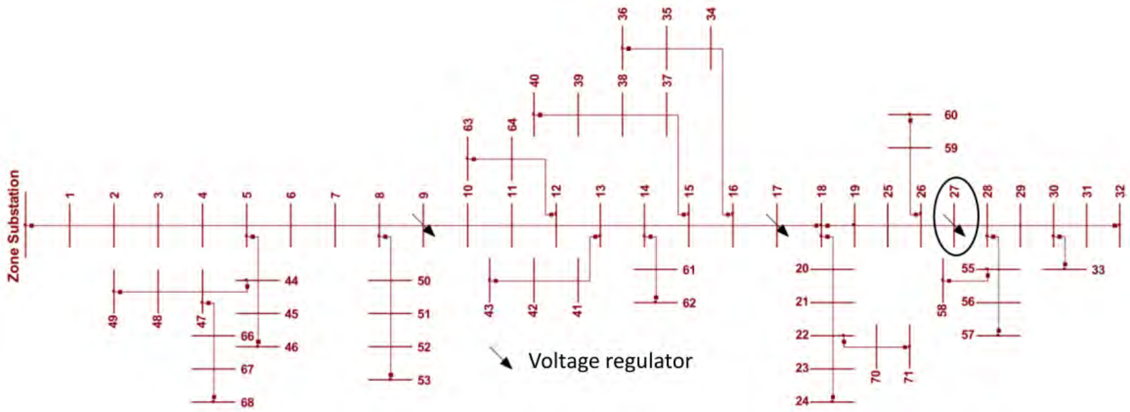

Figure 6.16 Case study LV distribution network [38]. Bus 27 is highlighted

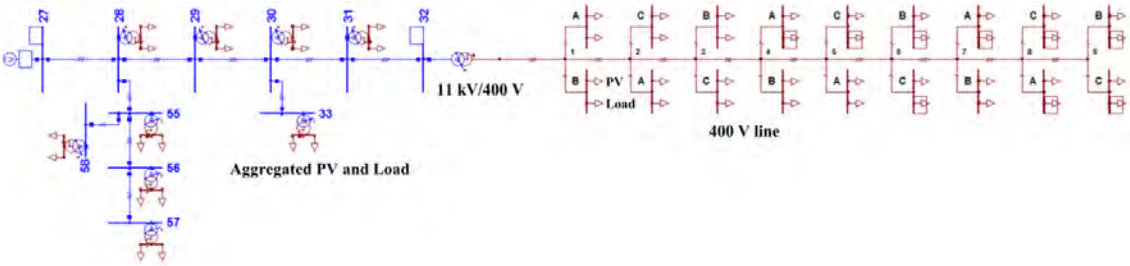

Figure 6.17 Representation of LV distribution network downstream of bus 27 and the *target 400 V line* connected at bus 32, taken from DIgSILENT

6.2.3.2 Set Points

Figure 6.18 gives the voltage set points calculated for the case study, the PV system and air-conditioning unit set points for the 6 households on each phase. The PV system set points are associated with the primary axis and the air-conditioning unit set points of the secondary. For the PV system set points an upper voltage limit of 253 V was selected, this was assigned to the last household of each phase. For the air-conditioning unit set points a lower voltage limit of 246 V was selected, this was assigned to the last household of each phase. 246 V was selected as it was exceeded regularly over the 10 days. A reduction in low voltage excursion up to 246 V was also achievable with a 40% load shedding limit – the assumed contribution of air-conditioning units to total household load at times when voltage management is required.

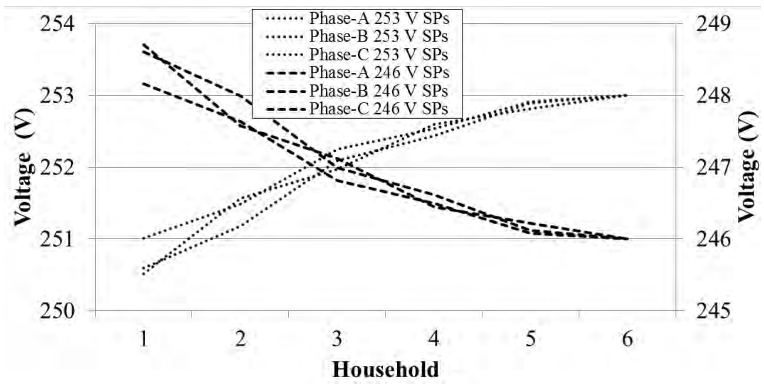

Figure 6.18 Voltage set points: PV set points on primary axis, A/C set points on secondary axis

TABLE 6.2 gives the PV system and air-conditioning unit power set points, for each phase, calculated for the case study.

TABLE 6.2 Power set points

	P_A^{PV} (kW)	P_B^{PV} (kW)	P_C^{PV} (kW)
253 V	-1.24	-1.12	-1.02
246 V	1.46	1.25	1.16

6.2.3.3 PV and Load Data

The same load and PV generation data set [117] as described in Section 6.1.2.1 is used for this case study. All households were randomly assigned PV and load profiles from the dataset. The PSPC+VSPC method was tested over the first 10 days of summer.

6.2.3.4 Simulation of the PSPC+VSPC method

The PSPC+VSPC method was simulated using DIgSILENT; Figure 6.19 presents a flow chart describing how the PSPC+VSPC method was programmed when applied to PV systems. The flow chart is the same for controlling air-conditioning units with the exception that a 40% load shedding limit is also included. For the 10 days, at each time step t, an unbalanced power flow calculation is performed. For each household on each phase, their measured net load ($P_{ph,h}^{net}$) is compared to their power set point for their phase (P_{ph}^{PV}) and their measured voltage ($V_{ph,h}$) compared to their voltage set point ($V_{ph,h}^{PV}$). The PV system generation ($PV_{ph,h}^{g}$) is then changed by the minimum of (6.4) and (6.5).

6.2.4 Results of Case Study

The results of testing for the case study are presented in this section. The PSPC+VSPC method is compared to two other methods. The first is the PSPC+VSPC method but where the power set point only is used for control, this method is termed the PSPC method. This method is equivalent to that proposed in [71]. It is also compared to the AS4777 standard, which uses *P(V)* droop control. This is a voltage set point only control method equivalent to that proposed in [72]. The PV system voltage set points used for the PSPC+VSPC method (Figure 6.18) are also used for the AS4777 method and the droop parameters were tuned to maximise accuracy. The comparison is made using three performance measures.

- The accuracy of the method.
- The efficiency of the method.
- How fairly the method allocates intervention across households.

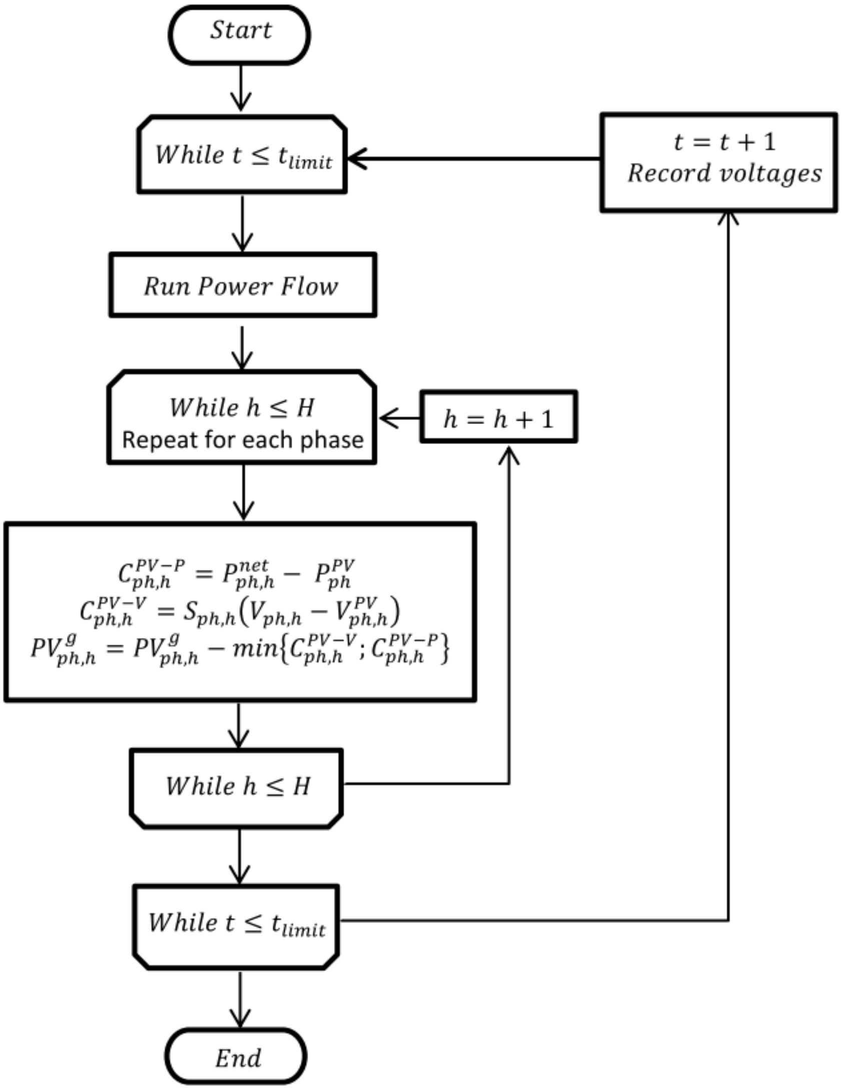

Figure 6.19 Flow chart describing how the PSPC+VSPC method was programmed in DIgSILENT. The flow chart is the same for controlling air-conditioning units with the exception that a 40% load shedding limit is included

6.2.4.1 Accuracy

The first performance measure is the accuracy of the method. When a breach of the upper voltage limit occurs, a method performing with perfect accuracy will manage intervention among PV systems such that the final voltage at the location of the breach is exactly the upper voltage limit. In reality, either the final voltage will be above the upper voltage limit, indicating insufficient intervention, or the final voltage will be under the upper voltage limit, indicating excessive intervention.

Figure 6.20 shows the accuracy of the PSPC+VSPC method. Figure 6.20 is a time-series plot, over the 10 days, of the voltage recorded at the last household on phase-C when there is no control (black dotted) and when all PV systems on the *target 400 V line* are operating under the PSPC+VSPC method (black solid). The red dashed line is the upper voltage limit, 253 V. A breach of the upper voltage limit occurs when the black dotted line is above the red dashed line. During these times, Figure 6.20 shows that the PSPC+VSPC method does not intervene excessively.

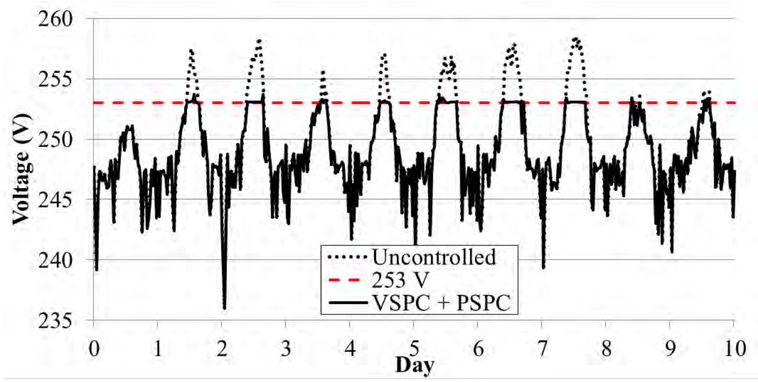

Figure 6.20 Voltages recorded, over the 10 days, for the last household on phase-C for uncontrolled (black dotted) and PSPC+VSPC (black solid)

Figure 6.21 gives a histogram of the voltage error for the three methods, PSPC+VSPC, PSPC and AS4777, providing a means to compare their accuracy. Voltage error is the difference between the uncontrolled voltage and the controlled voltage for times when there is no intervention and the difference between the controlled voltage and the upper voltage limit during intervention.

Figure 6.21 shows the PSPC+VSPC method to be the most accurate of the three. Its voltage error range is the smallest and centred closely to zero error. A positive voltage error indicates insufficient intervention and a negative voltage error indicates excessive intervention. Ranges are indicated by the horizontal arrowed lines on the chart. A range centred on zero indicates there is no bias towards either excessive or insufficient intervention.

The PSPC method has the lowest level of accuracy with the largest voltage error range of 2.25 V. It exhibits a heavy bias towards negative voltage error with the largest negative voltage error at -1.75 V. The PSPC method is therefore intervening excessively. Excessive intervention occurs with the PSPC method, and all power set point only methods, when its household has a high negative net load (high PV generation and low demand) and yet voltage levels are within limits, as the aggregate negative net load for all households is not sufficient to cause excessive voltage rise. The AS4777 method is more accurate than the PSPC method; it has a smaller range (2 V) which is also centred on zero, indicating no bias. Adjusting the *P(V)* droop parameters for the AS4777 method only shifted the voltage error range to be either more negative or more positive, it had little effect on the voltage error range.

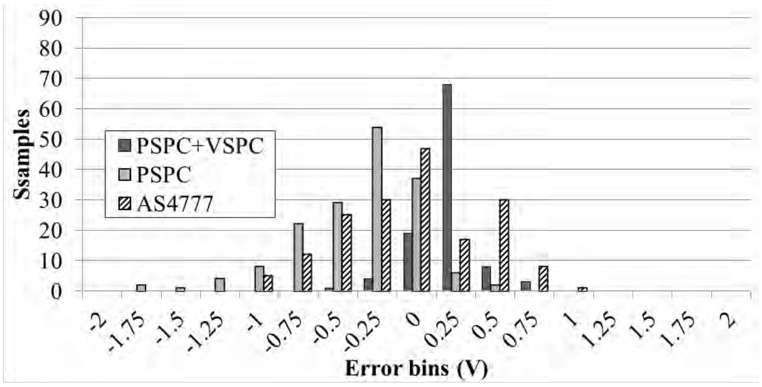

Figure 6.21 Histogram of voltage error for method, power set point only and AS4777 control

6.2.4.2 Efficiency

The second performance measure is efficiency. The less intervention required by a control method to ensure voltage limits are not exceeded, the more efficient it is. TABLE 6.3 gives the total amount of curtailment (kWh) across the 10 days for each control method.

In TABLE 6.3, the total amount of curtailment is also given for an optimal method. Its operation assumes comprehensive communication between all devices and therefore doesn't follow the principles outlined in Section 6.2.1. Its performance in terms of total curtailment however, does provide an appropriate comparison and way of measuring efficiency for the three control methods.

The optimal method operates as follows

- A power flow calculation is performed for each time step *t*, if a voltage above the upper voltage limit is detected; the real power of all PV systems is curtailed in small decrements until all voltages are within the upper voltage limit. The total curtailment for all PV systems is then recorded.

TABLE 6.3 shows that the PSPC+VSPC method is more efficient; curtailing the least over the 10 days compared to the other two control methods, whilst the PSPC method is the least efficient. TABLE 6.3 also gives further evidence of the excessive curtailment which occurs under a PSPC method.

TABLE 6.3 Total curtailment for each control method as well as an optimal control method over the 10 days (kWh)

Phase	Control method (kWh)			
	Optimal	PSPC	AS4777	PSPC+VSPC
A	322	564	421	324
B	531	850	664	645
C	447	705	546	565
Sum (kWh)	**1300**	**2119**	**1631**	**1534**

TABLE 6.4 gives the percentage increase in curtailment of the three control methods over the optimal method; this table is presented to more clearly show the efficiency of each control method.

TABLE 6.4 Percentage increase in curtailment over optimal method

Phase	Control method (% increase)		
	PSPC	AS4777	PSPC+VSPC
A	75.1	30.7	0.6
B	60	25	21.4
C	57.8	22.2	26.5
Average	64.3	26	16.2

6.2.4.3 Intervention Equity

The third performance measure calculates how fairly each method allocates intervention among households. Figure 6.22 and Figure 6.23 illustrate the equity of intervention allocation among households according to their net load contribution. Figure 6.22 gives the total curtailment for each household, combining data from all phases, over the 10 days as a percentage of the total curtailment across all households. Also given is the net load contribution for each household, again combining data from all phases, as a percentage of the total net load contribution across all households. For a method intervening with perfect equity, its intervention allocation (%) would be the same as the net load contribution (%) for each household.

Figure 6.23 is derived from the same data which generated Figure 6.22 and more clearly illustrates the difference in equity of allocation between the three control methods. Figure 6.23 gives the difference in intervention allocation (%) for each control method and the net load contribution (%) for each household. Results combine the data for all phases. As shown in Figure 6.23, the lower the difference between intervention allocation (%) and net load contribution (%), the more equitable the control method. By this measure, the PSPC+VSPC control method is the most equitable, with the least difference for all but household 2. The PSPC method is the least equitable at allocating intervention among households, with the greatest difference for four out of the six households. Despite being more equitable than the PSPC method, the AS4777 method is also shown to be significantly more iniquitous than the PSPC+VSPC method. Iniquitous intervention occurs with the AS4777 method and all voltage set point only methods, when a household has a low negative net load (PV generation similar to demand) and yet voltage levels are high as the aggregate negative net load for all households is excessive. Intervention of the PV system occurs at the household with low net negative load despite its small contribution to voltage rise. Incorporating a power set point as well prevents this, and greater intervention would occur at the households with higher net negative load. In [72], intervention is shown to be fairly allocated among households, but the method is tested under the condition that all PV systems have the same generation and load is zero. Under this condition, the situation under which unfair intervention allocation could occur is masked. The data used for testing in Section 6.2 is actual PV generation and load data, this type of data is necessary to test intervention equity.

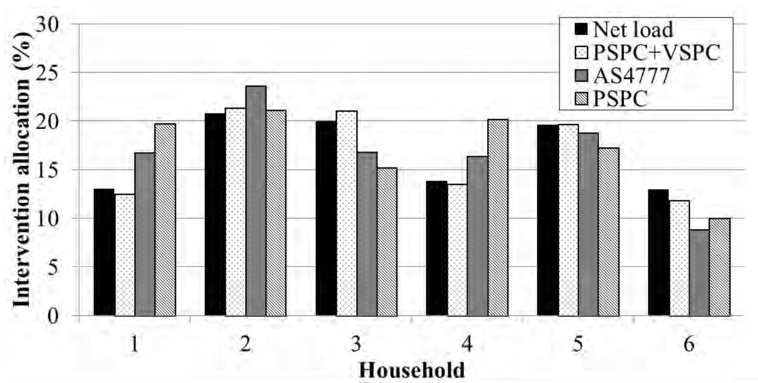

Figure 6.22 Intervention allocation (%) for each household for each control method. Also included is the net load contribution (%) for each household. Results combine the data for all phases

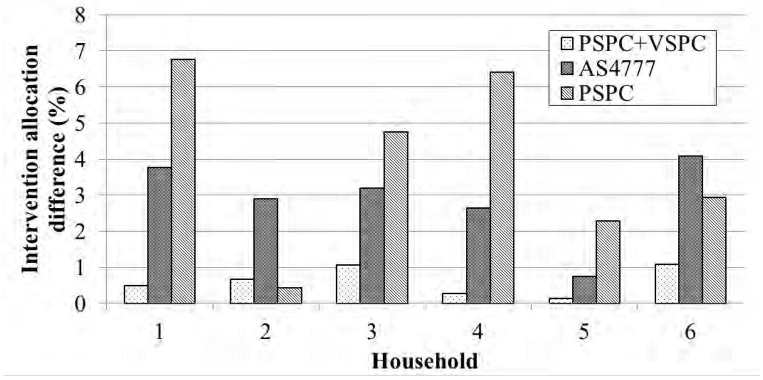

Figure 6.23 Difference in intervention allocation (%) for each control method and the net load contribution (%) for each household. Results combine the data for all phases.

6.2.4.4 Air-conditioning

The test results presented thus far are for PV system control only. As the voltage control method is the same for PV systems and air-conditioning units the performance of both will also be the same, therefore providing extensive results for air-conditioning units as well is unnecessary.

Figure 6.24 is included to show the effectiveness of PSPC+VSPC at ensuring a lower voltage limit is not exceeded through load shedding. The lower voltage limit is 216 V, but with a zero-load DTx voltage of 250 V, there is little chance of reaching this voltage. This case study illustrates how biased DTx tap settings are towards load; load has a 34 V voltage drop window whilst PV has only a 3 V voltage rise window. To test the method for air-conditioning units, the load was scaled higher relative to PV generation, to ensure excessive lower voltages would occur.

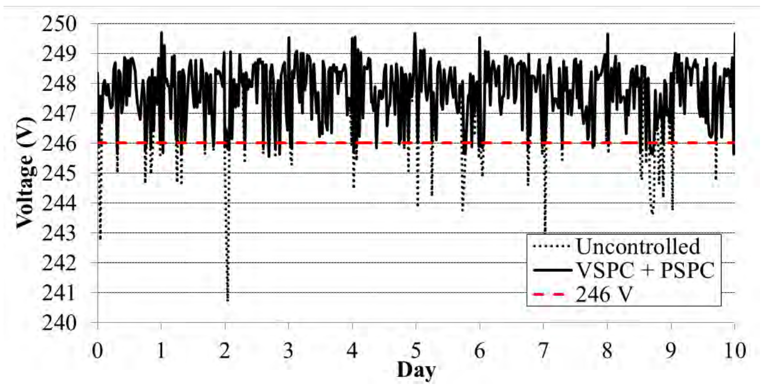

Figure 6.24 Voltages recorded for the last household of phase-C for uncontrolled (dotted) and PSPC+VSPC (solid) for air-conditioning units

It is possible that customers who have their air-conditioning units intervened be compensated; this is also the case for PV system owners who have their generation curtailed. However, the owners of air-conditioning units are already saving money, at the expense of some discomfort, by having their air-conditioners curtailed during peak times when the cost of electricity is highest. An examination into the economic implications of this is outside the scope of this study.

6.2.5 Drawbacks of the PSPC+VSPC Method

There are two drawbacks to the PSPC+VSPC method. The first is if a DNO does not have knowledge of the feeder configuration or the location of PV systems on a target 400 V line they would need to gather this information before the PSPC+VSPC method can be implemented.

The second is the procedure for entering settings (set points and sensitivities) into distributed devices (PV inverters and air-conditioning units). To enter device settings and not be in breach of principle a) likely requires a technician to travel to the households. A more efficient alternative, if possible, is the resident enters the settings. Also, set points need to be re-calculated and re-entered into devices when there is a (significant) change in feeder configuration or PV system deployment, the performance of the PSPC+VSPC method will be impacted otherwise.

Note that all methods currently proposed in the literature which calculate settings offline and use local measurements only for control [71-73, 80, 132], would also suffer from these two drawbacks.

A minor compromise on principle a) resolves the second drawback. Settings could be sent over the internet to PV inverters. This is not new technology and is used regularly for programmable logic controllers (PLCs) and remote telemetry units (RTUs). This compromise is not in breach of the motivation behind principle a). The PSPC+VSPC method would still use local measurements only to implement control. This detail, along with the method being more accurate, requiring less intervention and being more equitable, distinguishes the PSPC+VSPC method from those currently proposed in the literature.

6.2.6 Conclusion

The PSPC+VSPC method is a novel distributed voltage control method which can be applied to both PV systems and large controllable household loads like air-conditioning units. The voltage sensitivity of each household and a voltage and net real power set point are used to control PV system generation and load management of air-conditioning units. Control of PV systems ensures that an upper voltage limit is not exceeded whilst control of air-conditioning units ensures that voltage doesn't fall below the lower voltage limit. The PSPC+VSPC method follows the principles that distributed control methods should be accurate, efficient and fairly allocate intervention among households. For the case study presented, the PSPC+VSPC method is shown to outperform a PSPC method only and a *P(V)* only equivalent of the standard in AS4777 in terms of accuracy, efficiency and intervention equity. The set points and sensitivities only require changing if feeder characteristics change, number of houses, cabling etc., therefore, setting up a *target 400 V line* to use the PSPC+VSPC method, as per described in Section 6.2.2.4, is a set and forget type process. The method is also ideal for using PV system real power to charge a household battery, where at the voltage set point, PV system real power is diverted to charge the battery. The PSPC+VSPC method also uses local measurements only, a less complex approach which doesn't require extensive communication infrastructure and gives immediate support to the growth of DG in electrical distribution networks. That the PSPC+VSPC method can also be used for load management is an added benefit, although as air-conditioning is not the only cause for low voltage excursion, the ability for air-conditioning to ensure voltage levels is limited by its capacity.

7 Conclusions and Future Research

7.1 Summary

The aim of this thesis is to make a contribution towards the successful integration of DPVG into Australia's electricity network. This is to assist in the transition of Australia's generation portfolio to renewables. It is widely accepted that complete low carbon transformation of the global electricity sector is required to achieve global collective climate change goals. DPVG seems likely to play a key role in this transformation, but does raise some challenges for effective electricity industry integration.

The thesis contributes to this overall aim through original research in three areas concerning the technical integration of DPVG into distribution networks.

The first area is in PV generation variability characterisation. A comprehensive characterisation of PV generation variability is required to accurately quantify PV generation variability induced voltage fluctuations. This is necessary to accurately determine the impact on voltage management equipment and to assist network operators design appropriate voltage management equipment for sections of network with high levels of distributed PV deployment.

The second area is in the development of tools to assist network planning in relation to high penetration levels of DPVG. Network planning by DNOs is a time-consuming and resource-intensive exercise. The developed tools make this task easier and also make network operators more likely to consider DPVG in their planning.

The third area is in distributed voltage management. Existing methods may not be able to manage the increase in voltage variability and voltage rise introduced by high-penetration PV and new methods seem likely to be required as DPVG penetrations continue to climb.

7.2 Original Contribution

For the three research areas identified in Section 7.1, a number of knowledge gaps in the literature and limitations in existing industry practice were identified (Chapter 3). These knowledge gaps and limitations were then addressed through six original contributions.

7.2.1 Characterisation of PV Generation Variability

In Section 4.1, a characterisation of PV generation variability is conducted for a number of different PV technologies including fixed-tilt, single-axis and dual-axis tracking systems. The data used for the characterisation is taken from PV systems located at DKASC. The data is actual measured PV generation data, has a sample resolution of 5 min and covers an entire year. The characterisation is split according to season, week and hour. This research addresses characterisation knowledge gaps 1, 2, 5 and 6 defined in Section 3.1.1.

In Section 4.2, high resolution PV generation data is used to characterise the PV generation variability of a cluster of small-scale PV systems. The characterisation concentrates on variability hour to hour, and also categorises the analysis according to day type. Day type is defined according to cloud cover: sunny, partly cloudy and majority cloud. It also investigates aggregate generation variability. This research addresses characterisation knowledge gaps 2-5 defined in Section 3.1.1.

7.2.2 Tool Development to Assist Planning in Relation to High Penetration Levels of DPVG

In Section 5.1 an examination of the relationship between MPVG, feeder characteristics and load conditions is conducted. The MPVG is determined by the regulated upper voltage limit. For a range of feeder characteristics and load conditions, results are obtained through power flow calculations using DIgSILENT. The study assumes a number of simplifying conditions including evenly distributed PV generation and load, cable reactance of zero and load and PV system operating at unity power factor. General relationships are identified through analysis of the results data, primarily though graphical means, and an innovative method developed for deriving the MPVG. This research is a first step attempt to address MPVG knowledge gaps 1-4 defined in Section 3.2.1 and limitations 5-8 in current DNO PV installation assessment processes defined in Section 3.2.2.

An original method for calculating the MPVG is presented in Section 5.2, but is more sophisticated and widely applicable than that proposed in Section 5.1. The method is derived analytically and is an improvement to the method presented in Section 5.1 in terms of potential application under realistic network conditions. This research more completely addresses MPVG knowledge gaps 1-4 defined in Section 3.2.1 and limitations 5-8 in current DNO PV installation assessment processes defined in Section 3.2.2.

7.2.3 New Distributed Voltage Management Techniques

The context in which new methods for distributed voltage management are being developed is one which does not examine voltage management needs as a whole and often requires extensive communication infrastructure. In Section 6.1, a high-penetration PV case study is presented, where a probabilistic voltage and household impact analysis is conducted for a number of voltage management options. A typical LV feeder with high penetrations of PV is used for the case study. The objective of each option is a minimisation of voltage excursion, both higher and lower. The voltage management options simulated require no additional communication infrastructure. The results of the analysis are examined to select the most appropriate voltage management solution, which most effectively minimises voltage excursion as a whole. The study demonstrates a balanced approach to distributed voltage management. This research addresses voltage management knowledge gaps 1-3 defined in Section 3.3.1.

In Section 6.2, an original distributed voltage control method is proposed. The method controls PV inverters to ensure an upper voltage limit is not exceeded and activates controllable loads to ensure a lower voltage limit is not exceeded. Air-conditioning units are considered the most appropriate controllable load. The method can be applied to both PV inverters and controllable loads. The method uses both a voltage and a power set point for control; this ensures both a minimisation of intervention and a fair distribution of intervention among PV inverters and controllable loads on the feeder section. Local measurements only are required to implement the control method. This research addresses voltage management knowledge gaps 4-8 defined in Section 3.3.2.

7.3 Future Research

As always, the work of this thesis raises new questions and opportunities for future work. Research in the area of PV generation variability could be extended in the following ways

- A standardisation of the manner in which PV generation variability is characterised, for example, a characterisation template. The development of a characterisation template would allow for the development of planning tools which facilitated incorporating characterisation data into network planning and operation procedure.
- A comprehensive characterisation study on large scale centralised PV plant. The study would produce a meaningful quantification between PV plant variables, such as area and PV panel density, and potential PV plant generation variability. Quantification could be assessed according to day type, as described in Section 4.2, sunny, partly cloudy and majority cloud.

The MPVGEM, presented in Section 5.2, could be improved in the following ways

- The robustness of the MPVGEM could be improved with further testing of its accuracy at higher terminal counts on 400 V line, see Section 5.2.4.6.
- Including the facility to have PV systems which operated at non-unity power factor would enhance the utility of the MPVGEM.
- The MPVGEM could be programmed as a web application. If programmed in an intuitive fashion, it could be used by non-technical researchers looking for realistic PV generation values. It would also make it accessible to DNO's, in developing countries for example, who don't have access or who can't afford power flow software.

Research in the area of Distributed Voltage Management could be extended in the following ways

- For the case study in Section 6.1, an economic feasibility analysis as part of the decision making process could be introduced. This would incorporate a cost-benefit analysis comparing distributed options such as battery storage against standard augmentation and also possibly conventional MV voltage control such as STATCOM and LVR. It would also need to take into account customer compensation for PV and appliance tripping.

- Also for the case study in Section 6.1, the implications of (customer impact) inverters with Q(V) control instead of PV inverter tripping should be considered.
- A case study using the same approach as in Section 6.1 under different conditions should be undertaken. This would better demonstrate the benefits of a balanced approach to distributed voltage management. Different load demand and PV generation profiles, with different degrees of coincidence, would have a significant effect on the voltage profile, and hence the most appropriate voltage management solution.
- A simulated test of the PSPC+VSPC method should be conducted where every household on all 400 V lines for a LV distribution feeder should have the PSPC+VSPC method applied. In the case study presented in Section 6.2, all households within the LV distribution network are randomly allocated a load and PV generation profile, and contribute to power flow, but only one 400 V line has the PSPC+VSPC method applied.
- To properly test the potential effectiveness of the PSPC+VSPC method, a physical trial should be conducted. PV inverters and controllable loads would be configured to run the PSPC+VSPC method. The set points and sensitivities would be determined for the test network using power flow software, and modelled performance validated through real world application.

References

1. Heslop, S. and MacGill, I. *Operational characteristics of a cluster of distributed photovoltaic systems*. in *Innovative Smart Grid Technologies Asia (ISGT), 2011 IEEE PES*. 2011. IEEE.
2. Heslop, S. and MacGill, I. *A simple method for predicting the output of dual-axis tracking systems from fixed-tilt system outputs*. in *Universities Power Engineering Conference (AUPEC), 2012 22nd Australasian*. 2012. IEEE.
3. Heslop, S. and MacGill, I., *Comparative analysis of the variability of fixed and tracking photovoltaic systems.* Solar Energy, 2014. **107**: p. 351-364.
4. Heslop, S., et al., *Method for Determining a PV Generation Limit on Low Voltage Feeders for Evenly Distributed PV and Load.* Energy Procedia, 2014. **57**: p. 207-216.
5. Heslop, S., MacGill, I., and Fletcher, J. *Voltage Probability Analysis – PV and Load in Low Voltage Networks*. in *Asia Pacific Solar Research Conference 2015*. 2015. http://apvi.org.au/solar-research-conference/proceedings-from-past-conferences/.
6. Heslop, S.F., MacGill, I.F., and Fletcher, J.E. *Maximum PV generation estimation tool for residential low voltage feeders: First-stage*. in *2015 IEEE Power & Energy Society General Meeting*. 2015. IEEE.
7. Heslop, S., MacGill, I., and Fletcher, J., *Maximum PV generation estimation method for residential low voltage feeders.* Sustainable Energy, Grids and Networks, 2016. **7**: p. 58-69.
8. Ren, P., *Renewables 2016 global status report.* REN21 Secretariat: Paris, France, 2016.
9. (APVI), A.P.I., *Solar PV map*. 2015, Australian Photovoltaic Institute: http://pv-map.apvi.org.au/.
10. *NemSight Historical Electricity Tool*. Available from: http://analytics.com.au/energy-analysis/nemsight-trading-tool/.
11. Whitaker, C., et al., *Distributed photovoltaic systems design and technology requirements.* Sandia/SAND2008-0946 P, Tech. Rep, 2008.
12. Agüero, J.R. and Steffel, S.J. *Integration challenges of photovoltaic distributed generation on power distribution systems*. in *Power and Energy Society General Meeting, 2011 IEEE*. 2011. IEEE.
13. Ralph, M., et al. *Transmission and distribution deferment using PV and energy storage*. in *Photovoltaic Specialists Conference (PVSC), 2011 37th IEEE*. 2011. IEEE.
14. Pezeshki, H., Wolfs, P.J., and Ledwich, G., *Impact of high PV penetration on distribution transformer insulation life.* IEEE Transactions on Power Delivery, 2014. **29**(3): p. 1212-1220.

15. Agah, S. and Abyaneh, H.A., *Distribution transformer loss-of-life reduction by increasing penetration of distributed generation.* IEEE Transactions on Power Delivery, 2011. **26**(2): p. 1128-1136.
16. Issicaba, D., Lopes, J.A.P., and da Rosa, M.A., *Adequacy and security evaluation of distribution systems with distributed generation.* IEEE Transactions on Power Systems, 2012. **27**(3): p. 1681-1689.
17. Enslin, J.H. *Network impacts of high penetration of photovoltaic solar power systems*. in *IEEE PES General Meeting*. 2010. IEEE.
18. *Desert Knowledge Solar Centre*. Available from: http://dkasolarcentre.com.au/locations/alice-springs.
19. Lopes, L.A. and Sun, H., *Performance assessment of active frequency drifting islanding detection methods.* IEEE Transactions on Energy Conversion, 2006. **21**(1): p. 171-180.
20. Muttaqi, K. and Sutanto, D. *Assessment of distributed generation impacts on distribution networks using unbalanced three-phase power flow analysis*. in *Power and Energy Society General Meeting, 2011 IEEE*. 2011. IEEE.
21. Yan, R. and Saha, T.K. *Investigation of voltage variations in unbalanced distribution systems due to high photovoltaic penetrations*. in *Power and Energy Society General Meeting, 2011 IEEE*. 2011. IEEE.
22. Lee, K.-s., Yamaguchi, K., and Kurokawa, K., *Proposed distribution voltage control method for connected cluster PV systems.* Journal of Power Electronics, 2007. **7**(4): p. 286-293.
23. Yeh, H.-G., Gayme, D.F., and Low, S.H., *Adaptive VAR control for distribution circuits with photovoltaic generators.* Power Systems, IEEE Transactions on, 2012. **27**(3): p. 1656-1663.
24. Denholm, P. and Margolis, R.M., *Evaluating the limits of solar photovoltaics (PV) in traditional electric power systems.* Energy policy, 2007. **35**(5): p. 2852-2861.
25. Ari, G. and Baghzouz, Y. *Impact of high PV penetration on voltage regulation in electrical distribution systems*. in *Clean Electrical Power (ICCEP), 2011 International Conference on*. 2011. IEEE.
26. Yan, W., et al. *Operation strategies in distribution systems with high level PV Penetration*. in *ISES Solar World Congress*. 2011.
27. HiPerDNO. *HiPerDNO*. Available from: http://www.oerc.ox.ac.uk/projects/high-performance-distributed-network-operation-hiperdno.
28. Reese, C., Buchhagen, C., and Hofmann, L. *Enhanced method for voltage range controlled OLTC-equipped distribution transformers*. in *Power and Energy Society General Meeting, 2012 IEEE*. 2012. IEEE.

29. Tan, Y.T. *Impact on the power system of a large penetration of photovoltaic generation*. in *2007 IEEE Power Engineering Society General Meeting*. 2007.
30. Hsieh, W.-L., et al. *Impact of PV generation to voltage variation and power losses of distribution systems*. in *Electric Utility Deregulation and Restructuring and Power Technologies (DRPT), 2011 4th International Conference on*. 2011. IEEE.
31. Tan, Y.T., Kirschen, D.S., and Jenkins, N., *A model of PV generation suitable for stability analysis.* Energy conversion, IEEE Transactions on, 2004. **19**(4): p. 748-755.
32. *Part 3.5: Limits—Limitation of voltage fluctuations and flicker in low-voltage power supply systems for equipment with rated current greater than 16 A*. SAI Global: AS/NZS 61000.3.5:1998.
33. Lin, C.-H., et al., *Optimization of photovoltaic penetration in distribution systems considering annual duration curve of solar irradiation.* Power Systems, IEEE Transactions on, 2012. **27**(2): p. 1090-1097.
34. Demirok, E., et al. *Clustered PV inverters in LV networks: An overview of impacts and comparison of voltage control strategies*. in *Electrical Power & Energy Conference (EPEC), 2009 IEEE*. 2009. IEEE.
35. Thomson, M. and Infield, D., *Impact of widespread photovoltaics generation on distribution systems.* Renewable Power Generation, IET, 2007. **1**(1): p. 33-40.
36. Yan, R. and Saha, T.K., *Voltage variation sensitivity analysis for unbalanced distribution networks due to photovoltaic power fluctuations.* Power Systems, IEEE Transactions on, 2012. **27**(2): p. 1078-1089.
37. Yan, R. and Saha, T.K., *Analysis of unbalanced distribution lines with mutual coupling across different voltage levels and the corresponding impact on network voltage.* IET Generation, Transmission & Distribution, 2015. **9**(13): p. 1727-1737.
38. Alam, M.J., Muttaqi, K.M., and Sutanto, D., *A three-phase power flow approach for integrated 3-wire MV and 4-wire multigrounded LV networks with rooftop solar PV.* Power Systems, IEEE Transactions on, 2013. **28**(2): p. 1728-1737.
39. Alam, M.J.E., Muttaqi, K.M., and Sutanto, D., *Community energy storage for neutral voltage rise mitigation in four-wire multigrounded LV feeders with unbalanced solar PV allocation.* IEEE Transactions on Smart Grid, 2015. **6**(6): p. 2845-2855.
40. Alam, M.J.E., Muttaqi, K.M., and Sutanto, D., *Alleviation of neutral-to-ground potential rise under unbalanced allocation of rooftop PV using distributed energy storage.* IEEE Transactions on Sustainable Energy, 2015. **6**(3): p. 889-898.
41. Zahedi, A., *Maximizing solar PV energy penetration using energy storage technology.* Renewable and Sustainable Energy Reviews, 2011. **15**(1): p. 866-870.

42. Enslin, J.H. and Heskes, P.J., *Harmonic interaction between a large number of distributed power inverters and the distribution network.* Power Electronics, IEEE Transactions on, 2004. **19**(6): p. 1586-1593.
43. Papaioannou, I.T., et al. *Harmonic impact of small photovoltaic systems connected to the LV distribution network*. in *Electricity Market, 2008. EEM 2008. 5th International Conference on European*. 2008. IEEE.
44. Batrinu, F., et al. *Impacts of grid-connected photovoltaic plant operation on the harmonic distortion*. in *MELECON 2006-2006 IEEE Mediterranean Electrotechnical Conference*. 2006.
45. Piwko, R., et al., *Intermittency Analysis Project Appendix B: Impact of Intermittent Generation on Operation of California Power Grid*. 2007, Sacramento, California: California Energy Commission, PIER Research Development & Demonstration Program.
46. Lew, D., et al., *Impact of high solar penetration in the western interconnection.* Contract, 2010. **303**: p. 275-3000.
47. Mossoba, J., et al. *Analysis of solar irradiance intermittency mitigation using constant DC voltage PV and EV battery storage*. in *Transportation Electrification Conference and Expo (ITEC), 2012 IEEE*. 2012. IEEE.
48. Renné, D.S., et al., *Solar resource assessment*. 2008: National Renewable Energy Laboratory.
49. PVWatts. *PVWatts*. Available from: http://pvwatts.nrel.gov/.
50. Click, D.K., et al. *Effects of solar resource variability on the future Florida transmission and distribution system*. in *Transmission and Distribution Conference and Exposition (T&D), 2012 IEEE PES*. 2012. IEEE.
51. Jewell, W. and Ramakumar, R., *The effects of moving clouds on electric utilities with dispersed photovoltaic generation.* Energy Conversion, IEEE Transactions on, 1987(4): p. 570-576.
52. Mills, A., *Understanding variability and uncertainty of photovoltaics for integration with the electric power system.* Lawrence Berkeley National Laboratory, 2010.
53. Hoff, T.E. and Perez, R., *Quantifying PV power output variability.* Solar Energy, 2010. **84**(10): p. 1782-1793.
54. Mills, A.D. and Wiser, R.H. *Implications of geographic diversity for short-term variability and predictability of solar power*. in *Power and Energy Society General Meeting, 2011 IEEE*. 2011. IEEE.
55. Jenicek, D., Inam, W., and Ilic, M. *Locational dependence of maximum installable PV capacity in LV networks while maintaining voltage limits*. in *North American Power Symposium (NAPS), 2011*. 2011. IEEE.

56. Ilic, M.D. and Zaborszky, J., *Dynamics and control of large electric power systems*. 2000: Wiley New York.
57. Canova, A., et al., *Electrical impact of photovoltaic plant in distributed network.* Industry Applications, IEEE Transactions on, 2009. **45**(1): p. 341-347.
58. Tonkoski, R., Turcotte, D., and El-Fouly, T.H., *Impact of high PV penetration on voltage profiles in residential neighborhoods.* Sustainable Energy, IEEE Transactions on, 2012. **3**(3): p. 518-527.
59. Ueda, Y., et al., *Analysis results of output power loss due to the grid voltage rise in grid-connected photovoltaic power generation systems.* Industrial Electronics, IEEE Transactions on, 2008. **55**(7): p. 2744-2751.
60. Spertino, F., Di Leo, P., and Cocina, V., *Which are the constraints to the photovoltaic grid-parity in the main European markets?* Solar Energy, 2014. **105**: p. 390-400.
61. Shayani, R.A. and De Oliveira, M.A.G., *Photovoltaic generation penetration limits in radial distribution systems.* Power Systems, IEEE Transactions on, 2011. **26**(3): p. 1625-1631.
62. Conti, S., et al. *Study of the impact of PV generation on voltage profile in LV distribution networks*. in *Power Tech Proceedings, 2001 IEEE Porto*. 2001. IEEE.
63. Ayres, H.M., et al., *Method for determining the maximum allowable penetration level of distributed generation without steady-state voltage violations.* IET generation, transmission & distribution, 2010. **4**(4): p. 495-508.
64. Navarro, A., Ochoa, L.F., and Randles, D. *Monte Carlo-based assessment of PV impacts on real UK low voltage networks*. in *Power and Energy Society General Meeting (PES), 2013 IEEE*. 2013.
65. Ausgrid. *Guidelines for Photovoltaic Installations up to 200kW connected via Inverters to the Ausgrid Network*. Available from: http://www.ausgrid.com.au/~/media/00E8D0FB3FCF4E3A9C01A70F529B5975.ashx.
66. Energex and Ergon Energy. *Small Scale Parallel Inverter Energy Systems up to 30 kVA*. Available from: https://www.ergon.com.au/__data/assets/pdf_file/0005/198698/STNW1170ver2-Connection-Standard-for-IES-up-to-30kVA.pdf.
67. *AS4777.2:2015 Grid connection of energy systems via inverters - Inverter requirements*. 2015, SAI Global.
68. Liu, Y., et al. *Distribution system voltage performance analysis for high-penetration PV*. in *Energy 2030 Conference, 2008. ENERGY 2008. IEEE*. 2008. IEEE.
69. Kerber, G., Witzmann, R., and Sappl, H. *Voltage limitation by autonomous reactive power control of grid connected photovoltaic inverters*. in *Compatibility and Power Electronics, 2009. CPE'09.* 2009. IEEE.

70. Goodwin, S.E. and Krause, O. *Mitigation of voltage band violations through distributed active and reactive power control of inverter based PV generation on LV networks*. in *Power and Energy Society General Meeting (PES), 2013 IEEE*. 2013. IEEE.
71. Samadi, A., et al., *Coordinated active power-dependent voltage regulation in distribution grids with PV systems.* Power Delivery, IEEE Transactions on, 2014. **29**(3): p. 1454-1464.
72. Samadi, A., et al., *Multi-objective coordinated droop-based voltage regulation in distribution grids with PV systems.* Renewable Energy, 2014. **71**: p. 315-323.
73. Muttaqi, K.M., et al., *A Coordinated Voltage Control Approach for Coordination of OLTC, Voltage Regulator, and DG to Regulate Voltage in a Distribution Feeder.* Industry Applications, IEEE Transactions on, 2015. **51**(2): p. 1239-1248.
74. Paatero, J.V. and Lund, P.D., *Effects of large-scale photovoltaic power integration on electricity distribution networks.* Renewable Energy, 2007. **32**(2): p. 216-234.
75. Redfield, N. and Redfield, J. *The Garage of the Future: Maximizing the Economic Value of Solar Panels*. in *Green Technologies Conference, 2010 IEEE*. 2010. IEEE.
76. Blumsack, S., Brownson, J., and Rayl, J. *Matching photovoltaic orientation to energy loads*. in *System Sciences (HICSS), 2010 43rd Hawaii International Conference on*. 2010. IEEE.
77. Krauter, S. and Japs, E. *Integration of PV into the energy system: Challenges and measures for generation and load management*. in *Photovoltaic Specialist Conference (PVSC), 2014 IEEE 40th*. 2014. IEEE.
78. Riffonneau, Y., et al., *Optimal power flow management for grid connected PV systems with batteries.* Sustainable Energy, IEEE Transactions on, 2011. **2**(3): p. 309-320.
79. Heussen, K., et al., *Unified system-level modeling of intermittent renewable energy sources and energy storage for power system operation.* Systems Journal, IEEE, 2012. **6**(1): p. 140-151.
80. Marra, F., et al., *A decentralized storage strategy for residential feeders with photovoltaics.* Smart Grid, IEEE Transactions on, 2014. **5**(2): p. 974-981.
81. Marra, F., et al. *Energy storage options for voltage support in low-voltage grids with high penetration of photovoltaic*. in *Innovative Smart Grid Technologies (ISGT Europe), 2012 3rd IEEE PES International Conference and Exhibition on*. 2012. IEEE.
82. Blazic, B., et al. *Integration of photovoltaic systems with voltage control capabilities into LV networks*. in *Proceedings of the 1st international workshop on integration of solar power into power systems, Aarhus, Denmark*. 2011.
83. Alam, M., Muttaqi, K.M., and Sutanto, D., *Mitigation of rooftop solar PV impacts and evening peak support by managing available capacity of distributed energy storage systems.* Power Systems, IEEE Transactions on, 2013. **28**(4): p. 3874-3884.

84. Yao, E., et al. *Tackling the photovoltaic integration challenge in the distribution network with deferrable load*. in *Smart Grid Communications (SmartGridComm), 2013 IEEE International Conference on*. 2013. IEEE.
85. Scott, N.C., Atkinson, D.J., and Morrell, J.E., *Use of load control to regulate voltage on distribution networks with embedded generation.* Power Systems, IEEE Transactions on, 2002. **17**(2): p. 510-515.
86. Christakou, K., et al., *GECN: Primary voltage control for active distribution networks via real-time demand-response.* Smart Grid, IEEE Transactions on, 2014. **5**(2): p. 622-631.
87. Argiento, R., et al., *Distributed interruptible load shedding and micro-generator dispatching to benefit system operations.* Power Systems, IEEE Transactions on, 2012. **27**(2): p. 840-848.
88. Malik, O. and Havel, P., *Active demand-side management system to facilitate integration of res in low-voltage distribution networks.* Sustainable Energy, IEEE Transactions on, 2014. **5**(2): p. 673-681.
89. Steffel, S., et al., *Integrating solar generation on the electric distribution grid.* Smart Grid, IEEE Transactions on, 2012. **3**(2): p. 878-886.
90. Medina, J., Muller, N., and Roytelman, I., *Demand response and distribution grid operations: Opportunities and challenges.* Smart Grid, IEEE Transactions on, 2010. **1**(2): p. 193-198.
91. Sugihara, H., et al., *Economic and efficient voltage management using customer-owned energy storage systems in a distribution network with high penetration of photovoltaic systems.* Power Systems, IEEE Transactions on, 2013. **28**(1): p. 102-111.
92. Shahnia, F., Wishart, M.T., and Ghosh, A. *Voltage regulation, power balancing and battery storage discharge control by smart demand side management and multi-objective decision making*. in *Power Engineering Conference (AUPEC), 2013 Australasian Universities*. 2013. IEEE.
93. Douglass, P.J., et al., *Voltage-sensitive load controllers for voltage regulation and increased load factor in distribution systems.* Smart Grid, IEEE Transactions on, 2014. **5**(5): p. 2394-2401.
94. Hoke, A., et al., *Steady-state analysis of maximum photovoltaic penetration levels on typical distribution feeders.* Sustainable Energy, IEEE Transactions on, 2013. **4**(2): p. 350-357.
95. Keane, A., et al., *Enhanced utilization of voltage control resources with distributed generation.* Power Systems, IEEE Transactions on, 2011. **26**(1): p. 252-260.
96. Carigiet, F., et al., *Case study of a low-voltage distribution grid with high PV penetration in Germany and simulation analyses of cost-effective measures.* Progress in Photovoltaics: Research and Applications, 2015.

97. Shao, M., Walling, R., and Cleary, J. *Steady-state methodology for investigating the relationship between photovoltaic (PV) facility size, location, and voltage impact*. in *Power and Energy Society General Meeting, 2012 IEEE*. 2012. IEEE.
98. Baran, M.E., et al., *Accommodating high PV penetration on distribution feeders.* Smart Grid, IEEE Transactions on, 2012. **3**(2): p. 1039-1046.
99. Endeavour Energy. *Connection of a Power Generator System*. 2015; Available from: https://www.endeavourenergy.com.au/wps/wcm/connect/10b28580401ab9f387178fb80dd2df7b/23.+Brochure+Connection+of+a+Power+Generator+System_June+2014.pdf?MOD=AJPERES.
100. Western Power and Horizon Energy. *Western Australian Distribution Connections Manual 2015*. 2015; Available from: http://www.westernpower.com.au/documents/WA_Distribution_Connections_Manual.pdf.
101. Noone, B., *PV Integration on Australian Distribution Networks*. 2013, Australian PV Institute: http://apvi.org.au/wp-content/uploads/2013/12/APVA-PV-and-DNSP-Literature-review-September-2013.pdf.
102. Braun, M., et al., *Is the distribution grid ready to accept large-scale photovoltaic deployment? State of the art, progress, and future prospects.* Progress in photovoltaics: Research and applications, 2012. **20**(6): p. 681-697.
103. Energex. *Energex Power Quality Strategic Plan 2015-20*. 2015; Available from: https://www.aer.gov.au/sites/default/files/Energex - 29. Power Quality Strategic Plan - October 2014.pdf.
104. Australian Government. *Heating and Cooling*. 2013 [cited 2013 2013]; Available from: http://www.yourhome.gov.au/energy/heating-and-cooling.
105. Statistics, A.B.o., *Energy Use and Conservation Survey 2011*. 2011, Australian Bureau of Statistics: http://www.ausstats.abs.gov.au/.
106. Energex. *Residential Demand and Smart Control Network Tariffs Fact Sheet*. Available from: https://www.energex.com.au/__data/assets/pdf_file/0007/348046/Residential-Demand-and-Smart-Control-Network-Tariffs-Fact-Sheet.pdf.
107. Bebic, J., *Power system planning: emerging practices suitable for evaluating the impact of high-penetration photovoltaics. Subcontract report*. 2008, NREL/SR-581-42297. Available from: http://www.nrel.gov/docs/fy08osti/42297.pdf.
108. Saadat, N., Choi, S., and Vilathgamuwa, D.M. *A statistical approach to quantify the impact on voltage quality caused by PV generators*. in *Electric Utility Deregulation and Restructuring and Power Technologies (DRPT), 2011 4th International Conference on*. 2011. IEEE.
109. Miyamoto, Y. and Sugihara, H. *Demonstrative research on clustered PV systems*. in *Photovoltaic Specialists Conference (PVSC), 2009 34th IEEE*. 2009. IEEE.

110. Enslin, J.H. *Network impacts of high penetration of photovoltaic solar power systems*. in *Power and Energy Society General Meeting, 2010 IEEE*. 2010. IEEE.

111. Drury, E., et al., *Relative performance of tracking versus fixed tilt photovoltaic systems in the USA.* Progress in Photovoltaics: Research and Applications, 2014. **22**(12): p. 1302-1315.

112. SolFocus. Available from: http://www.solfocus.com/en/technology/.

113. Achilles, S., Schramm, S., and Bebic, J., *Transmission system performance analysis for high-penetration photovoltaics*. 2008: National Renewable Energy Laboratory.

114. *Australian Solar Industry Installs More Small PV than Germany in 2010*. 2011; Available from: www.renewableenergyworld.com.

115. Oozeki, T., et al. *An evaluation method for smoothing effect on photovoltaic systems dispersed in a large area*. in *Photovoltaic Specialists Conference (PVSC), 2009 34th IEEE*. 2009. IEEE.

116. Hoff, T. and Perez, R., *Quantifying PV Output Power Variability.* Clean Power Research, 2010.

117. *Solar home electricity data*. Available from: http://www.ausgrid.com.au/Common/About-us/Corporate-information/Data-to-share/Solar-home-electricity-data.aspx.

118. Chicco, G., et al., *Experimental Indicators of Current Unbalance in Building-Integrated Photovoltaic Systems.* Photovoltaics, IEEE Journal of, 2014. **4**(3): p. 924-934.

119. Australian Senate Committee. *Australian Senate Committee Report on Electricity Prices*. 2012; Available from: http://www.aph.gov.au/Parliamentary_Business/Committees/Senate/Former_Committees/electricityprices/electricityprices/report/c05.

120. Essential. *Essential Energy Applicance Guide 2011*. Available from: http://www.essentialenergy.com.au/asset/cms/PDF/Appliance_Nov2011.PDF.

121. Yang, Y., et al., *Sizing strategy of distributed battery storage system with high penetration of photovoltaic for voltage regulation and peak load shaving.* Smart Grid, IEEE Transactions on, 2014. **5**(2): p. 982-991.

122. Energex. *Energex Demand Side Management - Previous Programs*. Available from: https://www.energex.com.au/home/control-your-energy/positive-payback-program/positive-payback-for-households/our-previous-programs.

123. Western-Power. *Photovoltaic Forecast Public Version 2012*. 2012; Available from: http://www.westernpower.com.au/documents/Photovoltaic_Forecast_Public_Version_2012.pdf.

124. Energex. *Energex distribution annual planning report 2014/2015 to 2018/2019*. 2015; Available from: https://www.energex.com.au/__data/assets/pdf_file/0003/219720/DAPR-2014-15-to-2018-19-Volume-1.pdf.

125. Ausgrid. *Effect of small solar Photovoltaic (PV) systems on network peak demand*. Available from: http://www.ausgrid.com.au/~/media/Files/About%20Us/Newsroom/Discussions/Solar%20PV%20Research%20Paper.pdf.

126. Ausgrid. *Smart Grid, Smart City Distributed generation and storage trials*. Available from: https://www.ausgrid.com.au/~/media/Files/Customer%20Services/Homes/Solar/SGSCDGandDSResultsandOutcomes.pdf.

127. *AusNet Battery Energy Storage Trial*. Available from: http://www.hellogrid.com.au/innovation/ausnet-battery-energy-storage-trial-way/.

128. *Grid Utility Support System*. Available from: https://www.ergon.com.au/about-us/news-hub/talking-energy/technology/ergon-battery-energy-storage-systems-roll-out.

129. Brenna, M., et al., *Automatic distributed voltage control algorithm in smart grids applications.* Smart Grid, IEEE Transactions on, 2013. **4**(2): p. 877-885.

130. Yu, L., Czarkowski, D., and De León, F., *Optimal distributed voltage regulation for secondary networks with DGs.* Smart Grid, IEEE Transactions on, 2012. **3**(2): p. 959-967.

131. Sansawatt, T., Ochoa, L.F., and Harrison, G.P., *Smart decentralized control of DG for voltage and thermal constraint management.* Power Systems, IEEE Transactions on, 2012. **27**(3): p. 1637-1645.

132. Sondermeijer, O., et al. *Regression-based inverter control for decentralized optimal power flow and voltage regulation*. in *Power & Energy Society General Meeting. IEEE*. 2016.